# FUNCTIONAL CHARACTERIZATION OF GAP50: THE INTEGRAL MEMBRANE RECEPTOR FOR THE MYOSIN MOTOR COMPLEX IN *TOXOPLASMA GONDII*

**TEREZINA MARIE JOHNSON**

A dissertation submitted to the faculty of the University of North Carolina at Chapel Hill in partial fulfillment of the requirements for the degree of Doctor of Philosophy in the Department of Cell and Developmental Biology

Chapel Hill
2007

Approved by:

Con Beckers

Keith Burridge

Richard Cheney

Primal de Lanerolle

Kenneth Jacobson

**ABSTRACT**

Terezina M. Johnson
Functional Characterization of GAP50: The Integral Membrane Receptor for the Myosin Motor Complex in *Toxoplasma gondii*
(Under the direction of Con Beckers)

Toxoplasmosis is a serious disease caused by the obligate intracellular parasite *Toxoplasma gondii*. Lacking locomotive organelles such as flagellae, these parasites exhibit a unique substrate-dependent motion called gliding motility. Detailed studies in *Toxoplasma* and the closely related malarial agent, *Plasmodium*, have revealed that gliding motility is required for survival throughout many stages of the life cycle, including host cell invasion and egress. Although it has been demonstrated that parasite motility requires an active actin-myosin motility system, the structure and regulation of this system are not known in any detail (Dobrowolski et al., 1997; Meissner et al., 2002; Wetzel et al., 2003). The myosin involved in *Toxoplasma* motility, TgMyoA, is found in a complex with myosin light chain (TgMLC1), TgGAP45 and TgGAP50, the membrane anchor for the complex (Gaskins et al., 2004). The overall goal of this research is to determine the functional attributes of the gliding motility complex in these parasites, known as the glideosome. *Toxoplasma* motility is likely to be regulated at the level of this complex, and the importance of these accessory proteins is now being discovered.

This thesis will focus on two of the accessory proteins, TgGAP50 and TgGAP45 that accompany the driving myosin motor, TgMyoA. We have discovered that the TgMyoA anchor, TgGAP50, is immobilized in the outer face of the cholesterol-enriched inner membrane complex; a discovery that is fundamental to understanding the mechanism of force generation by TgMyoA. We have also determined that the lumenal domain and the first half of the transmembrane domain of TgGAP50 are required for targeting of the protein, while the cytoplasmic domain is necessary for glideosome formation and therefore, motility. Lastly, we have uncovered an unusual structural characteristic of TgGAP45, potentially revealing its function in motility, and have established a method for glideosome purification. These results shed light on basic cellular processes such as cell motility and may eventually reveal new targets for therapeutic interventions for diseases caused by parasites such as toxoplasmosis and malaria.

## TABLE OF CONTENTS

## LIST OF FIGURES

**Chapter I:**



**Chapter II:**

## LIST OF ABBREVIATIONS

| | |
|---|---|
| AAT | alpha-1 antitrypsin |
| BSA | bovine serum albumin |
| CE | cholesteryl |
| DRM | detergent-resistant membrane |
| FRAP | fluorescence recovery after photobleaching |
| GAP | gliding associated protein |
| HFF | human foreskin fibroblast |
| HLA-A2 | human class I histocompatibility protein |
| IMC | inner membrane complex |
| mβCD | methyl-β-cyclodextrin |
| PBS | phosphate buffered saline |
| PC | phosphocholine |
| PM | plasma membrane |
| PVM | parasitophorous vacuolar membrane |
| SAG | surface antigen |
| TBS | tris buffered saline |
| TLC | thin layer chromatography |
| TX | TritonX |
| YFP | yellow fluorescent protein |

# CHAPTER I

## COMPREHENSIVE LITERATURE REVIEW

## INTRODUCTION

"It's an incredibly smart parasite. It has ways of getting around all of the protective devices that the human body can throw at it, and that is one of the reasons why it's a difficult problem and it's a grand challenge." – Alan Cowman, PhD

### Apicomplexan parasites

The single-cell eukaryotic parasite *Toxoplasma gondii* may be one of the smartest parasites around. It does not have a high IQ, or an advanced degree, but it has the ability to avoid most protective mechanisms of its host, and even control host behavior. The parasite is able to infect any warm-blooded animal, where it forms a protective barrier in order to avoid recognition from the immune system of the host. It can then control expression of genes within the host by interfering with host cell signaling pathways (Saeij et al., 2007).

It was believed that these parasites could manipulate host behavior in order to increase their own transmission efficiency, known as the 'behavioral manipulation' hypothesis (Thomas et al, 2005, Klein, 2005). With the cat as the definitive host of the parasite, rats infected with *Toxoplasma* lose their innate avoidance of cats, increasing the likelihood that they will be eaten by a cat, therefore enabling the parasite to complete its life cycle (Webster, 2007). The behavior of rats is specific for its own selective benefit, since infected animals do not have an aversion to dogs, a predator that is not appropriate for parasite reproduction (Vyas et al., 2007).

Apoptosis, initiated in an infected cell by cytotoxic immune effector cells, is an important defense mechanism against pathogens (Barry and Bleackley, 2002); however, *Toxoplasma* can inhibit the apoptotic response of the host cell by interacting with many of the regulatory pathways (Carmen and Sinai, 2007). There is an increasing amount of data implicating behavioral changes of infected organisms in order for the parasite to exert control and continue propagation.

*Toxoplasma gondii* belongs to the Phylum Apicomplexa, of which the parasites are characterized by their polarized cell structure and a set of specialized organelles at their apical end that are necessary for motility and invasion of the parasite. They are obligate intracellular protozoan pathogens, so they must gain entry into their host cells in order to replicate and survive.

There are over five thousand parasitic species within the phylum Apicomplexa, of which many cause severe disease in humans and animals (Soldati and Meissner, 2004). Perhaps the most deadly and well-known member, *Plasmodium falciparum,* infects millions of humans worldwide, resulting in malaria. Other species include the wide-spread zoonotic organism *Cryptosporidium* which causes enteritis, as well as *Theileria*, *Babesia*, and *Eimeria*, the parasite responsible for coccidiosis in chickens (Black and Boothroyd, 2000). Although each of these parasites has a unique host, they all use the same mechanisms of motility and invasion for their survival within their respective host cell. Studies in *Toxoplasma* will likely lead to parallel discoveries in the highly similar parasites of this phylum, and lead to effective treatments of these diseases.

***Toxoplasma gondii***

*Toxoplasma gondii* was first described in 1908 by Nicolle and Manceaux in North America and by Splendore in Brazil. The scientific name was given based on the North American rodent from which the parasite was isolated (*Ctenodactylus gondi*) and the Greek word *toxon*, which means "bow" referring to the crescent shape of the parasites (Black and Boothroyd, 2000). The parasites can measure up to approximately 5µm long by 2µm wide during the rapidly growing phase of infection (Smith, 1995).

One of the key survival features of *Toxoplasma* is that it can infect any warm blooded animal (Dubey, 1998; Wong and Remington, 1993). The life cycle is divided into the sexual and asexual cycles, or the feline and non-feline cycles, respectively (Figure 1). Members of the cat family (Felidae) are the only known definitive hosts for the sexual stages of *T. gondii* and are therefore the main reservoirs of infection. Cats become infected with *T. gondii* by ingesting tissue cysts or oocysts from viable organisms such as mice. The cysts release parasites that invade epithelial cells of the small intestine where they undergo an asexual cycle followed by a sexual cycle and then form oocysts, which are excreted. The unsporulated oocyst takes 1 to 5 days after excretion to become infective. Although cats shed oocysts for only 1 to 2 weeks, large numbers may be shed and they are capable of survival in the environment for several months.

Human infection may be acquired in several ways, including the ingestion of undercooked infected meat containing tissue cysts, the ingestion of oocysts from fecally contaminated hands or food, organ transplantation, blood transfusion, or transplacental transmission. Infection is characterized by an acute and a chronic stage. The acute stage of toxoplasmosis, involves the rapidly replicating tachyzoite stage. Tachyzoites replicate every 8 hours, until approximately 40-60 hours later,

the number of parasites is too large for the host cell to support. At this point, the host cell ruptures and parasites are released to infect new host cells and continue the life cycle (Black and Boothroyd, 2000) (Figure 2). Approximately 7-10 days after infection, *in vivo* tachyzoites differentiate into bradyzoites, which are slow-growing forms of the parasite that form tissue cysts within the host (Black and Boothroyd, 2000). The chronic stage of the asexual cycle is defined by the formation of these long-lived cysts throughout the body, most commonly in skeletal muscle tissue and the central nervous system where they may remain throughout the life of the host (Black and Boothroyd, 2000).

Although the mechanism is not understood, bradyzoites are able to spontaneously differentiate back into tachyzoites at low frequencies, which can re-initiate an acute infection. In animals and humans, a rapid immune response prevents these tachyzoites from spreading, however in immunocompromised individuals, this infection leads to the disease toxoplasmosis.

**Toxoplasmosis**

Over 300 species of mammals and 20 species of birds have been reported as hosts for *Toxoplasma* and it is believed that all warm blooded animals are susceptible (Ortega, 2006). It should therefore come at no surprise that Toxoplasmosis is one of the most common human infections throughout the world, although infection is more common in warm climates and at lower altitudes than in cold climates and mountain regions (www.dpd.cdc.gov). A high prevalence of infection has been noted in France which may be due to a cultural preference for eating raw or undercooked meat, while high prevalence in Central America has been attributed to the higher number of stray cats residing in a climate favoring

oocyst survival. The overall prevalence in the United States was found to be 22.5% overall, with and 15% among women of childbearing age, as determined with specimens collected by the third National Health and Nutritional Assessment Survey (NHANES III) between 1988 and 1994 (Centers for Disease Control). Oocysts are resistant to most typical environmental conditions and can survive in moist conditions for months and even years. In addition to the traditional methods of transmission, invertebrates such as flies, cockroaches, and earthworms can spread oocysts mechanically (www.dpd.cdc.gov).

Whereas acute toxoplasmosis is especially problematic in immunocompromised individuals, an acute infection can also spread to a fetus and lead to severe congenital disease. This can result in neurological disorders such as blindness and mental retardation, and as a result, expectant mothers are advised to avoid changing cat litter boxes (Black and Boothroyd, 2000). In individuals with a weakened immune system, such as patients with AIDS, intracerebral lesions can cause toxoplasmic encephalitis (Wong and Remington, 1993). *Toxoplasma* infection of the eyes is a significant cause of retinochoroiditis in the United States, and can be the result of congenital infection, or infection after birth (Gilbert et al., 1995).

More recently, *Toxoplasma* infection has been linked to a variety of other diseases or conditions. In addition to altering the brain chemistry of rats so that they are less likely to avoid cats, *Toxoplasma* is thought to affect human behavior as well. Other protozoa are known to induce substantial behavioral changes upon brain infection, such as sleeping sickness caused by *Trypanosoma* and cerebral malaria caused by *Plasmodium* infection (Newton and Warrell, 1998). Recent studies indicate that *Toxoplasm*a infection may be correlated with cases of schizophrenia and human affective disorders (Torrey and Yolken, 2007; Webster et

al., 2006). Infection with the parasite has been associated with damaged astrocytes in the brain and schizophrenia has as well (Torrey and Yolken 2003). Studies have found that seropositive babies or babies born to seropositive mothers have an increased risk of later developing schizophrenia (Mortenson et al., 2007). One study suggests that subjects with latent toxoplasmosis have an almost three-fold higher risk of traffic accidents and that the actual risk decreases with the duration of infection, while another study shows that *Toxoplasma* infection could be skewing human sex ratios in favor of males (Lafferty, 2006; Flegr et al., 2007).

The current drug therapy consists of a combination of sulfonamide and pyrimethamine, which are effective at killing the tachyzoite stage parasite, but they are ineffective at removing parasites in the bradyzoites stage (Tenant-Flowers et al., 1991). Bradyzoite cysts may persist for the lifetime of the host; therefore long-term treatment is necessary for those with lowered immune responses. This partial efficiency of the current drug regimen, combined with their serious side effects, stresses the need for the development of novel, effective and safe treatment options.

## A UNIQUE EUKARYOTIC CELL: A LOOK INSIDE *TOXOPLASMA*

### Apical Complex

The name of the phylum apicomplexa refers to the presence of a number of unusual structural elements located at the anterior pole of the organism. This "apical complex" consists of the striking secretory organelles (micronemes, rhoptries and dense granules) and an unusual cylindrical organelle referred to as the conoid. The latter consists of 14 tightly wrapped microtubules and can move with respect to the remainder of the parasite. Two microtubules also extend from

the conoid to the center of the parasite, but their relevance is not understood (reviewed in Morrissette and Sibley, 2002a). (Figure 3). The cargo in the micronemes, rhoptries and dense granules are intimately involved in host cell invasion and the establishment of intracellular life (reviewed in Carruthers and Sibley, 1997). Micronemes are thin vesicular organelles at the apical end of the parasite that discharge their contents as the attachment to a host cell initiates invasion. As invasion continues, proteins are secreted from the rhoptries, the club-shaped organelles derived from Golgi, followed by the release of dense granules contents as invasion concludes.

**Pellicle**

The apicomplexan cell wall, known as the pellicle, consists of three membranes: one plasma membrane and two closely apposed membranes of the inner membrane complex (IMC), which are flattened cisternae that lie directly under the plasma membrane (Ogino and Yondeda, 1966). The IMC is present along the length of the organism, except the extreme anterior end (Dubremetz and Torpier, 1978). Breaks in the pellicle, called micropores, may be active sites of endocytosis since vesicles containing clathrin-like coats have been described in micropores (Nichols et al., 1994).

The formation of the inner membrane complex is not understood, but it appears to be constructed from either one or many flattened vesicles aligned in longitudinal rows joined by sutures (Porchet and Torpier, 1977; Dubremetz and Torpier, 1978; Dubremetz and Elsner, 1979). The IMC is characteristic of the group Alveolata in which apicomplexans belong (Cavalier-Smith, 1993). Freeze fracture data from several apicomplexan organisms have shown the presence of intramembranous

particles (IMPs) organized in parallel rows along the length of the parasite (Aikawa and Beaudoin, 1968) (Figure 3). The rows of IMPs extend along the parasite as single rows interspersed with double rows. Fourier analysis shows the IMPs to have a 32-nm periodicity longitudinally as do microtubule associated proteins (MAPs) (Morrissette et al., 1997).

**Subpellicular network**

The inner membrane complex is supported on its cytoplasmic side by a network of 10nm filaments that extend from the anterior end of the parasite to the posterior just underlying the IMC (Mann and Beckers, 2001). Upon detergent extraction, this network retains the shape of the parasite indicating it plays a role in maintaining cell shape. Two proteins were identified in this network, TgIMC-1 and TgIMC-2 (Mann and Beckers, 2001). These proteins show similarities to articulins, which form the membrane skeletons of protists such as *Euglena* as well as intermediate filament proteins (Morrissette and Sibley, 2002a).

**Microtubules**

The subpelliclular network is in turn associated with the 23 subpellicular microtubules (Morrissette et al., 1997). The microtubules radiate from a ring-like structure at the parasites' anterior end and extend two-thirds down the interior side of the parasite pellicle (reviewed in Morrissette and Sibley, 2002a). They are organized by their association with the apical polar ring and a circular microtubule organizing center (MTOC) in which the minus end of microtubules is attached (Nichols and Chiappino, 1987; Russell and Burns, 1984). These microtubules are thought to give both shape and polarity to the parasites as their depolymerization

causes parasites to be nonpolar, immotile and unable to invade (Hepler et al., 1966; Stokkermans et al., 1996).

**Actin**

A single gene, ACT1, encodes actin in *Toxoplasma*, *Plasmodium* and *Cryptosporidium* which most closely identifies with mammalian β and γ actin (Dobrowolski et al., 1997b). In *Toxoplasma*, actin localized beneath the parasite cell membrane and in clusters scattered within the cytosol. A striking feature of the actin in apicomplexans is that it is found mostly as monomers, making *in vivo* visualization of filamentous actin unusually difficult. Filaments cannot be detected by sedimentation or labeling with fluorescent phalloidin (Dobrowolski et al., 1997b). They can be visualized after treatment with jasplakinolide (JAS), an actin-polymerizing and filament stabilizing agent (Shaw and Tilney, 1999).

**Actin-related proteins**

Comparative genomic and phylogenetic studies reveal that most apicomplexan genomes contain only one conventional actin, yet they each have 8–10 additional actin-related proteins (ARPs) (reviewed in Gordon and Sibley, 2005). Apicomplexans do not have the highly conserved Arp2 or Arp3 proteins, suggesting they lost the Arp2/3 actin polymerization complex during the evolution towards becoming intracellular parasites. Among the ARPs, apicomplexans do have the highly conserved Arp1 protein thought to be part of a conserved dynactin complex, and Arp4 and Arp6 homologues, known to be subunits of the chromatin-remodeling machinery (Gordon and Sibley, 2005). Seven of these actin-like proteins (ALPs) are novel to apicomplexans and show no phylogenetic associations to the known Arp groups; therefore they are likely to have functions specific to this

group of parasites. The actin-binding protein coronin has been described in *Plasmodium*, and contains the characteristic five WD domains and a large C-terminal coiled-coil domain (Tardieux et al., 1998). Homologues of profilin, chronophin, and Adenylate cyclase-associated protein (CAP)-like proteins have been found in apicomplexan parasites (reviewed in Schüler and Matuschewski, 2006).

### Myosin

*Toxoplasma* has eleven of the actin-based motors known as myosins (TgMyoA through TgMyoK) and are found mainly to belong in class XIV amongst four subclasses (reviewed in Foth et al, 2006)). The class XIV myosins in *Toxoplasma* range in size from 93-125 kD and seem to have very different functions in the parasite as they are expressed in a stage-specific manner. TgMyoA is the smallest of the myosins at 93 kD and is the myosin responsible for parasite motility (Meissner et al., 2002). Aside from the six class XIV myosins, there are two myosins in class VI (TgMyoJ and TgMyoK) and one myosin each in class XXII (TgMyoF), XXIII (TgMyoG), and XXIV (TgMyoI) (reviewed in Foth et al., 2006).

## LET'S GET MOVING: SUBSTRATE-DEPENDENT GLIDING MOTILITY

### Movement types and characteristics

*Toxoplasma* locomotion utilizes a combination of three types of motility: circular gliding, upright twirling, and helical gliding (Frixione et al., 1996; Hakansson et al., 1999). Circular gliding involves the crescent shaped parasite lying on the right side, moving in counterclockwise circles. Upright twirling is a result of the parasite remaining attached to a substrate at the posterior end, causing it to move in a

spinning fashion. Helical gliding is substrate dependent and consists of a biphasic movement of a 180º clockwise revolution. This forward movement has been compared to 'corkscrewing' where the parasite must flip over to return to its original face and continue the helical motion. This helical gliding motility is the only type of movement that results in traveling across a substrate and is remarkably fast, occurring at rates of 1-10µm/sec, up to 10 times faster than most ameboid cells (Sibley, 2004).

**The MyosinA motor**

The mechanical power generated centers around one of the five unconventional class XIV myosins found in *Toxoplasma*, TgMyoA. This small myosin (93 kD) is a single-headed, non-processive motor whose conditional removal results in impaired host cell invasion and parasite spreading in cultured cells (Meissner et al., 2002). TgMyoA moves in steps of 5.3 nm with a velocity of 5.2 µm/sec toward the plus end of actin filaments. The protein exhibits unusual structural features that raise questions about its ability to power gliding motility (Herm-Gotz et al., 2002). The class XIV myosins do not follow the TEDS rule (Bement and Mooseker, 1995) in which an acidic or phosphorylatable residue is located at position 16 upstream of the DALAK sequence conserved in myosins (Heintzelman and Schwartzman, 1997; Hettmann et al., 2000). At the normal serine position TgMyoA contains a glutamic acid, which cannot be phosphorylated, implicating a novel mechanism for regulation and activation. The apicomplexan class XIV myosins also have a serine instead of the highly conserved glycine at position 699, the fulcrum point of the lever arm (Kinose et al., 1996). In addition, class XIV myosins do not possess the classical IQ motifs typically used for the binding of light chains. Rather, TgMyoA

contains a conserved stretch of amino acids that represents a very divergent form of this motif. Despite its structural divergences, TgMyoA is capable of binding F-actin in an ATP dependent manner (Heintzelman and Schwartzman, 1999; Hettmann et al., 2000). It has been shown that the tail region of TgMyoA is necessary and sufficient for its localization to the periphery of the parasite. However, unlike some myosins, a pair of arginine residues is responsible for the overall positive charge of the tail (Hettmann et al., 2000). Furthermore, our lab has found that TgMyoA may be phosphorylated, suggesting a potential role in the control of *Toxoplasma* motility (unpublished data).

**The glideosome**

The myosin involved in gliding motility, TgMyoA, resides in a complex with three other proteins: TgMLC1, the myosin-associated light chain and two novel proteins TgGAP45 and TgGAP50 (Gaskins et al., 2004). The myosin XIV motor complex, named the glideosome due to its role in gliding motility, has components that are conserved across the phylum (Baum, et al., 2006; Opitz and Soldati, 2002). Radiolabeling analysis found the four proteins in a ratio of approximately 1:1:1:1 indicating it is a single heterotetramer, consisting of one copy of each of the four proteins (Gaskins et al., 2004). The glideosome localizes to the inner membrane complex of the parasite and is anchored there by TgGAP50, providing the first report of an integral membrane protein acting as a receptor for a myosin motor. TgGAP45 is an essential protein, as attempts to knock-out this protein have proven to be lethal (Gaskins et al., 2004). Little is known about TgGAP45, although in *Plasmodium falciparum*, PfGAP45 is dually acylated with a myristate group and a palmitate group (Rees-Channer et al., 2006). In *Plasmodium*, MLC1 is referred to

as the MyoA tail domain interacting protein (MTIP), and the structure of the MTIP-MyoA tail complex was recently determined (Bergman et al., 2003; Bosch et al., 2006). The glideosome is an essential component for the net movement of the parasite, as force must be transduced via contacts with the host cell to the glideosome, through the IMC to the underlying cytoskeleton. The glideosome is assembled in two stages and will be discussed in the endodyogeny section of this chapter.

**Actin polymerization**

The susceptibility of the parasite to drugs that stabilize or destabilize F-actin as well as molecular-genetic studies confirm that actin nucleation and polymerization are critical for motility (Dobrowolski and Sibley, 1996). As previously mentioned, apicomplexans lack the ARP2/3 complex so they are likely use a variety of actin-binding proteins to orchestrate actin polymerization (reviewed in Schüler and Matuschewski, 2006). The difficulty in detecting actin filaments has impeded the research on motility. Recombinantapicomplexan actin forms filaments that are relatively short in length, measuring around 100 nm or an average of 50 protomers only (Schmitz et al., 2005). Actin filaments can be visualized after treatment with jasplakinolide (JAS), an actin-polymerizing agent. However, the polymerization achieved from high doses of the drug has been shown to inhibit motility and invasion (Shaw and Tilney, 1999). Conversely, low doses of JAS increase the speed of motility and reverse the direction of motion, possibly due to the random orientation of the newly formed filaments (Wetzel et al., 2003).

Two actin monomer-sequestering proteins have been identified in *Toxoplasma*, Actin-depolymerizing factor (ADF)/cofilin and toxofilin, suggesting these may play a

role in maintaining most actin in a monomeric form (Allen et al., 1997; Poupel et al., 2000). The ADF/cofilin homologue is probably involved in severing of filaments, and may contribute to the instability of actin filaments (Allen et al., 1997). Toxofilin, an actin-sequestering protein, may play a role in maintaining the large fraction of globular actin (Poupel et al., 2000). It is hypothesized that the actin polymerization process is highly dynamic, involving the continuous assembly and disassembly of very short filaments underlying the plasma membrane. These filaments interact with myosin, partially providing the necessary mechanical force for gliding motility.

**Plasma membrane proteins**

Gliding motility is associated with the discharge of adhesive proteins (MICs) from micronemes into the parasite plasma membrane. MIC secretion is regulated by intracellular calcium levels, causing them to bind to host-cell receptors, which contributes to attachment, motility, and invasion. MICs are thought to mediate interactions between the parasite and host surfaces. During invasion, a "tight junction" is formed between parasite and host-plasma membrane, which translocates toward the rear of the parasite via interactions between some of the MIC cytoplasmic tails and a cortical parasite actomyosin system discussed below. Most MIC proteins are proteolytically cleaved by the rhomboid protease microneme protein protease 1 (MPP1), which is responsible for intramembrane proteolytic cleavage (Dowse and Soldati, 2005). This event leads to the release of the MICs from the parasite surface, a process that is essential for invasion of apicomplexans.

**Gliding Motility**

Gliding motility is dependent on an actin-myosin interaction located between the plasma membrane and the inner membrane complex (IMC) (Figure 4). Motility is blocked by depolymerizing actin filaments with cytochalasin D, as well as the myosin ATPase inhibitor butanedione monoxime, indicating the importance of actin-myosin interactions (Dobrowolski and Sibley, 1996; Dobrowolski et al., 1997a; Meissner et al., 2002). The overall movement of the parasite (reviewed in Soldati and Meissner, 2004) begins with a $Ca^{2+}$ dependent event in which the adhesion protein MIC2, also known as thrombospondin-related anonymous protein (TRAP) in *Plasmodium*, is secreted from the parasite along with the MIC2-associated protein (M2AP) (Sultan et al., 1997; Huynh et al., 2003). On the outside of the parasite, MIC2/M2AP binds to components of the extracellular matrix or to molecules on the surface of the host cell, while the cytoplasmic domain of MIC2 binds to actin via the glycolytic enzyme aldolase, creating a bridge to the actin-myosin system (Jewett and Sibley, 2003; Buscaglia et al., 2003) (Figure 4). The action of TgMyoA and the glideosome moving the actin filaments causes movement of the actin/aldolase/MIC2/M2AP complex. During this process, MIC2 is translocated from the apical pole to the posterior pole through the plasma membrane (Carruthers et al., 2000). As MIC proteins are proteolytically cleaved by MPP1 in the plasma membrane, visible trails are formed behind the parasite (Dowse and Soldati, 2005). This system is conserved among apicomplexan parasites and propels the parasite forward by the backwards movement of the actin via the MIC2 complex powered by the TgMyoA via the glideosome (Kappe et al., 1999) (Figure 4).

## GETTING IN: HOST CELL INVASION

### Overview

Apicomplexan parasites infect a variety of cell types, although they share the same mechanism for motility and invasion. For some parasites it is very specific. For example, *Cryptosporidium* can only infect enterocytes of intestines, while *Toxoplasma* can infect any nucleated cell. Whereas bacterial pathogens can easily enter certain cells by induced phagocytosis, this task is much more challenging for the considerably larger protozoan parasites. Most intracellular parasites enter through host-mediated processes, but apicomplexan parasites use the active form of gliding motility to actively penetrate cells.

### Host cell recognition and attachment

Host cells are susceptible to invasion based on their surface receptors, as parasite association with these receptors is critical. Unlike phagocytosis, parasite entry apparently occurs independent of host cell processes and without any obvious alterations to the host cell cytoskeleton (Lovett et al., 2002 and 2003). Invasion is extremely fast, occurring in approximately 15 to 20 seconds and the attachment process utilizes two events: conoid protrusion at the apical end of the parasite and the induced secretion of microneme contents regulated by a calmodulin-like dependent protein kinase (Keeley and Soldati, 2004; Kieschnick et al., 2001). The spiral counterclockwise array of microtubules of the conoid are believed to penetrate the host cell to facilitate invasion (Morrissette and Sibley, 2002a).

### Microneme and rhoptry secretion

Microneme secretion is closely regulated by a calcium-mediated release pathway (Sibley, 2003). Proteins stored within the microneme are discharged through the apical end of the parasite surface, and then translocated along the surface of the parasite. These proteins are moved via the actin-based motility system described as the capping model, where they are eventually cleaved off at the posterior end of the parasite, forming trails behind the gliding parasite (Keeley and Soldati, 2004).

The rhoptries also release their contents during the process of invasion, contributing to the formation of the vacuole in which the parasite will reside and releasing components that affect the host cell (Hakansson et al., 2001; Bradley et al., 2005). Rhoptry proteins include adhesins, proteases and other secretory proteins (Zhou et al., 2007). ROP2 is one such protein that traffics to the vacuole to mediate association of host cell endoplasmic reticulum and mitichondria, as is the GPI-anchored protein Pf34 in *Plasmodium* which localizes to detergent-resistant domains in the rhoptries (Sinai and Joiner, 2001; Proellocks et al., 2007).

**Host cell entry and vacuole formation**

By entering the confines of a host cell, the parasite guarantees itself a readily available pool of nutrients as well as a method for avoiding the host cell's immune defense. Upon entry into the host cell, the parasites form a protective membrane called the parasitophorous vacuole membrane (PVM) which is formed from the invagination of host-cell plasma membrane combined with proteins from the rhoptries. This newly formed membranous structure does not contain integral membrane proteins from the host cell including the soluble N-ethylmaleimide-sensitive factor (SNARE) protein. The lack of this protein on the outside of parasite

vacuoles may be partly responsible for providing resistance to the fusion of lysosomes and acidification, and therefore guaranteeing parasite survival within the host cell (Keeley and Soldati, 2004). Alternatively, it has been demonstrated in *Plasmodium* that host plasma membrane proteins found in detergent resistant domains (DRMs) are incorporated into the PVM (Lauer et al., 2000). Once safely protected inside the vacuole, parasites replicate using mechanisms to exert control over host cell organelles (Sinai and Joiner, 2001).

## WITHIN THE HOST CELL: PARASITE REPLICATION AND ESCAPE

### Overview

Once the vacuole has formed, the parasite is ready to begin replicating. Dense granules are the third set of organelles that secrete their contents following the micronemes and rhoptries. Some of the contents include dense granule (GRA) proteins that are soluble when in the organelles, but become inserted into membranes once expelled (Karsten et al., 1998; Lecordier et al., 1999; Mercier et al., 1998). GRA3 has been proposed to act as a pore-forming complex in the PVM, since the PVM is a porous structure with a size exclusion of approximately 1.3 kD (Ossorio et al., 1994; Schwab et al., 1994).

### Aquiring the building blocks

These pores may be formed by dense granule proteins, which may facilitate the acquisition of purines in the form of host cytosolic ATP since *Toxoplasma* is auxotrophic for purine biosynthesis (Perotto et al., 1971; Schwartzman and Pfefferkorn, 1982). The parasites hydrolyze ATP into adenosine for purine salvage instead of utilizing the host ATP as an energy source. *Toxoplasma* requires

tryptophan and other essential amino acids, as well as a carbon source such as glucose for growth (Pfefferkorn, 1984; Fulton and Spooner, 1960). The mitochondria and endoplasmic reticulum of the host cell are also recruited to the PVM to possibly facilitate lipid transfer to the vacuole (Porchet-Hennere and Nicolas, 1983; Sinai et al., 1997; Trotter and Voelker, 1994).

**Cholesterol acquisition**

*Toxoplasma* is dependent on host cell cholesterol in the membrane to initiate invasion and trigger organelle discharge (Coppens and Joiner, 2003). Once in a vacuole within a host cell, the PVM has been found to contain cholesterol from the host cell plasma membrane. Cholesterol plays many roles in *Toxoplasma*, however the parasites cannot synthesize cholesterol *de novo* and rely upon the acquisition of low-density-lipoprotein (LDL) from the host cell (reviewed in Coppens et al., 2000). In mammalian cells, free cholesterol must be esterified in the endoplasmic reticulum before incorporation into lipid droplets (Liscum and Munn, 1999). The parasite internalizes free cholesterol and presumably directs the sterol to the parasite ER for esterification and subsequent storage in lipid droplets (Coppens et al., 2000). The GTPase Rab5 augments acquisition of host cell cholesterol by intracellular parasites, increases formation of lipid droplets and accelerates parasite growth rate (Robibaro et al., 2002).

**Endodyogeny**

The replication process for *Toxoplasma* is called endodyogeny and it is has been morphologically characterized by electron microscopy as well as real-time fluorescent microscopy (van der Zypen and Piekarski, 1967 and 1968; Striepen et

al., 2007). The beginning of endodyogeny starts in the middle of the cell where a rudimentary conoid and apical polar ring are formed, followed by other apical organelles such as rhoptries and micronemes (Figure 5) (Hu et al., 2002). Two IMC membranes are possibly formed from the Golgi complex, which will soon be the daughter cell IMC. The plastid-like organelle known as the apicoplast, the single mitochondrion, and the nucleus divide between the daughter cells as the inner membrane complex extends longitudinally (Black and Boothroyd, 2000). The daughter cells continue to grow until eventually the mother cell IMC disintegrates and the mother cell plasma membrane is used to form new daughter cell plasma membranes. A cleavage furrow is initiated at the anterior end which leaves the posterior end attached while the parasites continue to replicate. This attachment is what causes the rosette pattern of parasite replication in which the anterior ends are always pointed outward. This organization allows parasites to be able to exit the host cell at any point during intracellular growth if necessary.

During endodyogeny, the glideosome is assembled in two stages. First, TgMyoA, TgMLC1, and TgGAP45 associate in the cytosol as the protoglideosome, while TgGAP50 is inserted into the parasite ER and transported with the IMC of daughter cells (Gaskins et al., 2004). Once daughter cell IMC becomes mature IMC, TgGAP50 associates with the protoglideosome, and assembly of the glideosome is complete (Gaskins et al., 2004).

**Egress**

As part of the lytic cycle, *Toxoplasma* replicates inside a host cell until the number of parasites reach approximately 64-128, and the host cell is unable to support the size of the vacuole. The parasites have the ability to sense when the

host cell is under stress or dying so they can evacuate, or egress, in order to find new host cells to invade and continue their life cycle. The host cell plasma membrane becomes permeable two to three minutes prior to egress and it was demonstrated that the ensuing ionic change in host cytoplasm, specifically the loss of cytoplasmic potassium, actually triggers parasite egress (Moudy et al., 2001). Treatment with the ionophore nigericin, which selectively causes efflux of potassium from the cell without the need for permeabilization, effectively causes intracellular parasites to exit their host cell and is dependent on phospholipase C activity (Fruth and Arrizabalaga, 2007).

## THE PROBLEM: IDENTIFYING THE MECHANISMS OF GLIDEOSOME FUNCTION

### Overview

Parasite motility is key to infection of hosts. If *Toxoplasma* was not motile, Toxoplasmosis would not ensue, just as if *Plasmodium* was unable to migrate and invade, malaria would not be a worldwide problem. The intricate details of how motility occurs have not been elucidated, but it is known that an actin-myosin based system is responsible. The glideosome is at the heart of this operation holding the key myosin, TgMyoA, required for motility. Three other proteins make up this complex, so one must assume that their regulation and function play a role in the function of TgMyoA. This is the challenge: to understand the mechanisms and regulation of the underlying gliding motility system in apicomplexan parasites.

### Importance of integral membrane proteins

TgMyoA can attribute its ability to move along actin filaments to the integral membrane protein TgGAP50. TgGAP50 needs to be anchored in the inner

membrane complex to allow TgMyoA to transduce force and move along the substrate. Integral transmembrane proteins have many functions, acting as transporters, ion channels, enzymes, or receptors; however, TgGAP50 is the first evidence of an integral membrane protein acting as a receptor for myosin (Gaskins et al., 2004).

**Methods of anchoring integral membrane proteins**

Transmembrane proteins are often restricted in their movements even though a lipid bilayer is highly fluid. One might expect that these embedded structures would be relatively free to float in the plane of the membrane. For some transmembrane proteins this is the case; however, for others mobility is limited. Proteins exposed at the interior face of the plasma membrane of some cells are tethered to cytoskeletal elements such as actin filaments or to components of the extracellular matrix like collagen. Integral membrane proteins cannot pass through the tight junctions found between some cells as a way of keeping them compartmentalized.

Lipid microdomains or rafts in biological membranes that have a high sphingolipid and cholesterol content have also been described to contain protein such as GPI-anchored proteins (reviewed in Pike, 2004). Unlike the loosely packed, disordered phospholipids present in the bulk of membranes, raft lipids are organized in a tightly packed, liquid-ordered manner (Simons and Ikonen, 1997). Although the majority of integral membrane proteins are excluded from these domains, certain transmembrane proteins can reside in rafts (reviewed in Pike, 2004).

**Targeting of integral membrane proteins**

Membrane proteins can be sorted along the secretory pathway by elements present in the cytosolic, luminal or transmembrane domains. Determinants in transmembrane domains (TMDs) are presumed to influence sorting by interacting with lipid microdomains of a defined composition. Glycosyl transferases in the Golgi apparatus are believed to be retained there due to the interaction of their short TMD with the Golgi bilayer, which is thinner in size than the plasma membrane (Bretscher and Munro, 1993). It is also believed that the apical proteins in polarized epithelial cells are separated from basolateral proteins because of the interaction of apical proteins with lipid microdomains or rafts (Simons and Ikonen, 1997). For transmembrane proteins that have an amino-terminal signal sequence, the first transmembrane domain acts as the first signal sequence, targeting the protein to the ER membrane. Another integral membrane protein identified in *Toxoplasma*, PhiL1, does not have a transmembrane domain or lipid modifications (Gilk et al., 2006). Little is known about the mechanics of transmembrane protein topology and folding in *Toxoplasma*.

## Figure Legends

**Figure 1. The *Toxoplasma* life cycle.** Unsporulated oocysts are shed in cat feces which then sporulate in the environment and become infective. The sporulated oocysts infect humans through contaminated food, water and soil and infect animals or birds through contaminated feed, water and soil. The intermediary hosts include livestock and many other mammals such as sheep, goats, rats and birds, which may also infect each other through tissue cysts. Humans are infected by consuming cysts in tissues of intermediate hosts (raw and undercooked meat). Unborn babies are infected through tachyzoites transmitted through the placenta. Cats can be infected through cysts in the tissue of intermediate hosts. (Modified from Du, 2004).

**Figure 2. The *Toxoplasma* lytic cycle.** The first event is attachment of *Toxoplasma* to its host cell (step 1). As the parasite glides across the surface, it is reoriented to make contact with the host surface at its apical end and to initiate invasion (step 2). During the invasion event, the parasitophorous vacuole (PV) is formed. After the parasite enters its host, it stops moving and the vacuole closes at its posterior end by pinching off via a fission pore. The newly formed PV immediately recruits host mitochondria and portions of the host ER to assist with intracellular growth (step 3). The parasites undergo several rounds of replication (step 4) until they receive a signal for egress (step 5). Host cell egress is typically a destructive process that lyses the host cell and releases the parasites which quickly invade neighboring cells to complete the cycle (modified from Black and Boothroyd, 2000).

**Figure 3. The unique organelles and cytoskeleton of apicomplexan parasites.** (A) *Toxoplasma* subcellular structures involved in gliding motility and invasion (adapted from Soldati and Meissner, 2004). (B) Layers of *Toxoplasma* ultrastructure imaged by transmission electron microscopy (conoid), scanning electron microscopy (subpellicular network) and freeze fracture (IMC) (images from John Heuser and Naomi Morrissette).

**Figure 4. Substrate-dependent gliding motility model.** Apicomplexan motility model adapted from Baum et al., 2006) includes glideosome (GAP50, GAP45, MLC1, MyoA) associated with the IMC, moving along actin filaments. Treadmilling of actin is controlled by profiling and ADF/Cofilin. Actin associates with an aldolase tetramer which binds the adhesion (MIC2) that passes through the PM to make host cell contacts. Cleavage of MIC2 occurs within the plasma membrane and parasite movement is achieved.

**Figure 5. Diagram of endodyogeny.** As a parasite begins to divide, two inner membrane complexes begin to form in the middle of the cell from what appears to be a conoid and microtubule-organizing center (polar ring). As the IMC extends from these structures, the nucleus (N) and mitochondrion (Mitoch.) divide into these membranous outlines. Nascent apical organelles (NO) develop within the anterior poles as the daughter cells grow. The entire cytoplasm is eventually divided between the daughters and the IMC of the mother dissolves. A cleavage furrow divides the cells at the anterior pole and this division continues down the length of the cells until it reaches the posterior end, where it may leave a residual body connecting the two daughters. (adapted from Black and Boothroyd, 2000).

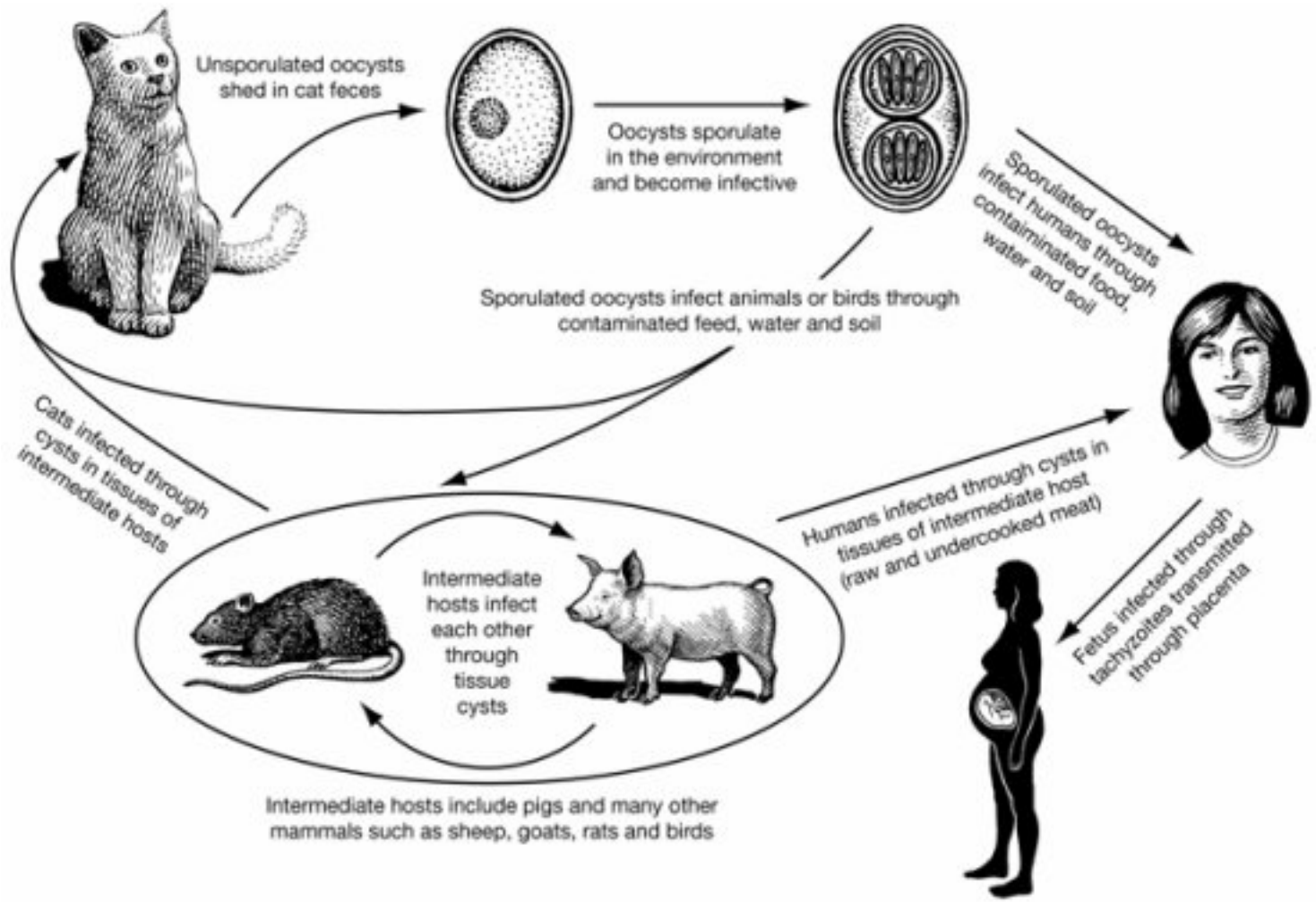


**Figure 1. The *Toxoplasma* life cycle.** (Du, 2004)

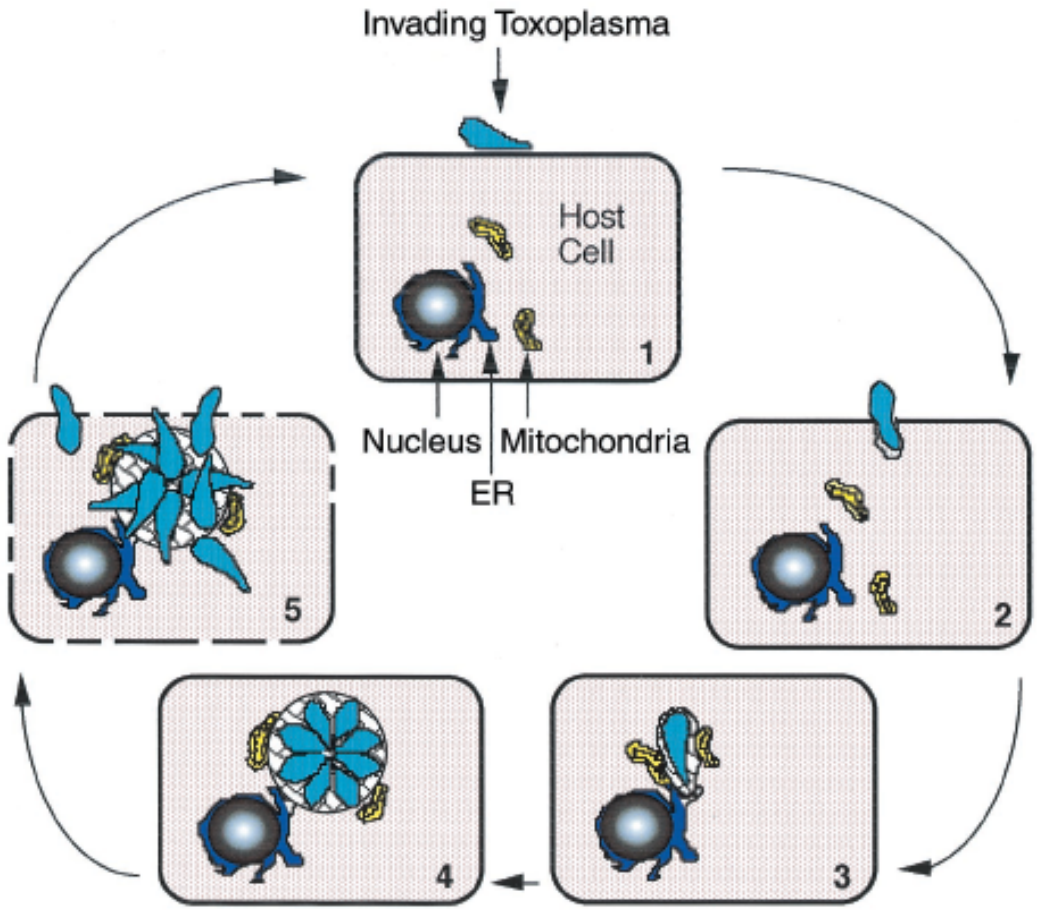


(Black and Boothroyd, 2000).

**Figure 2. The *Toxoplasma* lytic cycle.**

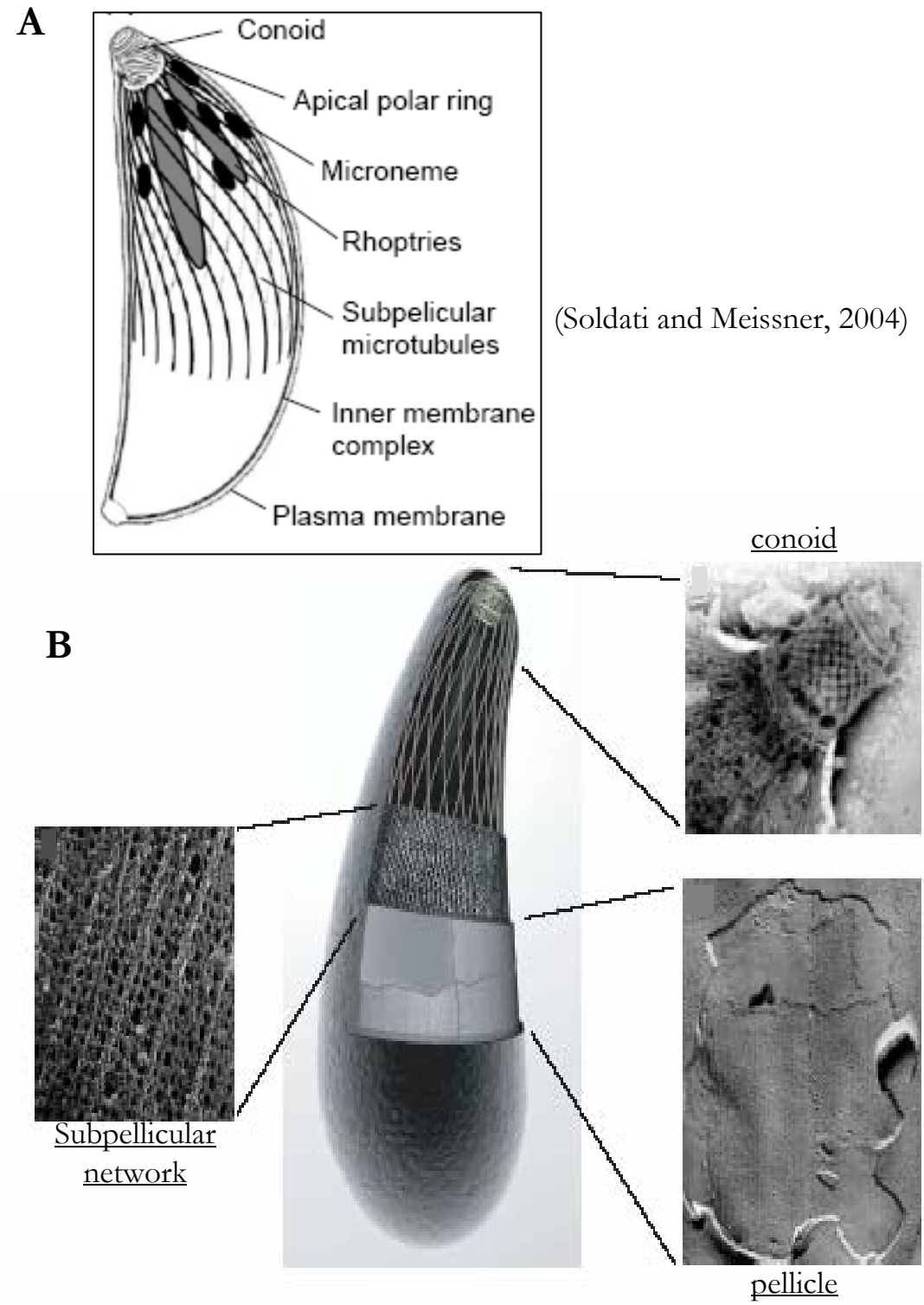


**Figure 3. *Toxoplasma* ultrastructure.**

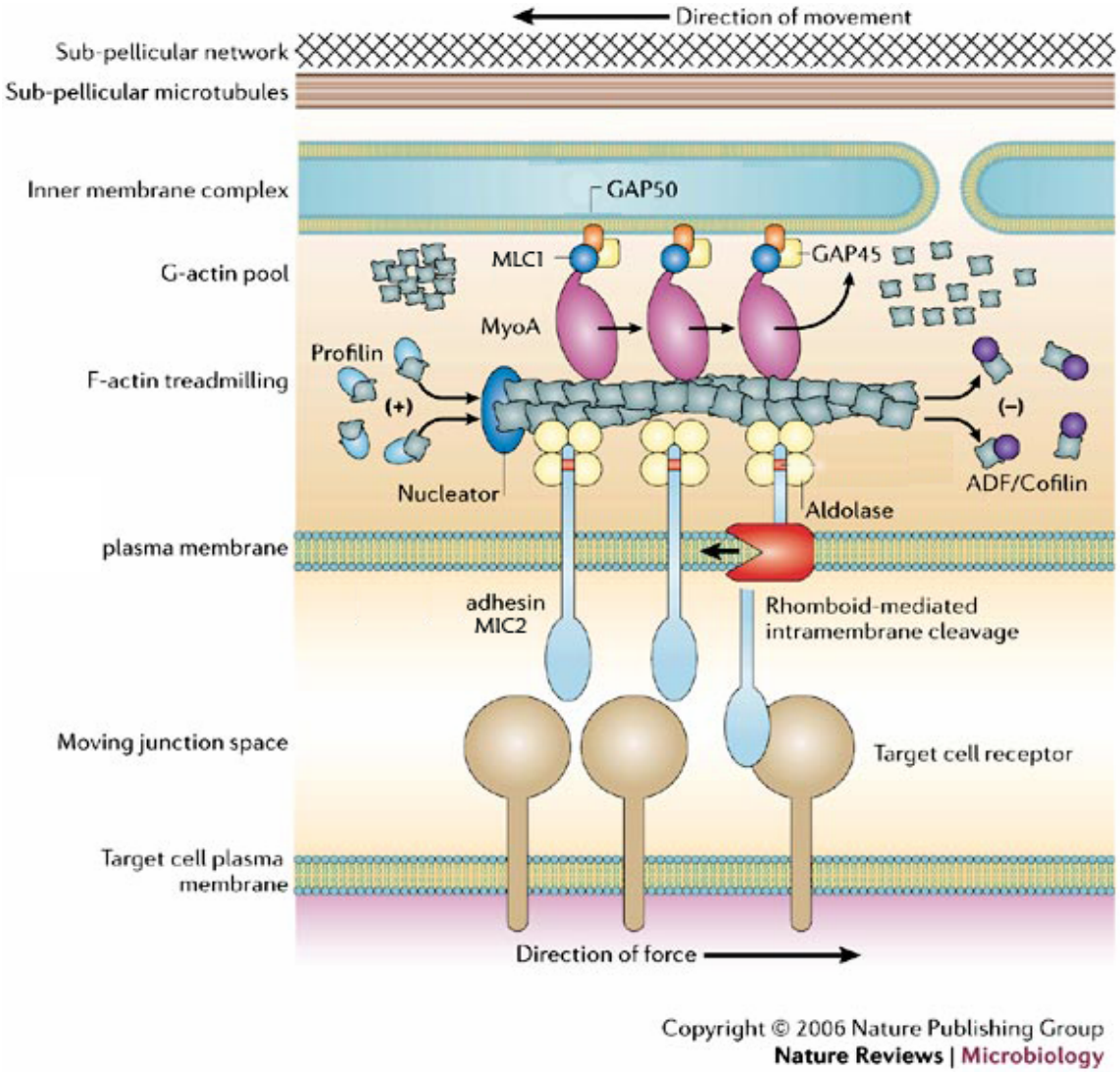


**Figure 4. Substrate-dependent gliding motility model.**

**(Baum et al., 2006)**

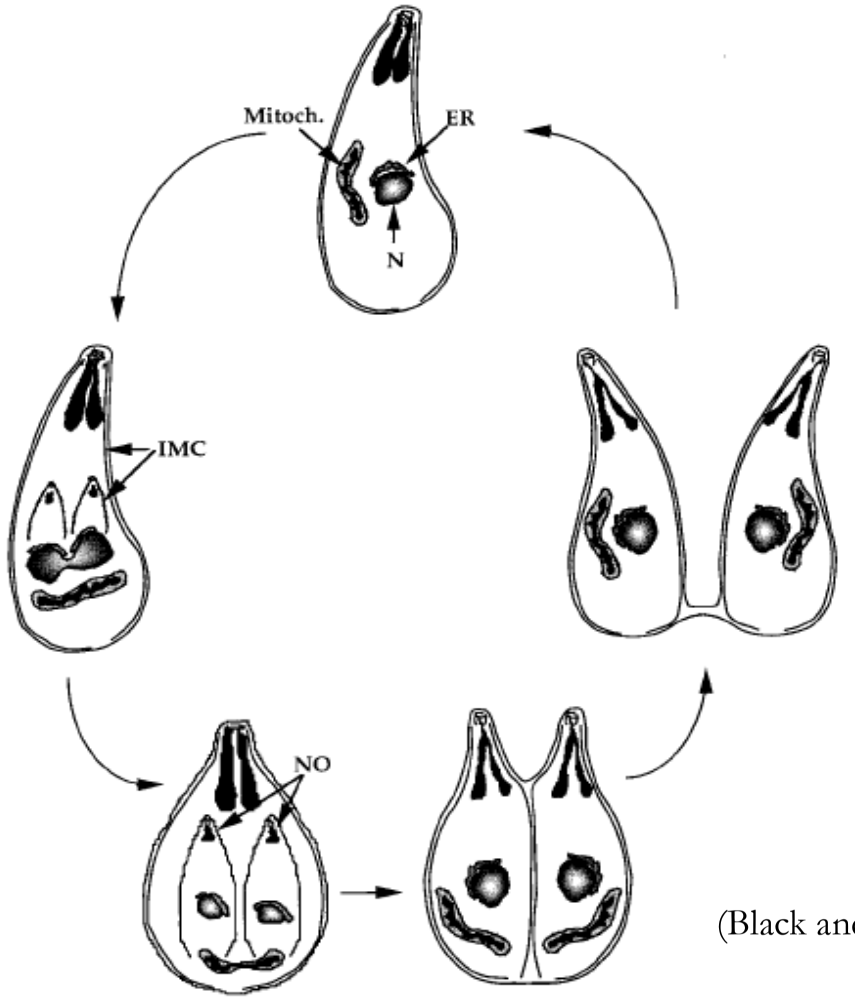


(Black and Boothroyd, 2000).

**Figure 5. Diagram of endodyogeny.**

**CHAPTER II**

# IMMOBILIZATION OF THE TYPE XIV MYOSIN COMPLEX IN *TOXOPLASMA GONDII*

Terezina M. Johnson, Zenon Rajfur, Ken Jacobson, Con J. Beckers

Molecular Biology of the Cell Vol. 18, Issue 8, 3039-3046, August 2007

Submitted January 18, 2007; Revised May 14, 2007; Accepted May 18, 2007

## Abstract

The substrate-dependent movement of apicomplexan parasites like *Toxoplasma gondii* and *Plasmodium* sp. is driven by the interaction of a type XIV myosin with F-actin. A complex containing the myosin-A heavy chain, a myosin light chain and the accessory protein GAP45 is attached to the membranes of the inner membrane complex through its tight interaction with the integral membrane glycoprotein GAP50. In order for the interaction of this complex with F-actin to result in net parasite movement, it is necessary that the myosin be immobilized with respect to the parasite and the actin with respect to the substrate the parasite is moving on. We report here that the myosin motor complex of *Toxoplasma* is indeed firmly immobilized in the plane of the parasite inner membrane complex. This does not appear to be accomplished by a direct interaction with other cytoskeletal elements of the parasite. Cholesterol does appear to be important for immobilization of the motor complex. Furthermore, both the motor complex and the cholesterol are found in detergent-resistant membrane domains that encompass a large fraction of

the inner membrane complex surface. The observation that the major myosin motor complex of *Toxoplasma* is immobilized within this cholesterol-rich membrane is likely to extend to closely related pathogens like *Plasmodium* as well as other eukaryotes.

## Introduction

Members of the phylum Apicomplexa are pathogenic protozoan parasites of humans and animals. They include *Plasmodium falciparum*, the causative agent of malaria, and *Toxoplasma gondii*, which causes severe disease in immunocompromised humans and congenital disease in infants (Dubey, 1994). The life cycle of apicomplexan parasites alternates between a motile extracellular phase during which they do not replicate and a non-motile phase within host cells where growth and replication occurs. Their ability to invade host cells is therefore critical for their survival. Their ability to egress from dying host cells after multiple rounds of replication is equally important, however, as this ensures survival and spread of the parasites. Both invasion and egress are dependent on active motility of the parasite (Meissner et al., 2002). The type of motility seen in apicomplexan parasites is quite unusual as it does not require typical locomotive organelles, such as filipodia or flagellae, but instead involves a unique substrate-dependent type of movement called gliding motility.

Gliding motility is dependent on the interaction of actin filaments and the type XIV myosin TgMyoA located in the parasite pellicle between the plasma membrane and inner membrane complex (IMC) (Heintzelman & Schwartzman, 1999; Meissner et al., 2002) (Supplemental Figure 1). Depolymerization of the actin filaments with cytochalasin D or inhibition of myosin ATPase activity with butanedione monoxime

blocks motility and host cell invasion completely, indicating the importance of actin-myosin interactions for the survival of the parasite (Dobrowolski and Sibley, 1996; Dobrowolski et al., 1997a; Meissner et al., 2002). Direct evidence for the essential role of TgMyoA in *Toxoplasma* motility and survival has come from elegant experiments in which expression of the MyoA gene was down-regulated, resulting in prominent defects in parasite motility and survival (Meissner et al., 2002).

In order for the interaction of actin with myosin to result in net movement of a parasite with respect to its substrate it is essential that one is immobilized with respect to the parasite and the other with respect to the substrate. For the F-actin in *Toxoplasma* and *Plasmodium* this appears to be accomplished through its interaction with the glycolytic enzyme aldolase which, in turn, interacts with MIC2/TRAP (Supplemental Figure 1). As the latter are cell surface adhesins that can mediate parasite attachment to host cells or extracellular matrix components, the actin-MIC2/TRAP-substrate interactions appear to be sufficient for immobilization of parasite F-actin filaments. (Jewett and Sibley, 2003; reviewed in Soldati and Meissner, 2004).

TgMyoA, on the other hand, has recently been shown to be associated with the IMC in a hetero-oligomeric complex called the glideosome (Gaskins et al., 2004). In addition to TgMyoA, this complex consists of a myosin light chain (TgMLC1) (Herm-Gotz et al, 2002) and two novel proteins, TgGAP45 and TgGAP50 (Gaskins et al., 2004). A similar complex has also been described in *Plasmodium* (Bosch et al., 2006) and is also found associated with the IMC (Bergman et al., 2003; Bosch et al., 2006). Whereas TgGAP45 appears to be an essential protein, its exact function in glideosome activity or membrane anchoring is not clear. TgGAP50, on the other hand, is an integral membrane glycoprotein of the IMC membranes and is essential

for anchoring of the glideosome in those membranes (Gaskins et al., 2004). These proteins that comprise the glideosome are conserved across the apicomplexan phylum indicating a common molecular mechanism for motility (Kappe et al., 1999; Baum et al., 2005).

For net parasite movement to occur it is not sufficient, however, for the glideosome to be merely associated with a membrane. It is also critical that the glideosome is immobilized within the plane of the IMC membrane. Here, we show that the glideosome is indeed immobilized within the plane of the IMC. We have found no evidence for the involvement of other IMC associated proteins in this immobilization. Instead, it appears that the lipid environment in the IMC, and specifically the presence of cholesterol, is an important factor in glideosome immobilization.

## Results

### TgGAP50 is immobilized in the inner membrane complex of *Toxoplasma*

TgGAP50 is an integral membrane glycoprotein that anchors the glideosome to the IMC membrane (Gaskins et al., 2004). In order for net movement to be achieved by the parasite, one would predict that TgGAP50 is immobilized within the plane of this membrane. To test this hypothesis, we used fluorescence recovery after photobleaching (FRAP) to determine the extent to which a functional but fluorescent derivative of TgGAP50, TgGAP50-YFP, is able to move within the plane of the IMC membrane. Intracellular parasites stably expressing TgGAP50-YFP were bleached in small regions at different locations of the IMC membrane. Images taken at 30 second time intervals for up to eight minutes thereafter reveal that TgGAP50-YFP does not migrate into bleached regions, indicating that the protein is

indeed immobilized in intracellular *Toxoplasma* (Figure 1A). In order to determine if TgGAP50 motility is increased when parasites are actually moving, we repeated the same experiments on motile, extracellular *Toxoplasma*. As can be seen in Figure 1B, no diffusion of TgGAP50-YFP was observed in actively moving parasites, indicating that the protein is immobilized within the plane of the IMC in both intracellular and extracellular parasites. As a control, we used a TgGAP45–YFP fusion protein which, unlike TgGAP50-YFP, does not associate with the other members of the glideosome (Supplemental Figure 2). Like wild-type GAP45, however, GAP45-YFP is also associated with the membrane of the IMC due to N-terminal palmitoylation and myristoylation of the protein (Johnson et al., manuscript in preparation). A similar modification has also been described for the protein found in *Plasmodium* (Rees-Channer et al., 2006). FRAP analysis on TgGAP45-YFP demonstrates that the protein is able to diffuse freely along the IMC (Figure 2A). As an additional control, cytoplasmic GFP was transiently expressed in COS7 cells in which fluorescence also recovered after photobleaching (Figure 2A). Further quantitative analysis indicates the recovery time of the TgGAP50-YFP mobile fraction was much slower than those of the controls, showing a diffusion coefficient of 0.019 $\mu m^2/s$ (Figure 2B). On average, TgGAP50-YFP had a mobile fraction of only 16.1% compared to 60.3% and 92.8% for TgGAP45-YFP and cytosolic GFP, respectively (Figure 2B). We did not observe a complete recovery of TgGAP45-YFP, an effect that appears to be due to a substantial fraction of the total protein being bleached. From these data, we can conclude that TgGAP50, and therefore the glideosome, is immobilized within the plane of the IMC.

**Glideosome immobilization does not appear to be a result of protein-protein interactions**

There are essentially two general mechanisms through which immobilization of the glideosome in the plane of the IMC membrane could be accomplished: protein-protein or protein-lipid interactions or a theoretical combination of the two. The glideosome behaves as a ~230 kD protein complex during velocity sedimentation, and radiolabeling analysis found the four proteins in a ratio of approximately 1:1:1:1 indicating it is a single heterotetramer, consisting of one copy of each of the four proteins (data not shown; Gaskins et al., 2004). Interaction of the four known glideosome subunits with other proteins could not be excluded because these interactions could either be generally weak or very sensitive to the lysis and immunoprecipitation conditions used. To test this hypothesis, we subjected parasites to a number of cross-linking reagents or prepared lysates in the presence of a variety of detergents, salts, and a number of potential cofactors. None of these conditions had a reproducible effect on the number and identity of proteins in the glideosome (Supplemental Table 1), suggesting that the glideosome only consists of the four known proteins, TgGAP50, TgGAP45, TgMyoA and TgMLC1. Although the subpellicular microtubules of *Toxoplasma* are located on the opposite side of the IMC, we also tested whether they might play a role in immobilization of the glideosome. Treatment of parasites with the microtubule-disrupting drug oryzalin (Morrissette and Sibley, 2002b) has no effect on anchoring of TgGAP50-YFP (data not shown). Taken together, these data indicate that protein-protein interactions

are unlikely to play an important part in immobilization of the *Toxoplasma* glideosome in the IMC.

**The glideosome is found in detergent-resistant domains of the IMC**

During our exploration of various glideosome solubilization methods, we noticed striking differences in the efficiency of glideosome extraction by different detergents. A variety of detergents, such as β-octylglucoside and CHAPS, solubilized the glideosome proteins efficiently in various buffers and at temperatures between 0 and 37°C. Triton-X100 in Tris-buffered saline (TX100/TBS) also solubilized the glideosome efficiently in the same temperature range. When parasites were subjected to extraction with 1% Triton-X100 in phosphate-buffered saline (TX100/PBS), however, we noted that glideosome proteins were solubilized efficiently at temperatures between 25°C and 37°C but remained insoluble when the extraction was performed at 4°C (Figure 3). To determine if this effect reflected a general property of *Toxoplasma* membranes or membrane proteins, we also tested the behavior of the plasma membrane protein SAG1, the rhoptry protein ROP2, the dense granule protein GRA3, and *Toxoplasma* BiP using a sequential extraction process with TX100/PBS and TX100/TBS (Figure 4A). Contrary to our observations with TgGAP50, extraction of parasites with TX100/PBS at 4°C resulted in the complete solubilization of SAG1, GRA3, ROP2, and BiP (Figure 4B). The membrane skeleton protein IMC1 remained, as expected, completely insoluble under either condition (Figure 4B). These results indicate that the insolubility of TgGAP50 in TX100/PBS on ice reflects a specific property of TgGAP50 and/or the IMC membrane it is embedded in.

To test these possibilities, we extracted parasites at 4°C in either TX100/PBS or TX100/TBS and examined these by light and transmission electron microscopy. As

can be seen in Figure 8A, the subcellular distribution of TgGAP50-YFP is not affected in an obvious fashion by extraction of parasites in TX100/PBS at 4°C whereas it is completely lost upon extraction in TX100/TBS. Analysis by transmission electron microscopy (Figure 5) demonstrates that the plasma membrane and most organellar membranes of the parasite are solubilized efficiently in TX100/PBS. The IMC membrane, however, appears to be largely resistant to extraction by TX100/PBS and can be seen as large sheets of double membranes that are still located adjacent to the underlying cytoskeleton. Extraction of parasites with TX100/TBS, on the other hand, resulted in the complete solubilization of *Toxoplasma* membranes, including the IMC membrane (Figure 5C).

To provide further proof that the detergent-resistant fraction of TgGAP50-YFP is indeed membrane-associated, we subjected this material to isopycnic centrifugation. The TX100/PBS-resistant material was adjusted to 1.6M sucrose, placed underneath a 0.25-1.4M sucrose gradient, and subjected to equilibrium density gradient centrifugation. Whereas the cytoskeletal protein IMC1 and tubulin remained at the bottom of the gradient, TgGAP50 was found exclusively at lower density fractions (density ~1.1M sucrose) indicating that it is present in membranes or lipid-rich structures (Figure 6). TgMyoA, TgGAP45 and TgMLC1 were also found in this fraction, indicating all proteins of the glideosome are similarly immobilized with TgGAP50. When the TX100/PBS-resistant material was incubated in TX100/TBS prior to centrifugation, TgGAP50 and glideosome proteins remained at the bottom of the gradient (data not shown). Taken together with our previous observations, these data support a model in which the *Toxoplasma*

glideosome is immobilized in detergent-resistant domains in the parasites' IMC membranes.

**The presence of cholesterol correlates with the immobilization of glideosome in the IMC membrane**

Detergent-resistant membrane domains (DRMs) in other eukaryotes are thought to be formed by the tight packing of cholesterol and the long and highly saturated fatty acids of sphingolipids, and contain a variety of proteins, including GPI-anchored, acylated, and integral membrane proteins (reviewed in Pike, 2004). To determine if the TX100/PBS-resistant IMC membranes of *Toxoplasma* also contained high concentrations of cholesterol we compared the lipid composition of total parasite membranes and the TX100/PBS-soluble and insoluble fractions by thin layer chromatography (TLC). The extraction efficiency of TgGAP50 was monitored in parallel by immunoblot analysis. As can be seen in Figure 7A, a substantial fraction of the total parasite-associated cholesterol is resistant to extraction in TX100/PBS but is solubilized completely by a subsequent extraction in TX100/TBS. To determine if the TX100/PBS-resistant fraction of cholesterol was indeed associated with the *Toxoplasma* IMC, we labeled parasites prior to extraction with BODIPY-cholesteryl ester (BODIPY-CE), a fluorescent cholesterol derivative that is commonly used as a qualitative tool to describe the subcellular distribution of cholesterol. As a control, parasites were also labeled with BODIPY-phosphatidylcholine (BODIPY-PC) to provide a marker for other parasite membranes.

As has been described previously (Coppens and Joiner, 2003), BODIPY-CE appears to accumulate in the *Toxoplasma* pellicle and in internal organelles that are consistent with the parasite rhoptries (Figure 8A). BODIPY-PC, on the other

hand, was found in membranes throughout the parasite (Figure 8B). Treatment of parasites with TX100/PBS resulted in a complete removal of parasite-associated BODIPY-PC as judged by both TLC analysis (Figure 7C) and fluorescence microscopy (Figure 8B). As we had already described for endogenous cholesterol, TLC analysis revealed that a substantial fraction of parasite-associated BODIPY-CE was retained after extraction in TX100/PBS (Figure 7B). Fluorescence microscopy revealed that this pool of BODIPY-CE was associated primarily with the parasite IMC as judged by the extensive overlap in distribution with TgGAP50-YFP (Figure 8A). A fraction of the fluorescent lipid also appeared to be associated with the extreme apical region of the parasite where TgGAP50-YFP was absent, suggesting this may represent a unique domain of the IMC membrane. When the TX100/PBS extraction was followed by extraction in TX100/TBS both BODIPY-CE and TgGAP50 were completely extracted, confirming that both are indeed associated with membranes (Figure 8A).

It is clear from the above that both cholesterol and the glideosome resist extraction by TX100/PBS and are solubilized efficiently by TX100/TBS. A number of explanations can be offered for these observations. First, the selective retention of both components in the IMC during the initial detergent extraction step could be caused by them being embedded independently in the IMC membrane. An alternative explanation is that both components closely interact with each other, and that the presence of cholesterol is critical for glideosome retention. In order to determine if the presence of cholesterol indeed contributes to the retention of TgGAP50, we analyzed whether the latter was sensitive to the cholesterol-sequestering agent methyl-β-cyclodextrin (mβCD). Short term incubation of intact parasites with mβCD did not affect TgGAP50, presumably because the IMC

membranes are shielded by the parasite plasma membrane. Incubation of TX100/PBS-extracted parasites with mβCD, on the other hand, resulted in the solubilization of TgGAP50 as judged by immunoblotting and fluorescence microscopy (Figure 9). All other members of the glideosome (TgMyoA, TgGAP45, and TgMLC1) were also solubilized in a similar manner as TgGAP50, indicating that the motor itself remains tightly associated to TgGAP50 in the IMC. Examination of the mβCD-treated parasites by electron microscopy revealed that cholesterol depletion actually results in the complete removal of the TX100/PBS-resistant IMC membranes (Figure 5). The effect of mβCD on TgGAP50 solubilization was due to its ability to sequester cholesterol as it was prevented by the addition of free cholesterol (Figure 9A). These observations indicate that cholesterol is clearly a very important structural element of the IMC membrane and is critical for the retention of the glideosome in that membrane.

## Discussion

Motility of *Toxoplasma* and other apicomplexan parasites depends on the activity of the MyoA myosin heavy chain and the associated myosin light chain-like protein MLC1, both of which are found in a complex with GAP45 and GAP50 (Gaskins et al., 2004). A general conservation of the glideosome components has been demonstrated between at least six apicomplexan genera, indicating that this complex plays an essential role in the invasion and motility of these protozoan parasites (Bergman et al., 2003; Gaskins et al., 2004). This notion is supported by the observation that *Toxoplasma* is not viable after the individual disruption of three glideosome subunits, TgMyoA, TgGAP45, and TgGAP50 (Meissner et al., 2002; Gaskins et al., 2004).

We have demonstrated previously that the integral membrane protein TgGAP50 anchors the glideosome complex in the *Toxoplasma* inner membrane complex (IMC), which consists of large flattened cisternae that underlie the parasite plasma membrane (Gaskins et al., 2004). It was not clear, however, if and how TgGAP50 and therefore the entire glideosome was immobilized in the plane of the IMC membrane, a prerequisite for net movement of the parasite with respect to its substrate. We have demonstrated here that TgGAP50 is indeed immobilized within the plane of the IMC and that the presence of cholesterol in the IMC membrane appears to play a role in this process.

We determined the extent of TgGAP50 immobilization in the plane of the IMC membranes by FRAP analysis of the fusion protein TgGAP50-YFP, in which YFP is attached to the short C-terminal cytoplasmic tail of TgGAP50. This fusion protein appears to be fully functional in that it is indistinguishable from TgGAP50 in its targeting to the IMC and its association with TgMyoA, TgMLC1, and TgGAP45 (Gaskins et al., 2004). Judged by our FRAP analysis, TgGAP50 does not diffuse freely within the plane of the IMC membranes. This is not the result of general diffusion barriers within the parasite or the IMC membrane, as proteins associated with the IMC membrane through acylation (TgGAP45-YFP) are able to recover within seconds. This observation proves that TgGAP50 is effectively immobilized in the IMC membrane. We considered a number of explanations for this observation. Stable cytoskeletal structures have not been described on the side of the IMC where the glideosome is located, the side facing the parasite plasma membrane or in the IMC lumen, where the bulk of TgGAP50 resides. The side of the IMC facing the cytoplasm of the parasite, on the other hand, is associated with a filamentous membrane skeleton and 23 subpellicular microtubules (Mann et al., 2001). We

tested whether the immobility of TgGAP50 was due to its interaction, or that of another glideosome subunit, with other proteins in the IMC or the associated membrane skeleton or microtubules. The use of a number of membrane-permeable and membrane impermeable chemical cross-linkers in various buffer conditions and the inclusion of a variety of potential co-factors such as ATP, GTP, calcium, and magnesium, did not alter the protein composition of the immunoprecipitated glideosome. Additionally, treatment of parasites with oryzalin, a microtubule destabilizing drug, does not alter the extraction properties of the glideosome, indicating a tight association with the IMC despite the lack of microtubule presence. These findings suggest that glideosome immobilization is not likely to be caused by its direct interaction with other proteins in the *Toxoplasma* IMC or cytoskeleton. If an additional protein is involved, these interactions may be very weak or transient and therefore unlikely to be strong enough to confer anchoring within a membrane. Alternatively, an interacting protein may be large or insoluble, thereby preventing the effective crosslinking and immunoprecipitation with TgGAP50.

In doing these various experiments, we noted that solubilization of the glideosome from the IMC by the detergent Triton-X100 is temperature and buffer-dependent. The glideosome was efficiently extracted from the IMC membrane using TX100 in PBS at room temperature but not on ice. This property was reminiscent of the detergent-insoluble domains or rafts described in other eukaryotes (Brown and Rose, 1992). Like the detergent-resistant structures observed by those authors, the detergent-resistant IMC fraction of *Toxoplasma* also consists of membrane-like structures. These differ from detergent insoluble membranes in other systems, however, in that their density is substantially higher (Figure 6). We

have found that this is not due to associated cytoskeletal proteins and is therefore probably a result of a higher protein/lipid ratio in the IMC membranes proper as compared to DRMs in other eukaryotes. Interestingly, the temperature-dependent solubilization of the glideosome observed in TX100 in phosphate-buffered saline is not observed using TX100 in Tris-buffered saline. In this regard, the IMC membrane appears to be similar to membrane domains found in myelin. These domains were also found to be insoluble in TX100 in phosphate buffer but were solubilized efficiently by TX100 in a Tris-based buffer (Arvanitis et al., 2005) and, like we observed for the IMC membrane, the TX100/phosphate-resistant myelin fraction was found to have a higher density than typical DRMs. It is interesting to note in this context that both the *Toxoplasma* IMC and myelin are composed of closely apposed membranes, suggesting that phosphate may play a role in their association.

Detergent-insoluble domains in other eukaryotes are characterized by a relative enrichment of cholesterol and sphingolipids (Simons and Ikonen, 1997). Analysis of the lipid composition of the TX100-resistant IMC membrane reveals that it too is enriched in cholesterol. The importance of cholesterol in the integrity of the IMC membrane and immobilization of the glideosome is illustrated by two observations. Treatment of the IMC with mβCD results in nearly complete disruption of the IMC membrane and the complete solubilization of the glideosome, without affecting the IMC-associated cytoskeleton. Sphingolipids, on the other hand, do not appear to be important for glideosome immobilization in the IMC membrane as this is not affected by sphingomyelinase treatment (data not shown). We have found that glideosome is enriched in these DRMs in the IMC, but we cannot conclude that this mechanism is fully responsible for anchoring TgGAP50.

Although other factors are likely to contribute to the immobilization of the glideosome in the IMC membrane of *Toxoplasma*, it is clear from our data that the presence of cholesterol plays a supporting role. *Toxoplasma* is a cholesterol auxotroph (Coppens et al., 2000) and appears to acquire this lipid from its host cell through the hijacking of endocytic host cell organelles carrying LDL particles. These are delivered to the parasitophorous vacuole surrounding the intracellular parasites from which they are taken up by the parasite. Once inside the parasite, cholesterol has many functions. It is found in lipid bodies (Murphy, 2001), rhoptries (Foussard et al., 1991; Vial et al., 2003), and the IMC (Coppens and Joiner, 2003). Treatment of parasite with progesterone resulted in the depletion of cholesterol from the rhoptries and lipid bodies. These parasites still exhibited IMC labeling with filipin, a cholesterol binding agent, indicating cholesterol is not depleted from this structure by progesterone treatment (Coppens and Joiner, 2003). When we attempted to extract cholesterol from intact parasites with mßCD, we also found that it was impossible to remove this lipid from the IMC. This particular observation is most likely due to the failure of mßCD to gain access to the IMC membrane in intact parasites. Both observations made it impossible for us to assess the effect of cholesterol depletion on motility of the intact parasite. When we first removed the parasite plasma membrane with TX100/PBS, however, mßCD extracted cholesterol efficiently from the TX100/PBS-resistant IMC membranes and resulted in a complete solubilization of the glideosome.

It is clear from these observations that cholesterol is involved in immobilization of the *Toxoplasma* glideosome in the IMC membrane. It is equally clear, however that this raises a number of new questions. Chief amongst these is whether glideosome immobilization involves a direct interaction of cholesterol and TgGAP50,

or whether it is due to the effect of cholesterol on the IMC membrane per se. As TgGAP50 is an abundant protein in the IMC membrane it is possible that the monomers are packed so closely together that a lattice of TgGAP50 molecules is created and stabilized by cholesterol. Removal of the cholesterol would then render the lattice unstable and prone to disruption by detergents. The possibility that the actual lipid composition, and specifically the presence of cholesterol, turns the IMC membrane into an unusually rigid structure that immobilizes TgGAP50 cannot be excluded at this point either, although it is unlikely that this is the only factor involved.

A second issue that needs addressing in this context is the organization of the detergent-resistant fraction of the IMC membrane. In other experimental models, these domains have been estimated to range in size from 40 to >500 nm (Prior et al., 2003; Brown and Lyles, 2003; Gupta and DeFranco, 2003), and to constitute up to 35% of a plasma membrane (Prior et al., 2003) depending on the cell type and isolation method used (Lucero and Robbins, 2004). Fluorescence and electron microscopy indicate that the overall appearance of the IMC membrane is not grossly affected by extraction in TX/PBS (figures 5 and 8). It is therefore possible that this membrane is detergent-resistant in its entirety. It can also be, however, that the IMC membrane resembles packed ice in that it consists of numerous smaller detergent-resistant domains that float as a closely-packed aggregate in an otherwise detergent-sensitive membrane.

Finally, the overall composition of the detergent-resistant domains also remains to be determined. Although cholesterol is clearly an important constituent, other lipids or proteins may play equally important roles in the formation and maintenance of this structure. It is also likely that, apart from immobilizing the

glideosome, the unusual IMC membrane domains we described here may play equally important roles in the localization and function of other factors required for parasite survival and its ability to cause disease.

## Acknowledgements

The authors would like to thank Yun Chen for assistance with the FRAP experiments and Hal Mekeel for help with electron microscopy. We would like to thank Richard Cheney and Vytas Bankaitis for many helpful discussions and suggestions, and Stacey Gilk, Sebastien Pomel and Flora Luk for critical reading of the manuscript.

## Materials and Methods

### Culture of *Toxoplasma*

The RH (HXGPRT-) strain of *Toxoplasma gondii* and its derivatives expressing various fusion proteins were maintained in human foreskin fibroblasts (HFF) as described previously (Gaskins et al., 2004). Metabolic labeling of parasite proteins were performed as described previously (Gaskins et al., 2004). Parasites were isolated from recently lysed cultures by passage through 18G and 25G needles and centrifugation at room temperature for 5 minutes at 800 x g. Parasites were resuspended in PBS and passed through 5 µm filters to remove the small amount of host cell debris and collected again by centrifugation as described above.

### Reagents

The generation of monospecific antisera to *Toxoplasma* IMC1 has been described previously (Mann et al., 2002). Monospecific antisera to YFP were generated by

injecting rabbits with purified recombinant YFP (Cocalico Biologicals, Reamstown, PA).

BODIPY-PC (2-(4,4-difluoro-5,7-diphenyl-4-bora-3a,4a-diaza-s-indacene-3-pentanoyl)-1-hexadecanoyl-sn-glycero-3-phosphocholine) and BODIPY-cholesteryl (cholesteryl 4,4-difluoro-5,7-dimethyl-4-bora-3a,4a-diaza-s-indacene-3-dodecanoate) were obtained from Molecular Probes (Eugene, OR). Methyl-β-cyclodextrin (mβCD) was purchased from Sigma-Aldrich (St. Louis, MO).

**FRAP experiments**

Fluorescence recovery after photobleaching (FRAP) measurements were performed on a custom built system based on a Leitz microscope (Leica Microsystems Inc., Bannockburn, IL) and Spectra Physics 164 argon ion laser (488 nm line).The laser beam was focused to 3.4 μm spot ($1/e^2$) using a 40x oil immersion objective (1.3 NA). The power of the bleaching beam was optimized for specimen spot photobleaching and varied from 50 mW to 300 mW (measured at the laser output). Fluorescence signals were detected by EMI cooled photomultiplier (S 20 photocathode) working in single photon counting mode. FRAP curves were obtained by collecting PMT signal in a multichannel scaler card (Ortec, Oak Ridge TN). Diffusion coefficients and immobile fraction were obtained by numerical analysis of FRAP curves using custom written software (Gordon et al., 1998). Cells on coverslips were mounted in custom made airtight chambers.

Video-FRAP was performed on an Olympus microscope (Olympus, Center Valley PA). The laser beam from a Spectra Physics Stabilite 2017 argon ion laser was focused to ~ 3 μm spot using 100x oil immersion objective (1.25 NA). Images were collected by Hamamatsu 4880 cooled CCD camera (Hamamatsu, Bridgewater NJ) driven by Metamorph imaging software (Universal Imaging Corp. Downington, PA).

Cells were kept in a 37°C environmental chamber (Warner Instruments, Hamden CT) and $CO_2$ was flushed over the culture dishes.

**Differential detergent extraction of *Toxoplasma* membranes**

Purified parasites (3 x $10^7$) were extracted for 10 minutes on ice in TX100/PBS (1% Triton X-100, 154 mM NaCl, 1.54 mM $KH_2PO_4$, 2.71 mM $Na_2HPO_4$ pH 7.4) in the presence of protease inhibitors (1:100) (Sigma-Aldrich). The TX100/PBS-soluble and insoluble material was collected by centrifugation at 16,000 x g for 10 minutes at 4°C. The TX100/PBS-insoluble material was subsequently extracted for 10 minutes on ice in TX100/TBS (1% Triton X-100, 150 mM NaCl, 25 mM Tris-HCl pH 7.4) in the presence of protease inhibitors (1:100) (Sigma-Aldrich), and the TX100/TBS soluble and insoluble material collected by centrifugation as described above.

**Transmission Electron Microscopy**

Parasites were treated as described above in either TX100/PBS, TX100/TBS, or TX100/PBS plus mβCD. Insoluble parasite material was incubated in 1% glutaraldehyde (Electron Microscope Sciences [EMS], Fort Washington PA) in PBS for 20 minutes on ice. Parasites were washed in PBS and collected by centrifugation at 16,000 x g for 10 minutes at 4°C. Parasites were then resuspended in 1% tannic acid (EMS) for 20 minutes on ice, washed again, and incubated in 1% OsO4 (EMS) for 20 minutes at room temperature. Parasites were washed twice in PBS, dehydrated in a 50-100% ethanol series and after two washes propylene oxide embedded in epon.

The polymerized bocks were sectioned at 60 nm with a Leica Ultracut UCT ultramicrotome (Leica Microsystems Inc., Bannockburn, IL). Sections were stained

with 2% uranyl acetate and Sato's lead stain, and viewed on an FEI Tecnai 12 electron microscope (FEI Company, Hillsboro, OR). Images were collected with a Gatan model 794 multi-scan digital camera (Gatan Inc., Pleasanton, CA).

**Fluorescent Lipid Labeling**

Parasites were incubated in either 10 µM BODIPY-PC or BODIPY-cholesteryl for 3 hours at 37°C in Intracellular (IC) buffer (Moudy et al., 2001). Cells were washed once in PBS and collected by centrifugation for 5 minutes at 800 x g. Parasites were extracted in TX100/PBS or TX100/TBS at 4°C for 10 minutes in the presence of 5 µM BODIPY-CE or BODIPY-PC for lipid labeling.

**Thin Layer Chromatography**

Parasites (6-9 x $10^8$) were isolated and extracted as described above to obtain subcellular fractions. Lipids were extracted in chloroform/methanol by the method of Bligh and Dyer (1959) and separated by mono-dimensional TLC on Partisil LK6D silica gel 60 A plates (Whatman, Clifton, NJ). Lipids were separated in a solvent system composed of hexane/ether/acetic acid (70:30:1) for cholesterol and methanol/chloroform/ammonium hydroxide/water (60:72:7.5:10.5) for phospholipids. Authentic cholesterol standard (Avanti Polar Lipids, Alabaster, AL) was run in parallel and all cholesterol was visualized by spraying with 3% cupric acetate in 8% $H_3PO_4$ and baking at 100°C for one hour. Fluorescent lipids were detected by exposure to 450 and 635 nm light with a STORM Scanner Control Version 5.03 (Amersham Biosciences, Piscataway, NJ) and visualized with ImageQuant TL software (Amersham Biosciences).

**Cholesterol depletion of the *Toxoplasma* IMC membranes**

Parasites were extracted in TX100/PBS for 10 minutes at 4ºC in the presence of protease inhibitors (1:100) (Sigma-Aldrich) and the TX100/PBS-resistant fraction was collected by centrifugation at 9,400 x g for 10 minutes at 4ºC. This material was subsequently resuspended in either PBS, 30 mM mβCD in PBS, or 30mM mβCD with 5 µg of cholesterol in PBS and incubated at 37ºC for 45 minutes. Extraction of the glideosome under these conditions was monitored by fluorescence microscopy and differential centrifugation. For fluorescence microscopy, an aliquot of the treated and untreated parasites were washed once in PBS and then allowed to adhere to poly-L-lysine coated coverslips. TX100 was added to the remainder of the reactions to a final concentration of 1% and, after a 10 minute incubation at 4ºC, the soluble and insoluble material was separated by centrifugation for 10 minutes at 9,400 x g at 4ºC and analyzed by SDS-PAGE and immunoblot.

**Sucrose gradient centrifugation**

Parasites (2-4 x $10^8$) were lysed in TX100/PBS for 10 minutes on ice in the presence of protease inhibitors (1:100) (Sigma-Aldrich). Material was divided into two aliquots and centrifuged at 9,400 x g for 10 minutes at 4ºC. The TX/PBS-resistant material was incubated in PBS in the presence or absence of mβCD as described above, followed by the addition of TX100 to a final concentration of 1% and an additional incubation on ice for 20 minutes. Samples were then adjusted to a total volume of 500 µl and 1.6M sucrose, transferred to 13 x 51 mm centrifuge tubes (Beckman, Fullerton, CA) and overlaid with 500 µl each of 1.4M, 1.2M, 1.1M, 1.0M, 0.9M, 0.8M, 0.7M, 0.6M, and 1 ml 0.25M sucrose. Gradients were centrifuged for 2 hours at 120,000 x g and 4ºC in a MLS-50 swinging bucket rotor.

Fractions (500 µl) were collected from the bottom and pellets were resuspended in 500 µl PBS for analysis by western blot.

**Fluorescence Microscopy**

Cells labeled with fluorescent lipids were allowed to adhere to poly-L-lysine coated coverslips, and fixed with 3% paraformaldehyde in PBS for 7 minutes at room temperature. For immunofluorescence, cells were permeabilized in 0.5% TX100 in PBS for 7 minutes at room temperature and incubated with primary antibody (Rabbit α-IMC1) for 30 minutes in 3%BSA in PBS. Samples were washed and incubated with Alexa Fluor®350-conjugated secondary antibodies (Invitrogen Corporation, Carlsbad, CA) in 3%BSA in PBS for 30 minutes at room temperature. Images were captured using an epifluorescence Nikon Eclipse TE-2000 microscope (Nikon Inc., Melville, NY) and a Hamamatsu 1394 cooled digital CCD camera (Hamamatsu) and Metamorph® imaging software (Universal Imaging Corp.). Adobe Photoshop® (Adobe Systems Inc., San Jose, CA) was used to crop images.

**SDS-PAGE and immunoblotting**

Protein preparations were separated by SDS-PAGE on 10% polyacrylamide mini gels. Transfer to nitrocellulose and immunoblot analysis was performed as described previously (Mann and Beckers, 2001).

## Figure Legends

**Figure 1.** GAP50 is immobilized within the inner membrane complex of *Toxoplasma gondii.* (A) Parasites stably expressing GAP50-YFP were allowed to infect an HFF monolayer. In these video-FRAP experiments, prebleach images were captured and fluorescence at the indicated portion of the IMC was photobleached. Images were taken at two minute intervals thereafter to monitor diffusion into the bleached region. (B) FRAP on motile extracellular parasites also demonstrated that GAP50-YFP is immobilized. Parasites were harvested and allowed to move along poly-L-lysine coated coverslips during FRAP analysis. Scale bars = 5 μm.

**Figure 2.** Quantitative analysis of GAP50-YFP mobility in the inner membrane complex. A) Fluorescence intensity was measured as a function of time after photobleaching for GAP50-YFP and two controls: GAP45-YFP, which localizes to the IMC but does not associate with glideosome, and COS7 cells expressing GFP. Asterisks indicate level of fluorescence prior to bleaching. (B) Mobile fractions and diffusion coefficients were averaged for all three samples confirming the slow recovery of GAP50-YFP. For GAP50-YFP n= 9, GAP45-YFP n=6, COS7 with GFP n= 3. AU = arbitrary unit.

**Figure 3.** Glideosome solubility in Triton-X100 is temperature and buffer-dependent. Parasites were harvested and subjected to detergent extraction in either 1%TX100 in PBS or 1%TX100 in TBS. Extractions were performed for 10 minutes at 37°C or on ice. Extracts were subjected to centrifugation for 10 minutes at 14,000 x g and 4°C. Proteins were resolved by SDS-PAGE, transferred to nitrocellulose and incubated with antisera to glideosome proteins and the membrane skeleton protein IMC1.

**Figure 4.** Sequential extraction of the glideosome from *Toxoplasma gondii.* (A) Diagram of the differential solubilization of *Toxoplasma* structures during sequential extraction in 1%TX100/PBS and 1%TX100/TBS. (B) Parasite fractions obtained during these extractions were analyzed by immunoblots for the presence of the glideosome subunits (TgMyoA, TgGAP50, TgGAP45, and TgMLC1), the membrane skeleton (IMC1), plasma membrane (SAG1), endoplasmic reticulum (BiP), dense granules (GRA3), and rhoptries (ROP2). Red italicized symbols indicate fractions containing glideosome proteins.

**Figure 5.** The IMC membrane is largely resistant to extraction by TX100/PBS. (A) Isolated pellicles of non-extracted parasites possess an intact plasma membrane, IMC membrane, and the associated cytoskeleton. (B) Extraction in TX100/PBS removes the plasma membrane but does not affect the appearance of the IMC membrane. (C) The IMC membrane is solubilized efficiently by extraction in TX100/TBS as well as by treatment with mβCD (D). Subpellicular microtubules are indicated by asterisks. Scale bars: 100 nm.

**Figure 6.** Sucrose density gradient centrifugation analysis of the TX100/PBS-resistant IMC fraction. Parasites were lysed in 1% TX100 in PBS on ice and the TX100-soluble and insoluble material was separated by differential centrifugation.

The pellet fraction was resuspended, adjusted to 1.6M sucrose, overlaid with a gradient of 1.4M, 1.2M, 1.1M, 1.0M, 0.9M, 0.8M, 0.7M, 0.6M, and 0.25M sucrose, and subjected to centrifugation for 2 hours at 120,000 x g. Fractions were collected from the bottom of the gradient and analyzed by SDS-PAGE and immunoblotting for IMC1 and TgGAP50.

**Figure 7.** Cholesterol is selectively enriched in the *Toxoplasma* IMC. Parasites were harvested and incubated with (A) no dye, (B) BODIPY-CE, or (C) BODIPY-PC for 3 hours at 37°C. Sequential detergent extractions were performed as described above using 1%TX100 in PBS followed by 1%TX100 in TBS, both on ice. Lipids were extracted from all fractions and analyzed by thin layer chromatography. The extraction efficiency of TgGAP50 in these buffers was confirmed by immunoblot analysis. STD = lipid standard.

**Figure 8.** The TX100/PBS-resistant cholesterol and TgGAP50 in the IMC are efficiently extracted with TX100 in TBS. (A) BODIPY-cholesteryl ester accumulates in the *Toxoplasma* IMC, as judged by the overlap with GAP50. IMC-associated BODIPY-CE is resistant to extraction by TX100/PBS but is solubilized by TX100/TBS. (B) BODIPY-PC is found throughout the parasite and is completely extracted in TX100/PBS. Scale bars = 5μm.

**Figure 9.** TX100/PBS-resistant cholesterol and TgGAP50 are completely extracted by mβCD. (A) The TX100/PBS-resistant fraction was incubated in PBS or in PBS containing 30 mM mβCD or 30 mM mβCD and 5μg of cholesterol for 30 minutes at 37°C. TritonX-100 was added to 1% and parasites were incubated on ice for 10 minutes. Soluble and insoluble fractions were separated by centrifugation at 14,000 x g for 10 minutes at 4°C and analyzed for the presence of TgGAP50 by SDS-PAGE and immunoblot analysis. (B) The TX100/PBS-resistant fraction of parasites pre-labeled with BODIPY-CE was incubated in the presence or absence of 30mM mβCD for 45 minutes at 37°C and analyzed by fluorescence microscopy. Scale bars = 2μm.

**Supplementary Table 1.** Summary of the various crosslinking and immunoprecipitation conditions tested in this study. As indicated in the text, glideosome solubilization was only found to be temperature dependent using the detergent TX100 in 150 mM NaCl, 5 mM EDTA, 50 mM Na3PO4. Crosslinking experiments were performed using a variety of water insoluble (DSP, DSS, BMH) and water soluble (BS3) crosslinkers. Reactions were carried out for various times at room temperature and ice in phosphate-buffered saline (PBS) and quenched by the addition of 1M Tris or glycine, pH 7.5 to a final concentration of 50mM.

**Supplementary Figure 1.** Current model of the *Toxoplasma* motile apparatus.

**Supplementary Figure 2.** TgGAP45-YFP does not associate with other members of the glideosome complex. *Toxoplasma* tachyzoites expressing TgGAP45-YFP were labeled for 20 hours with [35S] methionine/cysteine and, after lysis in TX100/TBS, subjected to immunoprecipitation with antisera to TgGAP45 or YFP. Asterisks indicate degradation products of TgGAP45 and TgGAP45-YFP.

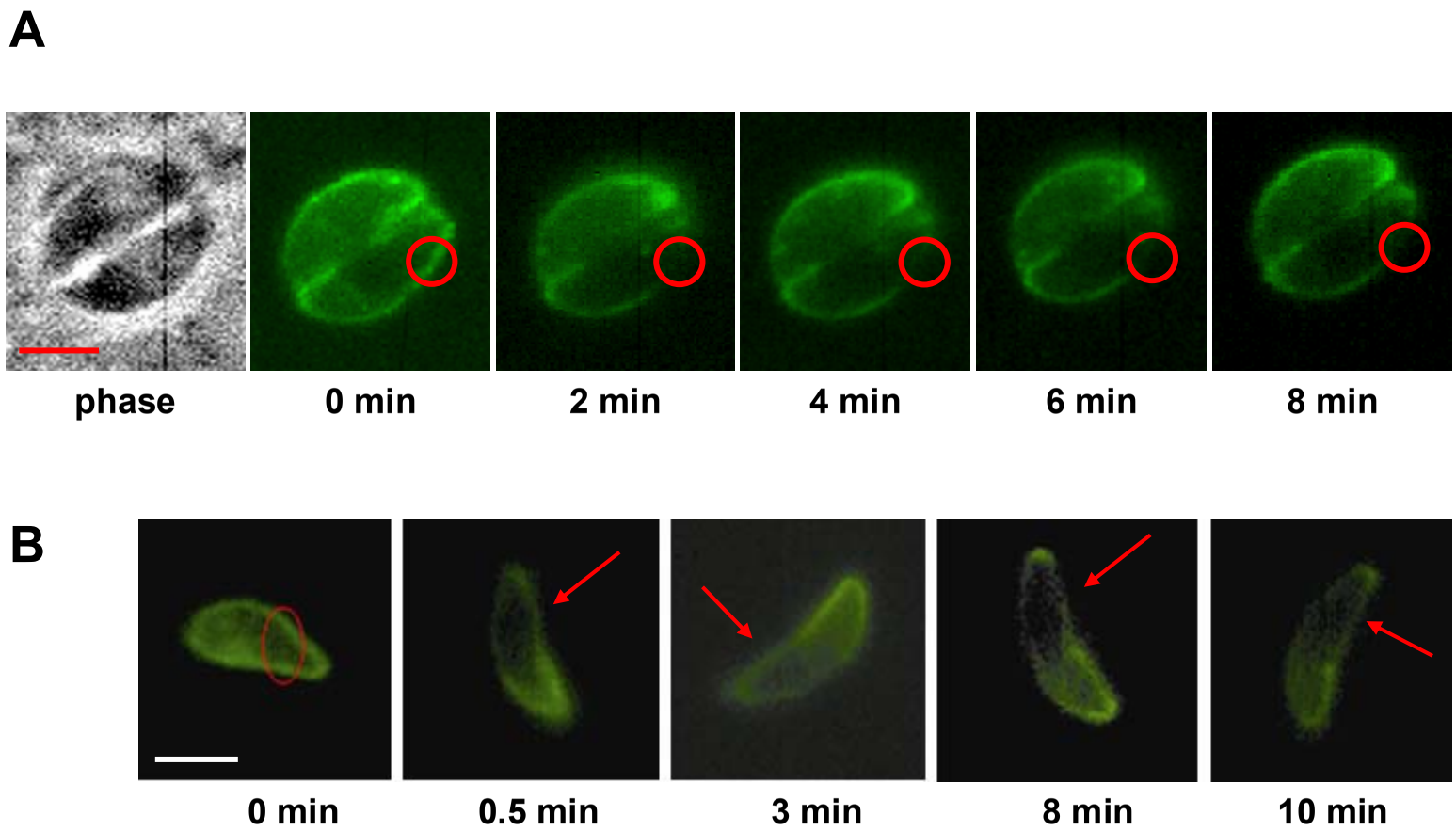


Figure 1. GAP50 is immobilized within the inner membrane complex of *Toxoplasma gondii*.

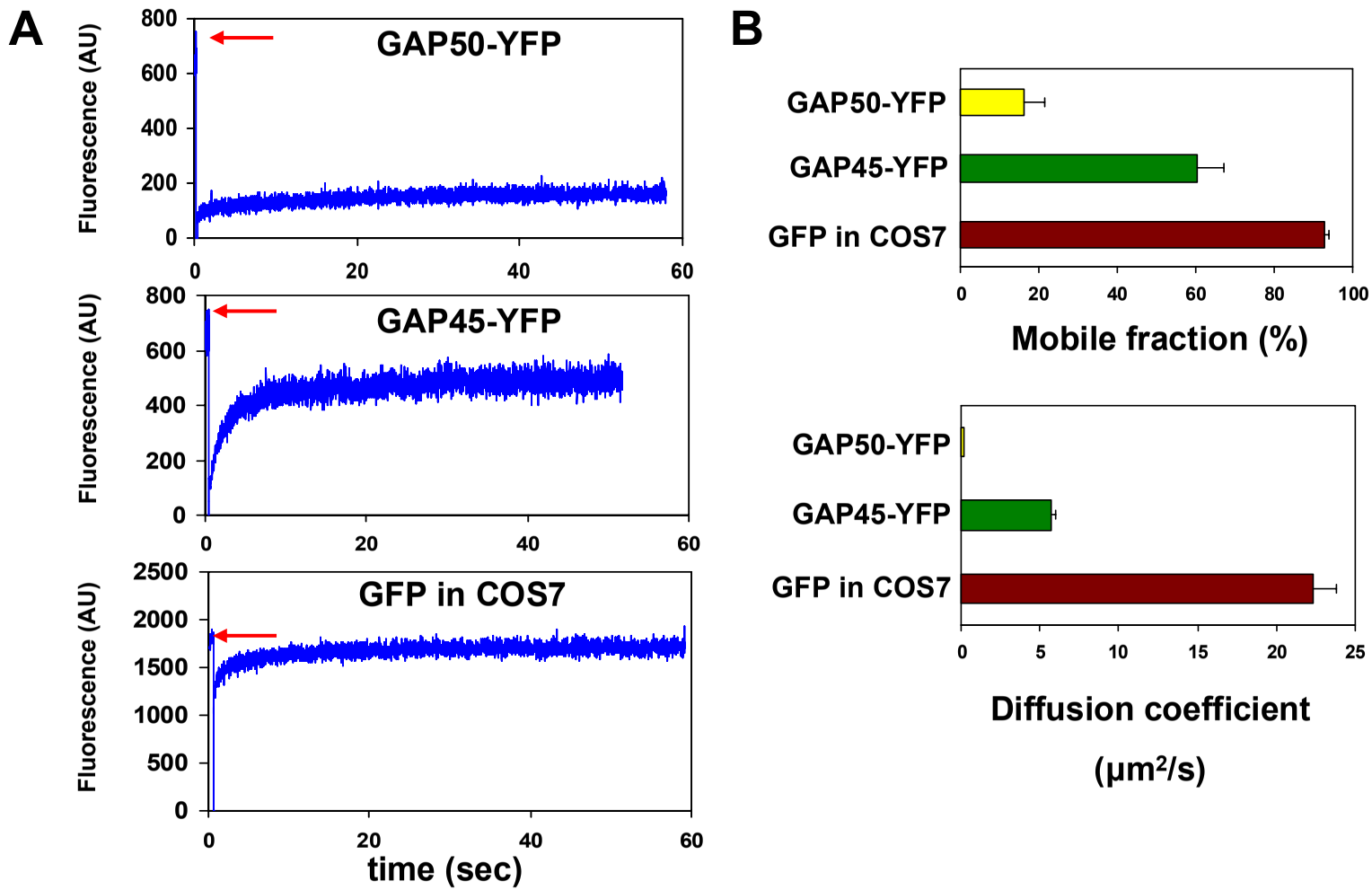


Figure 2. Quantitative analysis of GAP50-YFP in the inner membrane complex.

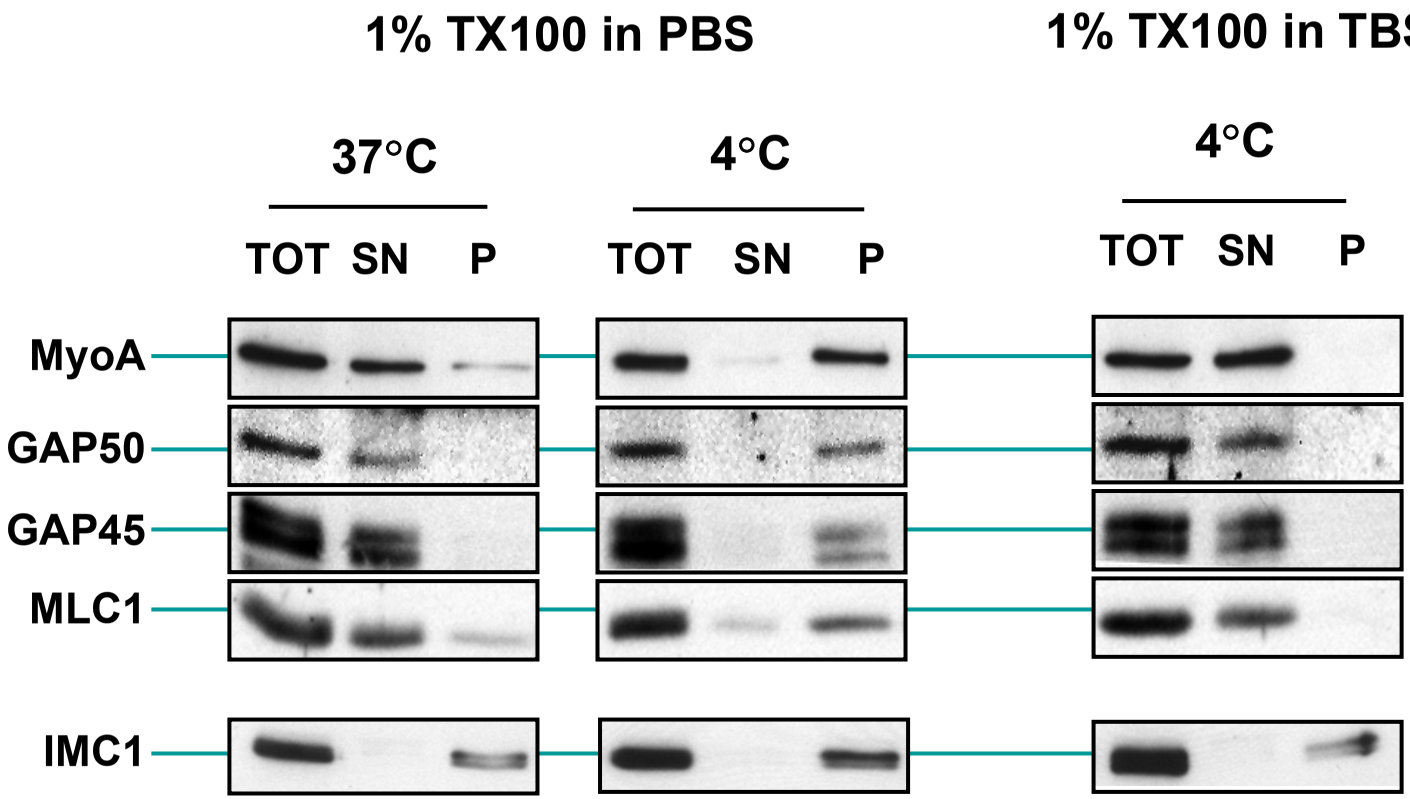


**Figure 3. Glideosome solubility in Triton-X-100 is temperature and buffer-dependent.**

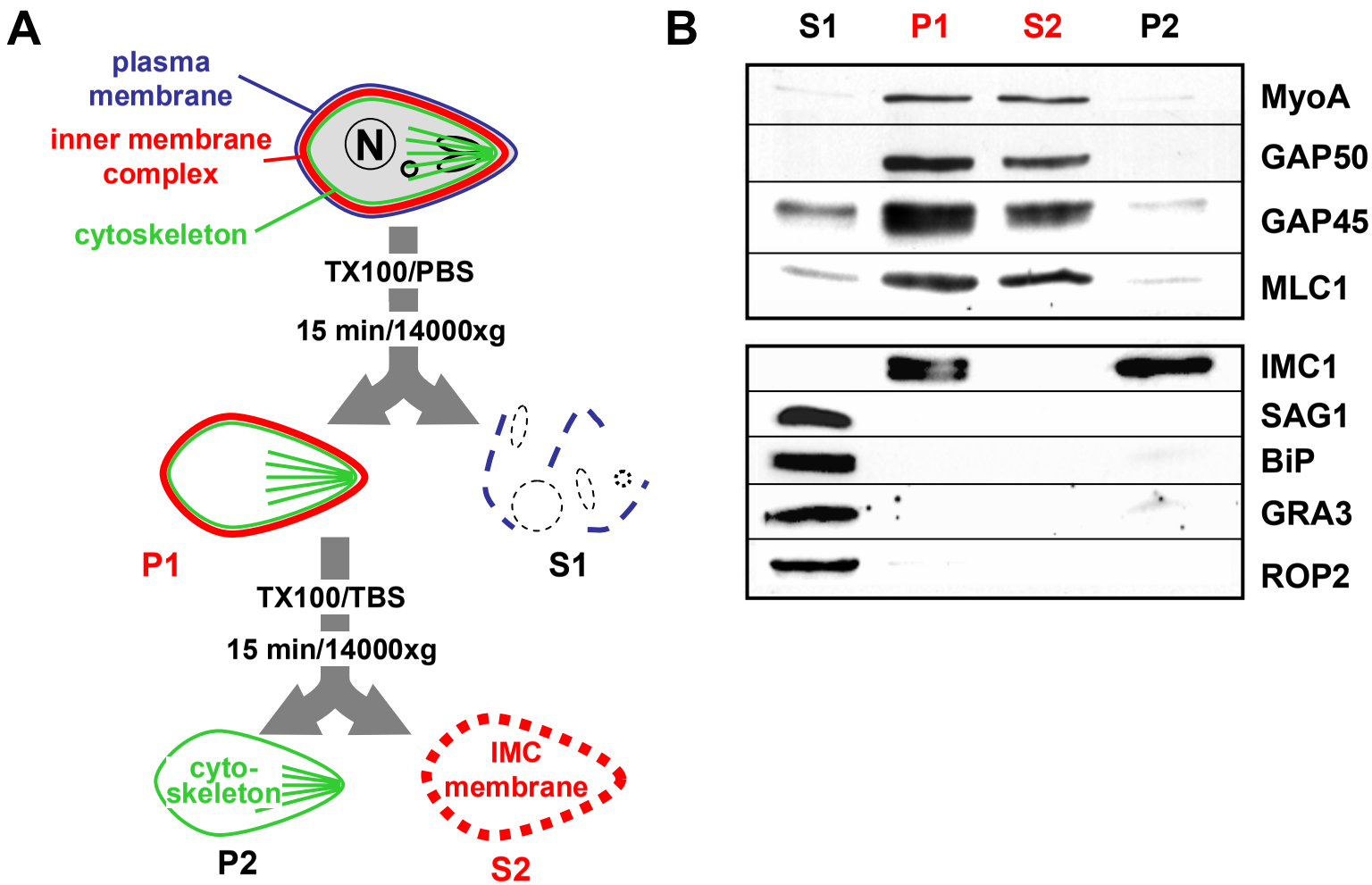


Figure 4. Sequential extraction of the glideosome from *Toxoplasma gondii*.

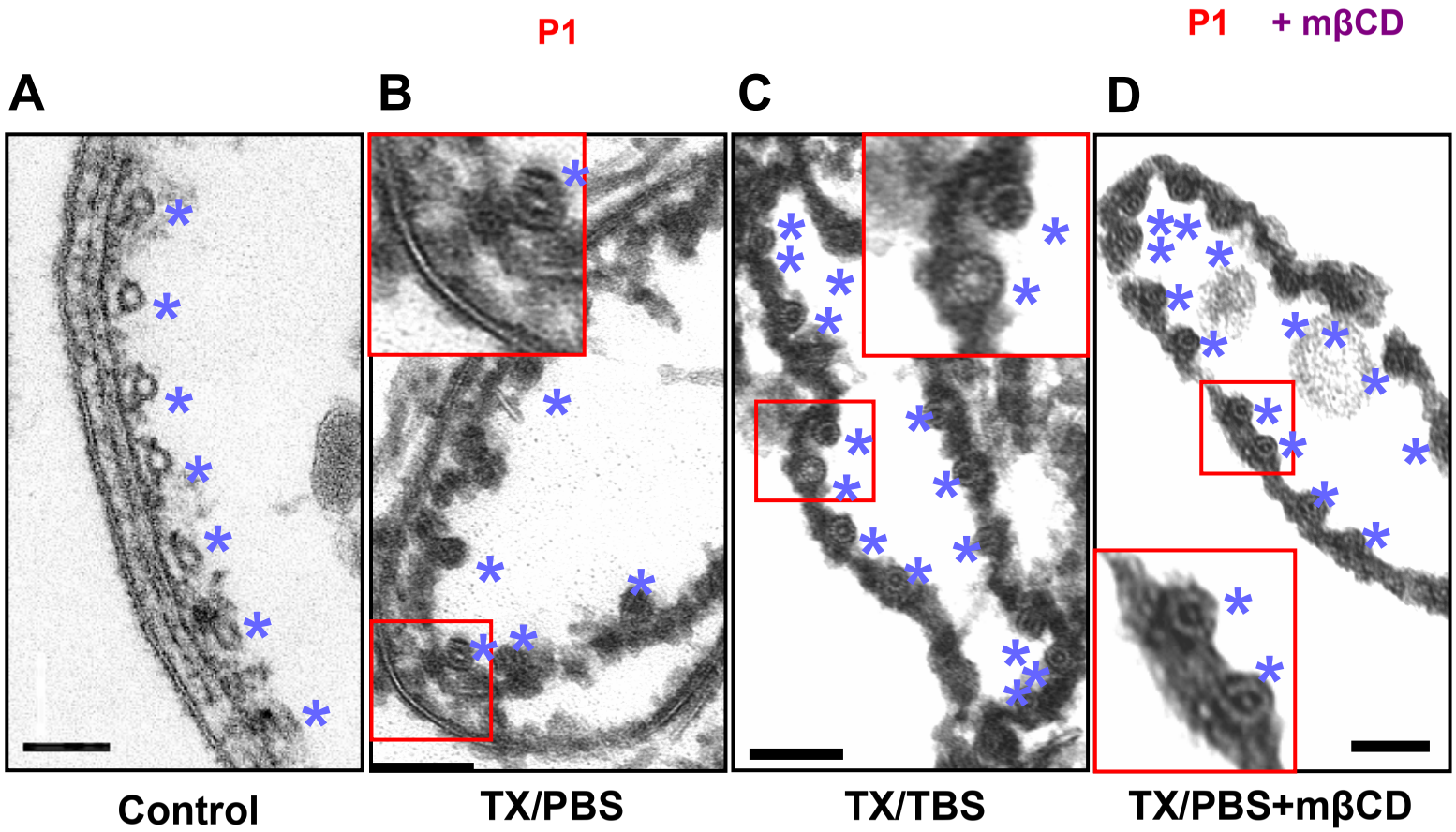


Figure 5. The IMC membrane is largely resistant to extraction by TX100/PBS.

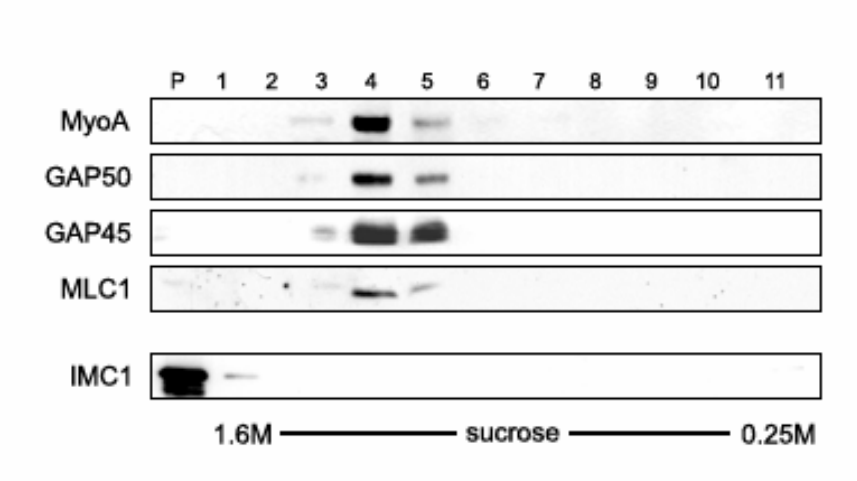


**Figure 6. Sucrose density gradient centrifugation analysis of the TX100/PBS-resistant IMC fraction.**

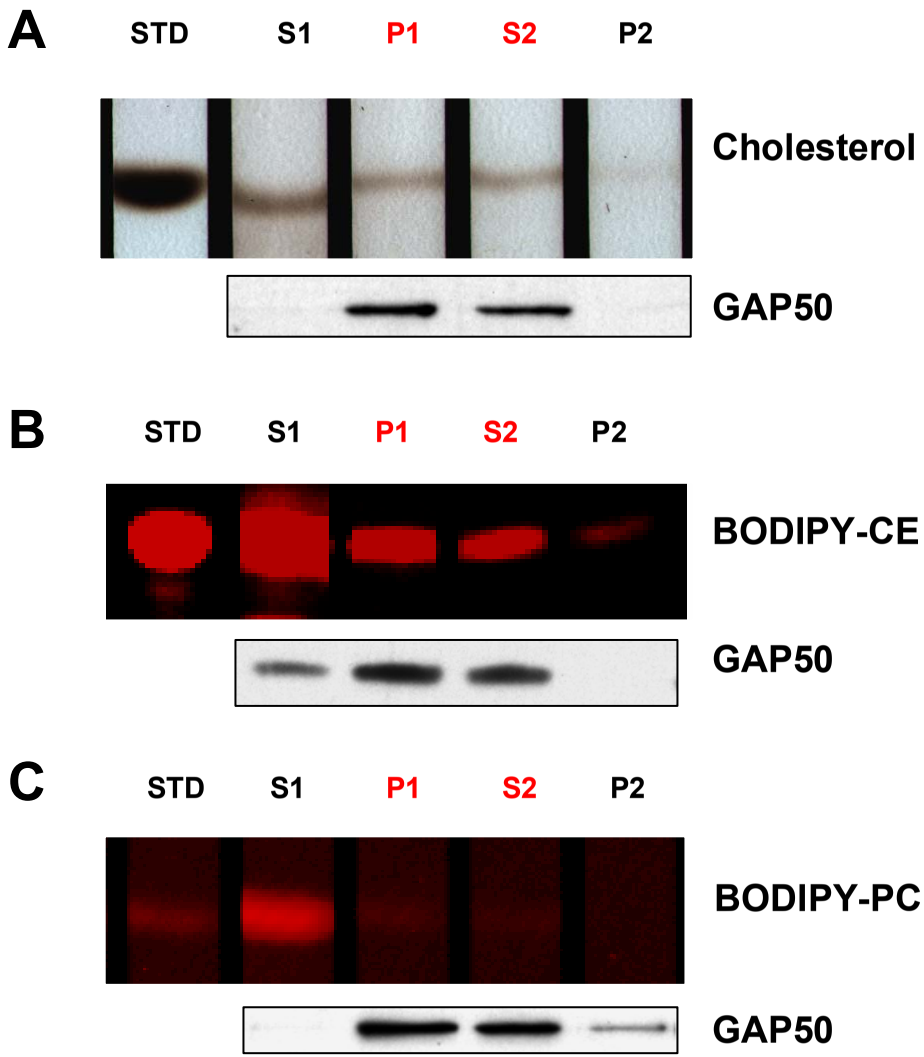


Figure 7. Cholesterol is selectively enriched in the *Toxoplasma* IMC.

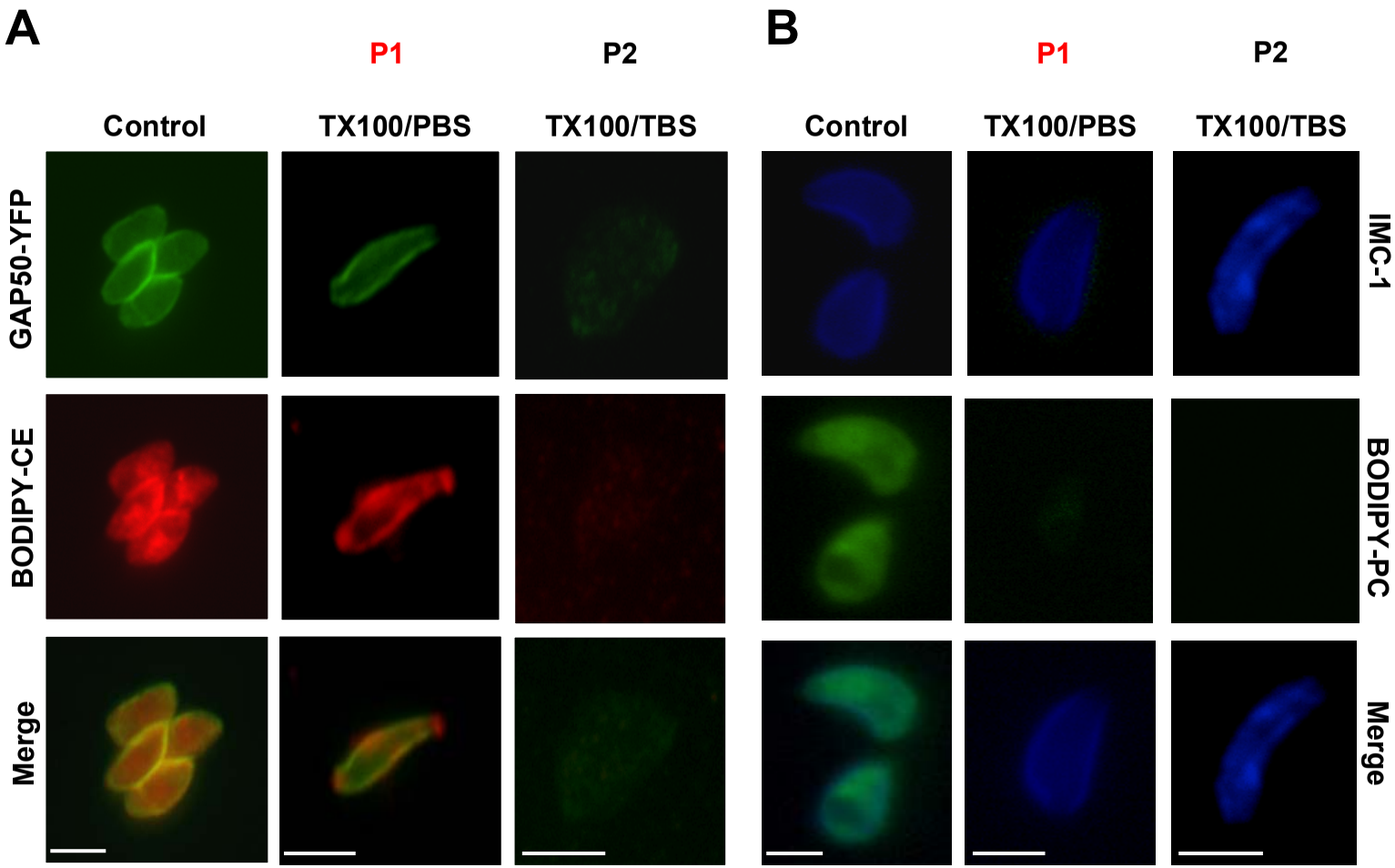


**Figure 8. The TX100/PBS-resistant cholesterol and TgGAP50 in the IMC are efficiently extracted with TX100 in TBS.**

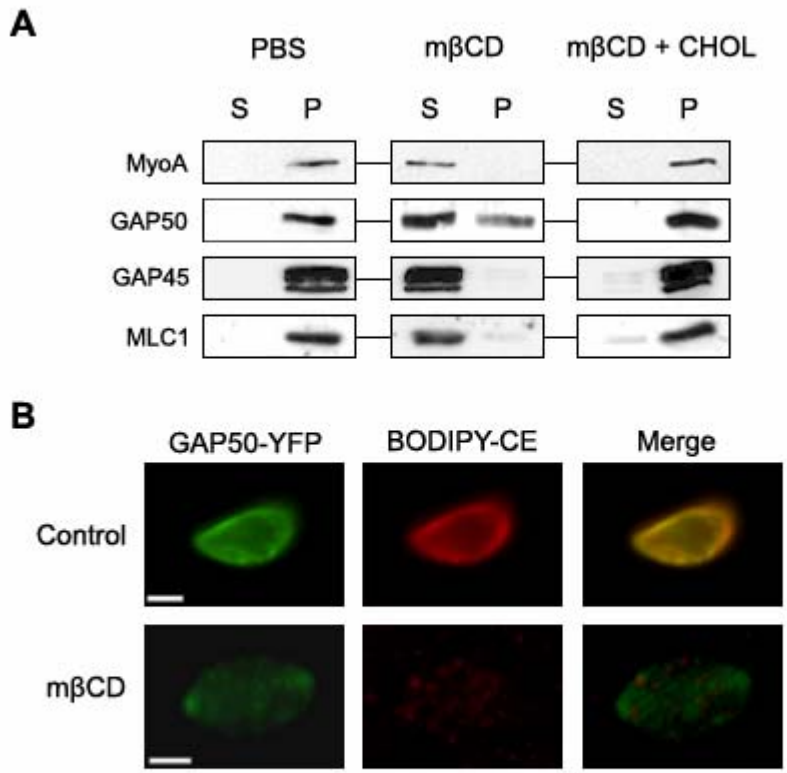


**Figure 9. TX100/PBS-resistant cholesterol and TgGAP50 are completely extracted by mβCD.**

| **Crosslinkers tested** | **Concentration tested** |
|---|---|
| Dithiobis[succinimidylpropionate] (DSP) | 0.1mM, 1mM |
| Disuccinimidyl suberate (DSS) | 0.1mM, 1mM |
| Bismaleimidohexane (BMH) | 0.1mM, 1mM |
| Bis[sulfosuccinimidyl]suberate (BS3) | 0.1mM, 1mM |

**Detergents tested:**

1%, 0.5%, 0.2% TX100 in 150 mM NaCl, 5 mM EDTA, 50 mM Tris-HCl pH 7.5 or pH 8.0

1%, 0.5%, 0.2% TX100 in 150 mM NaCl, 5 mM EDTA, 50 mM $Na_3PO_4$ pH 7.5 or pH 8.0

1% CHAPS in 150 mM NaCl, 5 mM EDTA, 50 mM Tris-HCl pH 7.5 or pH 8.0

1% β-octylglucoside in 150 mM NaCl, 5 mM EDTA, 50 mM Tris-HCl pH 7.5 or pH 8.0

**Potential co-factors tested:**

0.5mM $CaCl_2$ in 1% TX100, 150 mM NaCl, 50 mM Tris-HCl pH 7.5 or pH 8.0

2 mM EGTA in 1%TX100, 150 mM NaCl, 5 mM EDTA, 50 mM Tris-HCl pH 7.5 or pH 8.0

2mM $MgCl_2$ in 1%TX100, 150 mM NaCl, 50 mM Tris-HCl pH 7.5 or pH 8.0

1mM ATP, 2mM $MgCl_2$ in 1%TX100, 150 mM NaCl, 50 mM Tris-HCl pH 7.5 or pH 8.0

1mM GTP, 2mM $MgCl_2$ in 1%TX100, 150 mM NaCl, 50 mM Tris-HCl pH 7.5 or pH 8.0

0.1 mM GTPγS, 2 mM $MgCl_2$ in 1%TX100, 150 mM NaCl, 50 mM Tris-HCl pH 7.5 or pH 8.0

## Supplemental Table 1. Summary of the various crosslinking and immunoprecipitation conditions tested in this study.

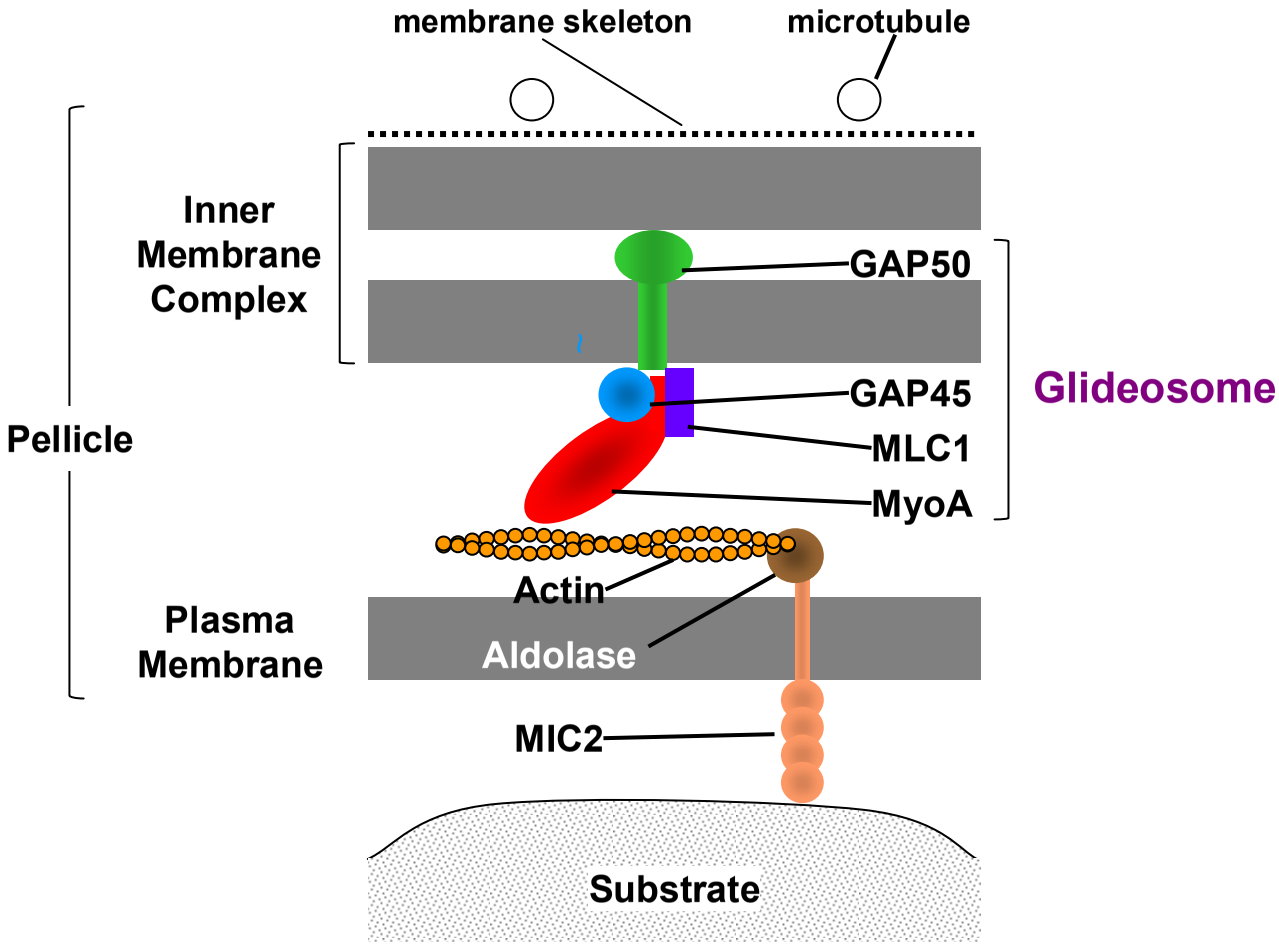


Supplemental Figure 1. Current model of the *Toxoplasma* motile apparatus.

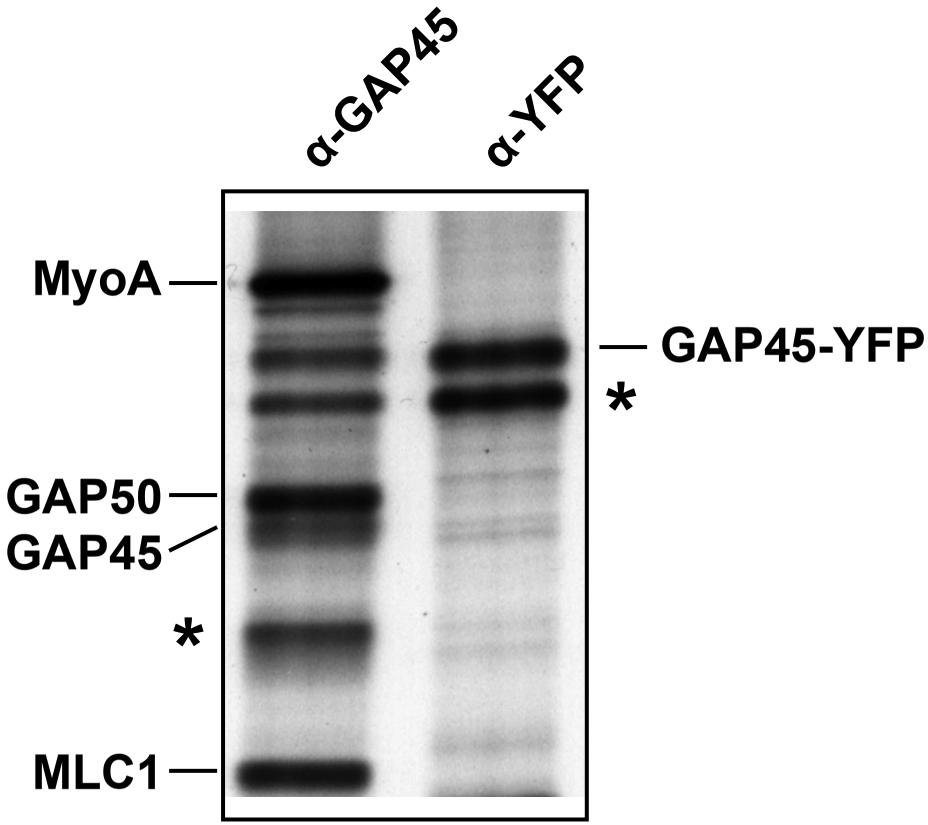


**Supplemental Figure 2. TgGAP45-YFP does not associate with other members of the glideosome complex.**

# CHAPTER III

# THE LUMENAL AND TRANSMEMBRANE DOMAINS OF THE MYOSIN XIV ANCHOR TGGAP50 IN *TOXOPLASMA GONDII* ARE NECESSARY FOR PROPER TARGETING

## INTRODUCTION

### Parasites

Infectivity of the protozoan parasite *Toxoplasma gondii* occurs worldwide and is known to affect humans and warm-blooded animals. Infection can be life-threatening in immunocompromised individuals and can cause congenital disease in infants (Dubey, 1994). Other members of the apicomplexan phylum such as *Plasmodium*, *Cryptosporidium*, and *Eimeria* are also medically relevant parasites for which treatments are inadequate or still not available.

The life cycle of apicomplexan parasites alternates between a motile extracellular phase and a non-motile phase within host cells where growth and replication occurs. Both the invasion of host cells and egress are dependent on active motility of the parasite and therefore critical for their survival (Meissner et al., 2002). The type of motility seen in apicomplexan parasites is quite unusual as it does not require typical locomotive organelles, such as filipodia or flagellae, but instead involves a unique substrate-dependent type of movement called gliding motility.

**Glideosome**

Gliding motility is dependent on the interaction of actin filaments and the type XIV myosin TgMyoA located between the plasma membrane and inner membrane complex (IMC) of the parasite pellicle (Heintzelman & Schwartzman, 1999; Meissner et al., 2002). Depolymerization of the actin filaments with cytochalasin D, inhibition of myosin ATPase activity with butanedione monoxime, and knock-down of TgMyoA all block motility and host cell invasion completely, indicating the importance of actin-myosin interactions for the survival of the parasite (Dobrowolski and Sibley, 1996; Dobrowolski et al., 1997a; Meissner et al., 2002).

TgMyoA has been shown to be associated with the IMC in a hetero-oligomeric complex called the glideosome (Gaskins et al., 2004). In addition to TgMyoA, this complex consists of a myosin light chain (TgMLC1) (Herm-Gotz et al, 2002) and two novel proteins, TgGAP45 and TgGAP50 (Gaskins et al., 2004) which have also been described in *Plasmodium* (Bergman et al., 2003; Bosch et al., 2006).

In order for the interaction of actin with myosin to result in net movement of a parasite, it is essential that the myosin is immobilized with respect to the parasite and the actin with respect to the substrate. The immobilization of parasite F-actin filaments appears to be accomplished through its interaction with the glycolytic enzyme aldolase which, in turn, interacts with MIC2/TRAP in the plasma membrane (Jewett and Sibley, 2003; reviewed in Soldati and Meissner, 2004). TgMyoA is anchored in the cholesterol enriched inner membrane complex (IMC), immobilized as a part of the glideosome through its tight association with TgGAP50 (Johnson et al., 2007).

**TgGAP50**

Database searches have found that orthologues of TgGAP50 exist in as many as six other apicomplexan parasites including *Plasmodium* and *Cryptosporidium* (Figure 1). The orthologues are highly homologous (41-58% identity) with the exception of the N-terminal signal sequence region, which is highly divergent. TgGAP50 shows homology with purple acid phosphatases (22-26% identity) however, the amino acids required for enzymatic phosphatase activity are not conserved. TgGAP50 is a 431-residue protein with a predicted molecular weight of 46.6 kD and direct amino acid sequencing of TgGAP50 begins with amino acid 51, indicating the first 50 residues of the protein contain a cleavable signal sequence (Gaskins et al., 2004). This sequence may be responsible for the orientation in the membrane, but its function is unknown in the role of targeting (Goder and Spiess, 2001). Aside from this 50 amino acid sequence, TgGAP50 is predicted to be comprised of three domains: the 351-residue luminal domain, a single transmembrane domain of 24 residues, and a 6-residue cytoplasmic domain. The lumen of TgGAP50 is modified by N-linked glycosylation on three locations, amino acids 101, 136, and 228 (Gaskins et al., 2004). Deletion of the cytoplasmic domain does not allow TgGAP50 to associate with the other three proteins of the glideosome indicating the importance of TgGAP50 in glideosome assembly and function (Gaskins et al., 2004).

This integral membrane glycoprotein localizes to the IMC membranes of both daughter cells in replicating parasites and mature parasites. TgGAP50 is found to be associated with detergent-resistant, raft-like domains in the IMC, so the targeting of TgGAP50 is potentially influenced by these domains (Johnson et al., 2007). The lumen of TgGAP50 is oriented between the two layers of the IMC with the transmembrane domain only passing through one face of IMC membrane. The

ability of TgGAP50 to anchor the gliding motility apparatus relies on proper targeting to the IMC. A sequence alignment of TgGAP50 with other apicomplexan parasites shows many regions of homology, including a very high conservation in one half of the transmembrane domain indicating a possible conserved function for this region.

Little is known about how TgGAP50 is inserted into the IMC and what part or parts of the protein are responsible for targeting. We constructed a variety of chimeric proteins to determine which of the three domains are critical for targeting of TgGAP50 to the IMC. Our results show that the lumen and the conserved half of the transmembrane domains of TgGAP50 are important for localization to the IMC, while the cytoplasmic domain is not.

## Results

### Generation of TgGAP50 hybrid proteins

TgGAP50 consists of three domains: lumenal (L), transmembrane (TM), and cytoplasmic (C) (Figure 2). To analyze which of these domains are important for the targeting of TgGAP50 to the IMC, we constructed hybrids utilizing combinations of TgGAP50 domains with domains of other proteins, expressed these hybrids in parasites, and assessed their localization. Domains of other proteins were chosen based on properties that were similar to TgGAP50, such as sequence length, function, and shape (Figure 2). The lumen of TgGAP50 was replaced with the lumen of the similarly sized alpha-1-antitrypsin (AAT) protein (Parfrey et al., 2003). For the replacement of transmembrane and cytoplasmic domains, we used the human class I histocompatibility protein, HLA-A2, which has a single

transmembrane domain, and similar sized domains as TgGAP50 (Jordan et al., 1985). All hybrids have YFP at the carboxy terminus.

**The lumenal domain of TgGAP50 is necessary but not sufficient for targeting to the inner membrane complex**

In order to determine if the lumen of TgGAP50 is necessary for targeting, we overexpressed a hybrid containing the AAT lumen in place of the TgGAP50 lumen (L-hybrid) in parasites. Although the parasites were not able to retain expression of this protein, transient transfections demonstrate that the protein is not targeted to the IMC but is instead cytoplasmic (Figure 3). Expression of the ΔTMC-hybrid which lacks both the TgGAP50 transmembrane and cytoplasmic domains with no substituted domains also remains nuclear and in the cytosol, and was not able to be expressed under stable conditions (data not shown). Two other attempts were made to replace the lumenal domain of TgGAP50, using either bacterial β-lactamase or a smaller myc peptide sequence in place of the lumen; however, all of these constructs had the same localization properties (data not shown). It is possible that the YFP tag is being cleaved, and the inability to maintain prolonged expression makes this issue difficult to address. These data suggest that the lumenal domain of TgGAP50 may be necessary for proper targeting of TgGAP50, a finding that is not surprising considering the domain encompasses 81.4% of the total protein.

**The transmembrane domain is critical for TgGAP50 targeting to the IMC, but the cytoplasmic domain is not**

To test the importance of the cytoplasmic domain in targeting, we expressed a hybrid in which the cytoplasmic domain of TgGAP50 was replaced with that of HLA-A2 (C-hybrid). Our lab has previously found that the absence of TgGAP50 cytoplasmic sequence still allows proper targeting to the IMC, although the other members of the glideosome are not able to bind (Gaskins et al., 2004). The substitution of the cytoplasmic domain of TgGAP50-YFP with that of HLA-A2 (C-hybrid) has similar properties, localizing to the pellicle of the parasite (Figure 3). To determine the role of the transmembrane domain in IMC targeting of TgGAP50-YFP, we expressed the hybrid in which only the transmembrane domain was replaced with that of HLA-A2 (TM-hybrid). We found that this protein also localizes to the pellicle of the parasite. The expression of the TMC-hybrid, in which both the transmembrane and cytoplasmic domains of TgGAP50 are replaced with those of HLA-A2 localizes to the pellicle in a similar manner.

It is unclear if these hybrids that localize to the pellicle are associated with the IMC or the plasma membrane (Figure 3). To ascertain which pellicle membrane these two hybrids are targeting to, we looked for the presence of the three YFP tagged hybrid proteins in replicating parasites. Wild-type TgGAP50 is inserted in the IMC of developing daughter cells during replication (Figure 4) whereas plasma membrane proteins are not found to colocalize with daughter cells. We found that the C-hybrid localizes to daughter cells as does wild-type TgGAP50-YFP, while the TM-hybrid and the TMC-hybrid do not (Figure 4). These data indicate the cytoplasmic domain has no effect on localization; however the transmembrane domain is necessary for proper targeting to the IMC.

**The TgGAP50 cytoplasmic domain is not necessary for targeting, but is required for motility**

While the C-hybrid protein still localizes to the IMC, however it is unable to bind the other three members of the glideosome, similar to TgGAP50-YFP lacking the cytoplasmic residues (data not shown and Gaskins et al., 2004). To determine if the overexpression of the C-hybrid or any of the other hybrids has an effect on parasite motility, we utilized a gliding motility assay. As parasites move, they shed a variety of proteins such as actin and surface antigen 1 (SAG1) in a circular trail pattern. By using a monospecific antibody against SAG1 we can visualize these trails and therefore visualize parasite movement. Extracellular parasites expressing wild-type TgGAP50-YFP and parasites overexpressing each hybrid protein were incubated on coated coverslips for 30 minutes at 37°C. We found that parasites were motile if they expressed a protein in which the TgGAP50 transmembrane domain was replaced (TM-hybrid and TMC-hybrid) while parasites expressing hybrid proteins with a wild-type TgGAP50 transmembrane domain intact were not as motile (C-hybrid) with the exception of the fully intact protein with no substituted domains (Figure 5). Invasion of these less motile C-hybrid parasites was normal, however, plaque size of infected HFF monolayers were smaller in size (data not shown). These data suggest gliding motility is affected in the absence of certain TgGAP50 domains, alluding to the mechanism of the glideosome itself.

**The conserved half of the TM domain is critical for IMC targeting**

To further investigate the properties of the TgGAP50 transmembrane domain, we analyzed the amino acid sequence by homology to five other apicomplexan

parasites. The first 12 residues of the 24 amino acids in this domain are almost completely conserved while the last 12 residues are not even similar (Figure 6). This region of homology shows the most conservation compared to the various domains of the protein indicating a likely conserved function among parasites. Based on the data from the C-hybrid and the TM-hybrid, we attempted to analyze the localization properties of the conserved domain versus the non-conserved domain. We constructed hybrids containing either the conserved half of the TgGAP50 transmembrane domain with the second half of the HLA-A2 transmembrane domain ($C^{1/2}$TM-hybrid) or the first half of the HLA-A2 transmembrane domain followed by the non-conserved half of the TgGAP50 HLA-A2 transmembrane domain ($NC^{1/2}$TM-hybrid) (Figure 6). Both proteins were targeted to the pellicle of the parasite, but when daughter cells were analyzed, only the $C^{1/2}$TM-hybrid showed colocalization with immature IMC suggesting the $NC^{1/2}$TM-hybrid is in the plasma membrane (Figure 7). This indicates the first 12 amino acids of the TgGAP50 transmembrane domain are necessary for proper targeting of the protein.

## Discussion

Integral membrane proteins have many functions from tethering cytoskeletal proteins and maintaining structure to acting as receptors to initiate signaling cascades. Regardless of function, it is imperative that these proteins are targeted to the proper membrane in order to carry out its function. The ability of TgGAP50 to anchor the gliding motility apparatus relies on proper targeting to the inner membrane complex.

Our results show that the lumen and the conserved half of the transmembrane domains of TgGAP50 are important for localization to the IMC, while the cytoplasmic domain is not. Our efforts to replace the lumen domain with a number of proteins (AAT, β-lactamase, myc tag) or the deletion of the lumen have proven to be difficult because they are difficult to express. Protein that is expressed does not target to the IMC, but remains cytoplasmic and nuclear, indicating the lumen is important for targeting TgGAP50. In all hybrids, the 50 amino acid signal sequence is present at the N-terminus.

Transmembrane domains are found in a variety of proteins, and can be either alpha-helical or beta-barrel in structure. The majority of transmembrane proteins are alpha-helical and can consist of a single transmembrane α-helix (bitopic membrane protein) or it can be a polytopic α-helical protein with more than one membrane spanning domain. Tail-anchored transmembrane proteins are known to contain an extracellular and cytoplasmic portion of protein with only one transmembrane domain towards the extreme C-terminal end. These proteins do not have an N-terminal signal sequence, so the mechanism of how these proteins get inserted into the membrane is still under investigation (Rayner and Pelham, 1997).

The process of how TgGAP50 is inserted into the IMC is still largely unknown, but it is found in both the immature daughter cell IMC of replicating parasites as well as mature IMC. Although similar in topology to tail-anchored proteins, TgGAP50 does have a signal sequence and it is speculated to be required for proper orientation of the protein in the IMC; however it is not sufficient to target the protein to the IMC. There are no other known proteins in the IMC of *Toxoplasma*

*gondii*, so it is unknown if the sequence of the conserved TgGAP50 transmembrane domain is a defining element of these proteins.

TgGAP50 is found to be associated with detergent-resistant raft-like domains in the IMC, so the targeting of TgGAP50 is potentially influenced by these domains (Johnson et al., 2007). Many proteins associate with lipid rafts or raft-like domains via the sequence of a transmembrane domain. Prohormone convertase 3 (PC3) associates with lipid rafts through a twenty amino-acid stretch in the transmembrane domain, but when this sequence is altered, raft association is lost (Lou et al., 2007). Many virus proteins also exhibit this effect, such as the influenza virus neuraminidase (NA) type II protein which relies on lipid rafts for association and virus budding (Barman et al., 2004). Other integral membrane proteins do not exhibit sequence specific targeting to rafts. Respiratory syncytial virus F envelope protein associates with lipid rafts, but the exchange of the transmembrane domain with that of a non-raft protein, localization was not altered (Fleming et al., 2006).

For some hybrids, overexpression led to the accumulation of protein in cytosolic compartments. The $NC^{1/2}$TM-hybrid localizes to the plasma membrane however a portion of protein was detected in the organelles of the secretory pathway. Co-transfections using a Golgi apparatus protein, GRASP-RFP, or antibodies to an endoplasmic reticulum protein, BiP, demonstrated that the $NC^{1/2}$TM-hybrid accumulates in the Golgi complex (data not shown).

It has previously been shown that the cytoplasmic domain of TgGAP50 is necessary for the association of the other glideosome proteins, MyoA, GAP45, and MLC1 (Gaskins et al., 2004). The other members of the glideosome do not associate with TgGAP50 until the IMC is mature and replication is complete.

Preliminary data shows that the requirements for glideosome formation are that TgGAP50 targets properly and has the cytoplasmic domain intact although we have not tested the effects on glideosome immobilization. It is possible that the second half of the transmembrane domain has a role in immobilization, depending on how the lipid domains are ordered.

A model can be made based on the motility defect seen in the C-hybrid, but not the other hybrids. Overexpression of a hybrid lacking the cytoplasmic domain (C-hybrid) localizes to the IMC, but if this space was not previously occupied by a TgGAP50 molecule, it will not have an effect on motility as the number of TgMyoA molecules does not change (Figure 8A). If the TgGAP50 molecules are tightly packed in the IMC, replacement of endogenous molecules with non-glideosome-binding TgGAP50 would have an effect on motility, as there would be fewer molecules of TgMyoA available to interact with polymerizing actin (Figure 8B). We do find a defect in motility, indicating Figure 8B is more probable. Ideally, FRAP experiments on parasites expressing these hybrids will determine to what extent each domain is responsible for immobilization of the glideosome.

## Materials and Methods

### Culture of *Toxoplasma*

The RH (HXGPRT-) strain of *Toxoplasma gondii* and its derivatives expressing various fusion proteins were maintained in human foreskin fibroblasts (HFF) as described previously (Gaskins et al., 2004). Parasites were isolated from freshly lysed cultures by passage through 18G and 25G needles and centrifugation at room temperature for 5 minutes at 800 x g. Parasites were resuspended in PBS

and passed through 5 µm filters to remove the small amount of host cell debris and collected again by centrifugation as described above.

**Hybrid construction and expression in *Toxoplasma***

To generate the TgGAP50-YFP hybrids inverse PCR was used to engineer sites into TgGAP50-YFP to include a MfeI site between the signal sequence and lumenal domain, an AatII site between the lumenal and transmembrane domain, and a PstI site between the transmembrane and cytoplasmic domains. The luminal domain of TgGAP50 was replaced with AAT using MfeI and AatII. Transmembrane and cytoplasmic domains of TgGAP50 were replaced by the corresponding HLA-A2 domains using the enzymes AatII and PstI and/or an AvrII site at the C-terminus of TgGAP50. Inserts were then cloned into pTUB-YFP/CAM (Hu et al., 2002), and confirmed by sequencing. Hybrids were transfected into parasites by electroporation, and stable transfectants were obtained by selection with chloramphenicol (Mann et al., 2002).

**Immunofluorescence**

Parasites were allowed to invade a human foreskin fibroblast (HFF) monolayer overnight at 37°C. They were then fixed with 3% (w/v) paraformaldehyde in PBS for 15 minutes at room temperature. Cells were permeabilized in 0.5% (v/v) TX100 in PBS for 7 minutes at room temperature and incubated with primary antibody (Rabbit α-IMC1) for 30 minutes in 3% (w/v) BSA in PBS. The generation of monospecific antisera to *Toxoplasma* IMC1 has been described previously (Mann et al., 2002).

Samples were washed in PBS and incubated with Alexa Fluor®594-conjugated secondary antibody (Invitrogen Corporation, Carlsbad, CA) in 3% (w/v) BSA in PBS for 30 minutes at room temperature. Coverslips were washed and mounted in Mowiol. Images were captured using an epifluorescence Nikon Eclipse TE-2000 microscope (Nikon Inc., Melville, NY), a Hamamatsu 1394 cooled digital CCD camera (Hamamatsu) and Metamorph® imaging software (Universal Imaging Corp.). Adobe Photoshop® (Adobe Systems Inc., San Jose, CA) was used to crop and process images.

**Gliding motility assays**

Freshly harvested parasites were added to Cell-Tak-coated coverslips in HH medium (Hanks balanced salt solution [Invitrogen], 50 mM HEPES pH 7.0, and 1% [v/v] dialyzed FBS) and allowed to glide for 30 minutes at 37°C. Trails were fixed with 3% (w/v) paraformaldehyde in PBS for 15 minutes at room temperature, followed by a 20 minute incubation in 3% (w/v) BSA and immunofluorescence using a mouse anti- SAG1 primary antibody and Alexa488-conjugated secondary antibody. Images were captured as described above.

**Metabolic labeling and Immunoprecipitations**

For metabolic labeling with [$^{35}$S]-methionine/cysteine, $10^7$ parasites were added to a confluent HFF monolayer in a T25 flask. After 14-16 hours, cells were incubated for 1 hour in methionine/cysteine-free DMEM (Hyclone, Logan, UT) containing 1% (v/v) FBS prior to the addition of 0.7 mCi [$^{35}$S] methionine/cysteine (GE Biosciences, Piscataway, NJ). Parasites were collected after labeling for an additional 20-24 hours.

Extraction was performed in TX/TEN buffer (1%TX100, 10 mM Tris pH 8, 150 mM NaCl, 2 mM EDTA, 1:100 protease inhibitors) and insoluble material was collected by centrifugation at 16,000 x g for 10 minutes at 4ºC. The supernatants were incubated for 1 hour at 4°C with 1:1000 anti-YFP rabbit sera (UNC2-11) or anti-GAP45 rabbit serum, followed by incubation with protein-A-Sepharose (Zymed, San Francisco, CA) for 1 hour at 4ºC. The beads were washed four times in TX/TEN buffer, and bound proteins were eluted in reducing SDS-PAGE sample buffer containing 4% (v/v) β-mercaptoethanol (Laemmli, 1970). Immunoprecipitated proteins were separated by SDS-PAGE on 10% polyacrylamide mini gels, incubated in En$^3$hance (Perkin-Elmer, Boston, MA) for 60 minutes, followed by incubation in water for 30 minutes. Gels were dried and exposed to film.

**Gel Filtration Chromatography**

Approximately 48 hours after transfection, parasites (3 x $10^7$) were harvested by scraping, passed through a 27G needle, and collected by centrifugation for 5 minutes at 400 x g. After one wash in PBS, parasites were extracted for 10 minutes on ice in TX/TEN buffer. Insoluble material was removed by centrifugation for 10 minutes at 14,000 x g and 4°C, and the supernatant spun through a 5 μm spin filter to remove any remaining debris (Millipore, Bedford MA). The filtrate was then loaded onto a Superdex200 column of an AKTA FPLC system (GE Biosciences) equilibrated in TX/TEN buffer, and 0.5 ml fractions were collected. Fractions were precipitated with trichloroacetic acid (TCA) and acetone, resuspended in reducing SDS-PAGE sample buffer containing 4% (v/v) β-mercaptoethanol (Laemmli, 1970), run on 12% SDS-PAGE gels. Transfer to

nitrocellulose and immunoblot analysis was performed as described previously (Mann and Beckers, 2001).

## Figure Legends

**Figure 1. Multiple sequence alignment of TgGAP50.** Orthologues of the TgGAP50 amino acid sequence include E. tenella (EtGAP50), P. falciparum (PfGAP50), and P. yoelii (PyGAP50) aligned with rat purple acid phosphatase (RnAPP5). Markings are as follows: highlighted in black, 3 out of 4 residues are identical; highlighted in gray, similar residues; arrow, N-terminus of mature TgGAP50; boxed, putative transmembrane domain; ###, potential N-glycosylation sites; asterisks, residues in rat phosphatase required for metal binding and phosphatase activity. (Gaskins et al., 2004)

**Figure 2. TgGAP50-YFP hybrids.** All constructs contain the 50 amino acid signal sequence peptide and a C-terminal YFP tag. The three domains of TgGAP50 are swapped with either the human class I histocompatibility molecule (HLA-A2) or alpha-1-antitrypsin (AAT). Domains: L, lumen; TM, transmembrane; C, cytoplasmic.

**Figure 3. Localization of TgGAP50 hybrids.** Immunofluorescence assays show the distribution of YFP-tagged hybrids compared to the inner membrane complex, which was detected using monospecific antisera to TgIMC1. Full length TgGAP50-YFP localizes to the IMC. Scale bars, 2µm.

**Figure 4. Localization of TgGAP50 hybrids in replicating parasites.** Immunofluorescence assays show the distribution of YFP-tagged hybrids in daughter cells of replicating parasites compared to the inner membrane complex. Full length TgGAP50-YFP localizes to the IMC in both replicating and non-replicating parasites. Scale bars, 2µm.

**Figure 5. Motility assays demonstrate a motility defect for the C-hybrid.** Extracellular parasites expressing wild-type TgGAP50-YFP and parasites expressing each hybrid protein were incubated on coated coverslips for 30 minutes at 37°C followed by IFA with antisera to SAG1 to detect trails. Trail length and direction are compared to wild-type TgGAP50-YFP. Scale bars, 5µm.

**Figure 6. TgGAP50 transmembrane domain hybrids.** Two hybrids were made based on the conservation of TgGAP50 sequence in the transmembrane domain. The $C^{1/2}$TM-hybrid contains the conserved half of the TgGAP50 transmembrane domain with the second half of the HLA-A2 transmembrane (TM) domain and the $NC^{1/2}$TM-hybrid contains the first half of the HLA-A2 transmembrane domain followed by the non-conserved half of the TgGAP50 HLA-A2 transmembrane domain. All other domains of TgGAP50 remain intact with a C-terminal YFP tag.

**Figure 7. Localization of TgGAP50 transmembrane domain hybrids.** Immunofluorescence assays show the distribution of YFP-tagged transmembrane hybrids ($C^{1/2}$TM-hybrid [A] and $NC^{1/2}$TM-hybrid [B]) in mature parasites and daughter cells of replicating parasites compared to the inner membrane complex. Scale bars, 3µm.

**Figure 8. Model of TgGAP50 distribution in the inner membrane complex.** Overexpression of a hybrid lacking the cytoplasmic domain (C-hybrid) localizes to the IMC, but if this space is not previously occupied by a TgGAP50 molecule, it may not have an effect on motility as the number of TgMyoA molecules does not change (A). If the TgGAP50 molecules are tightly packed in the inner membrane complex (IMC), replacement of endogenous molecules with non-glideosome-binding TgGAP50 would have an effect on motility, as there would be fewer molecules of TgMyoA available to interact with polymerizing actin (B). We do find a defect in motility, indicating B is more probable.

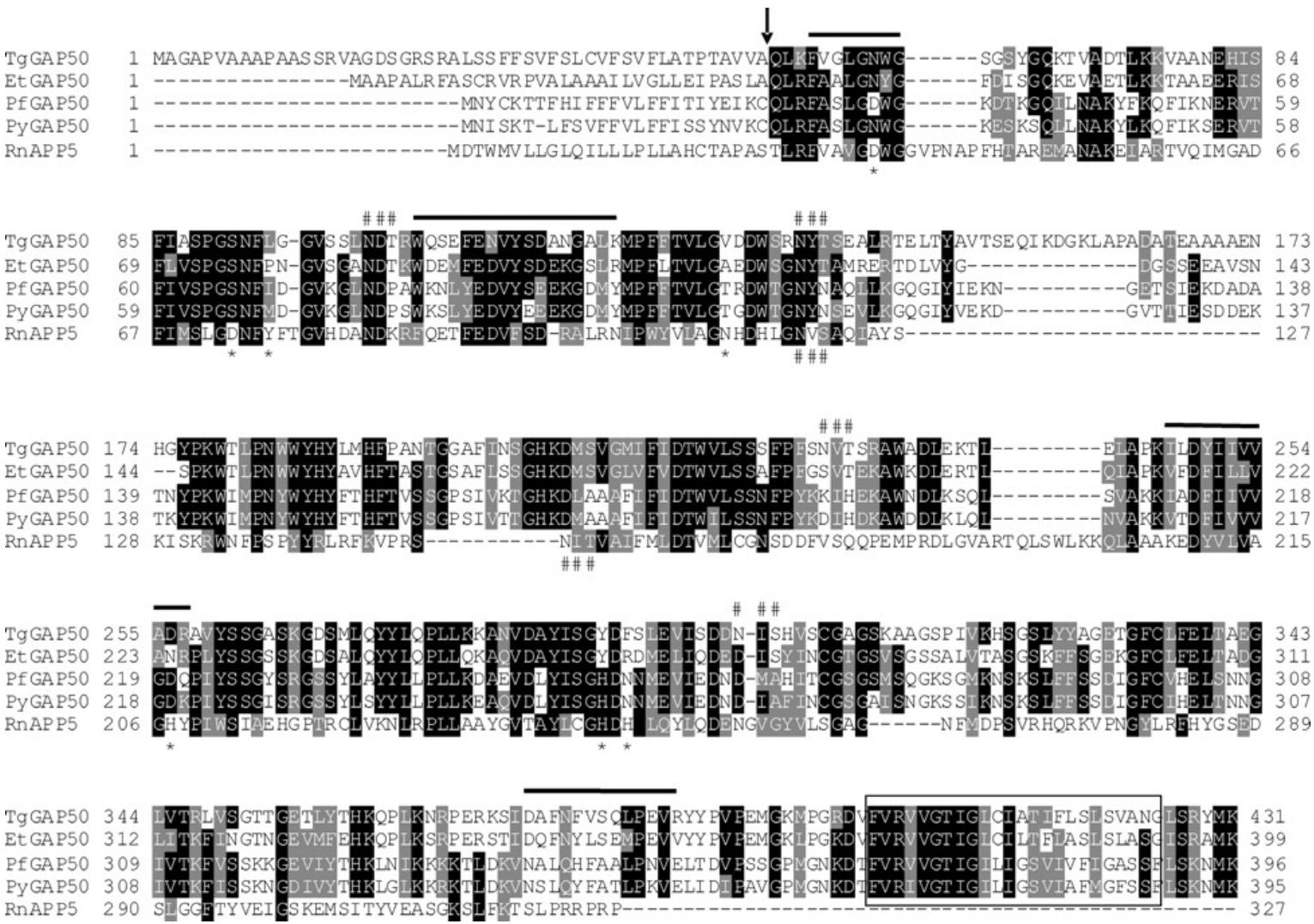


**Figure 1. Multiple sequence alignment of TgGAP50.** (Gaskins et al., 2004)

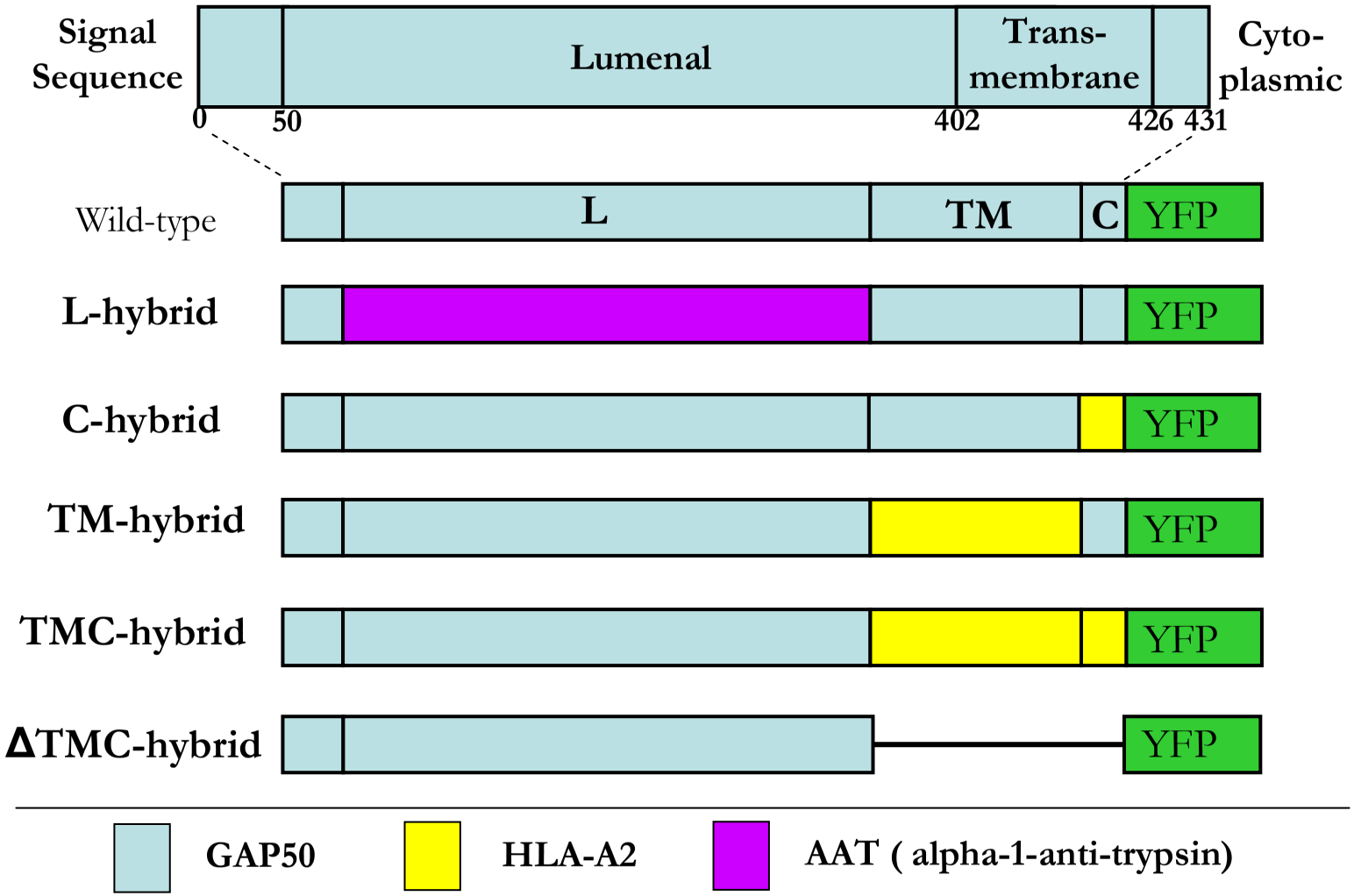


**Figure 2. TgGAP50-YFP hybrids.**

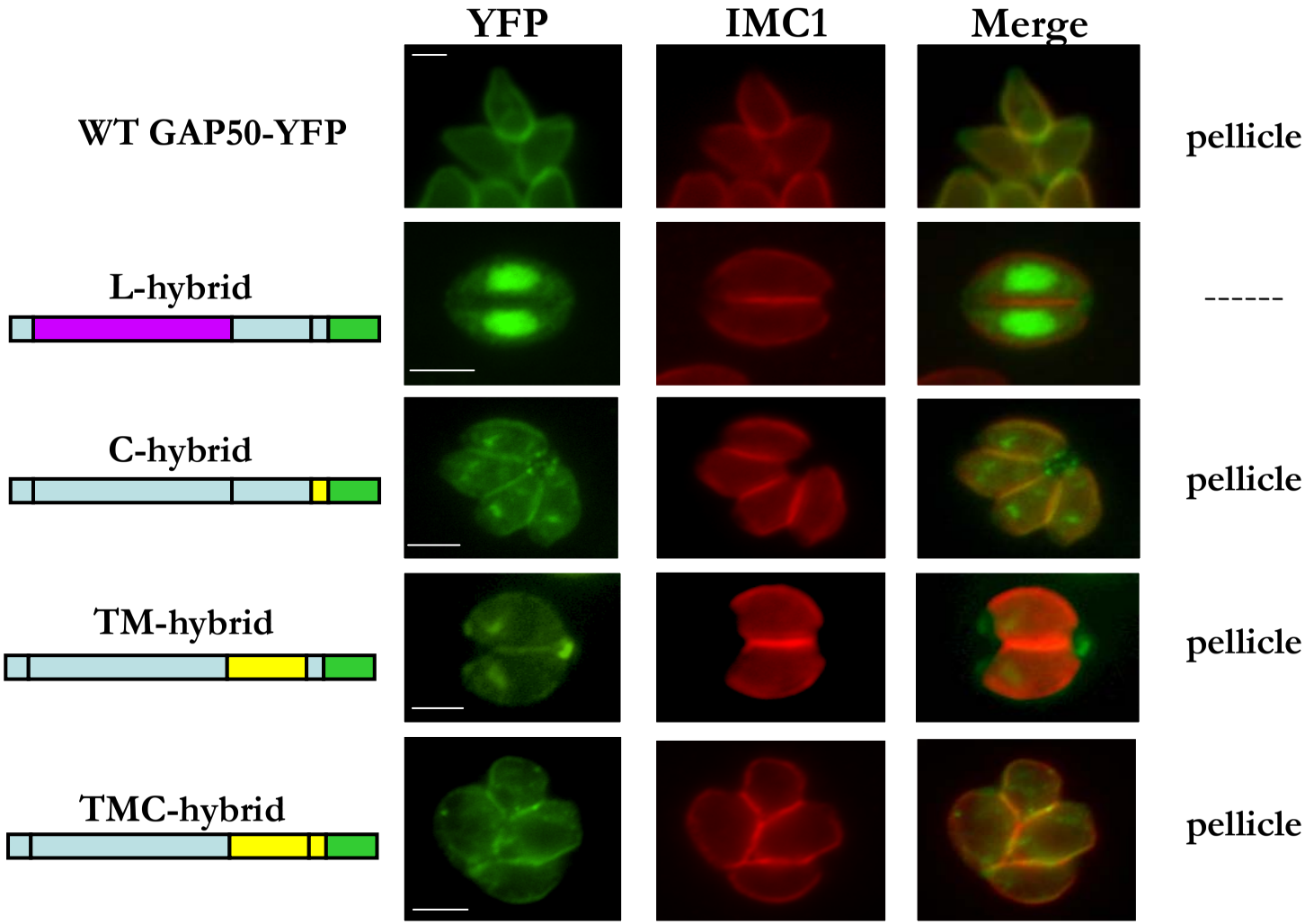


Figure 3. Localization of TgGAP50 hybrids.

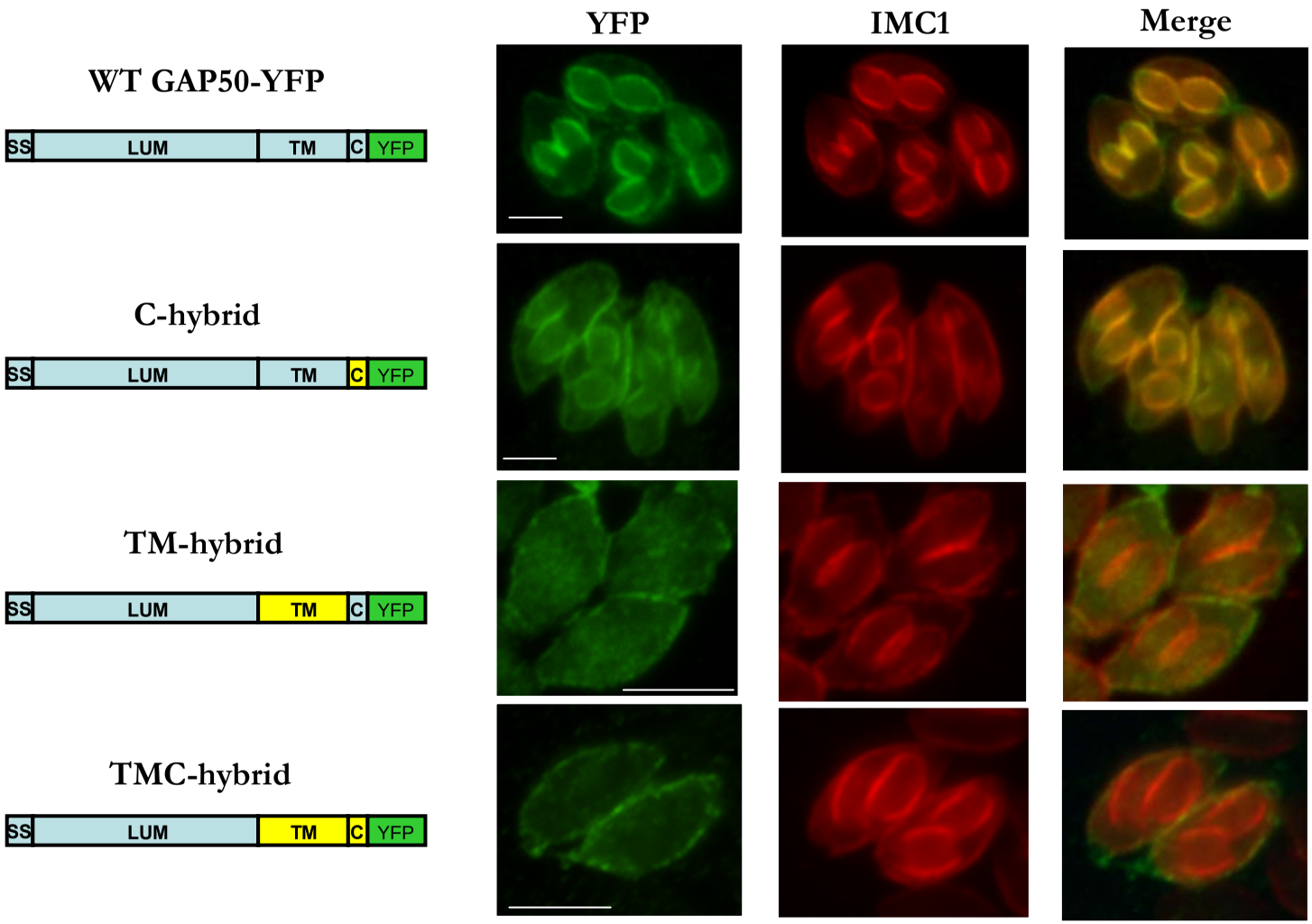


Figure 4. Localization of TgGAP50 hybrids in replicating parasites.

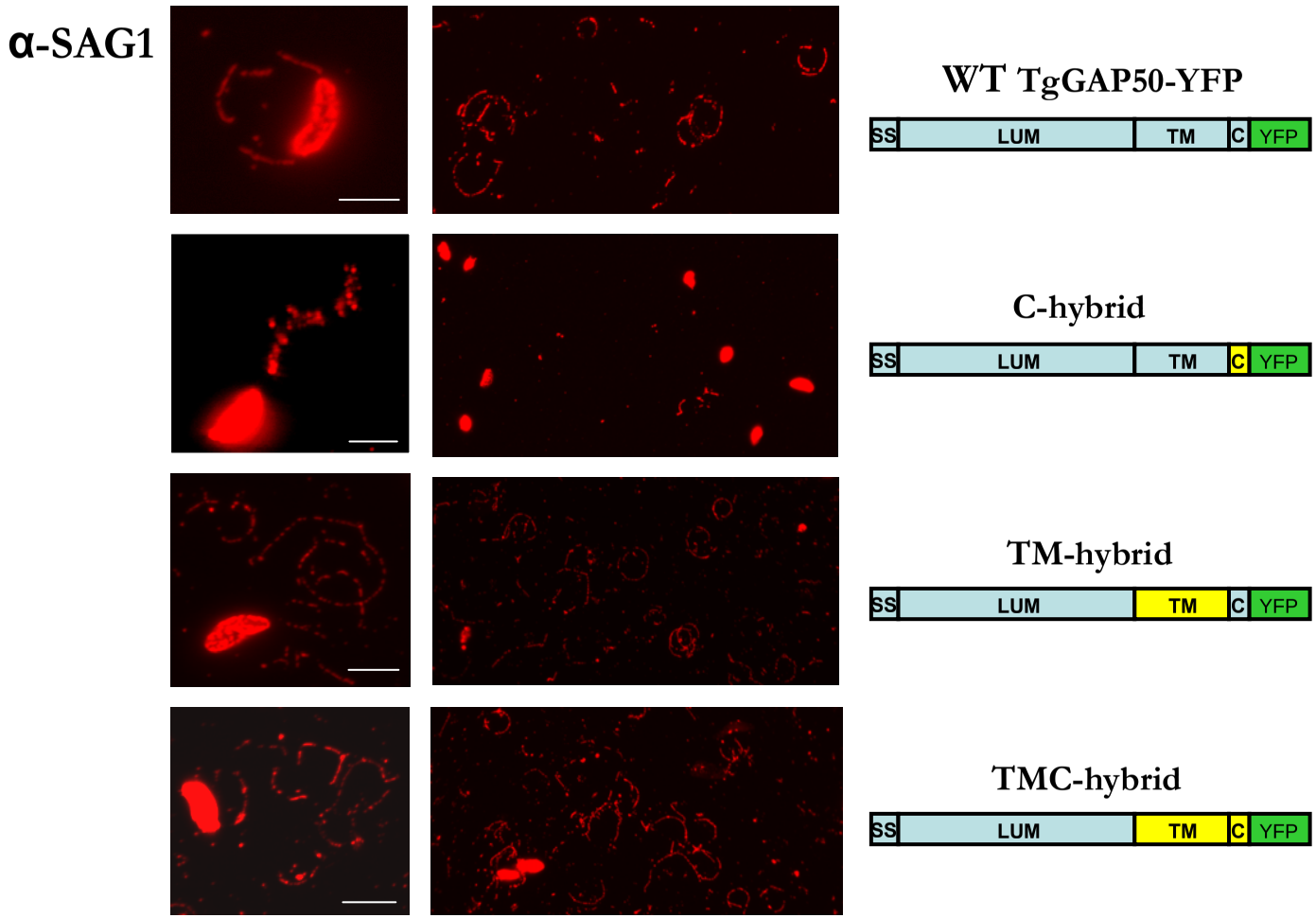


**Figure 5. Motility assays demonstrate a motility defect for the C-hybrid.**

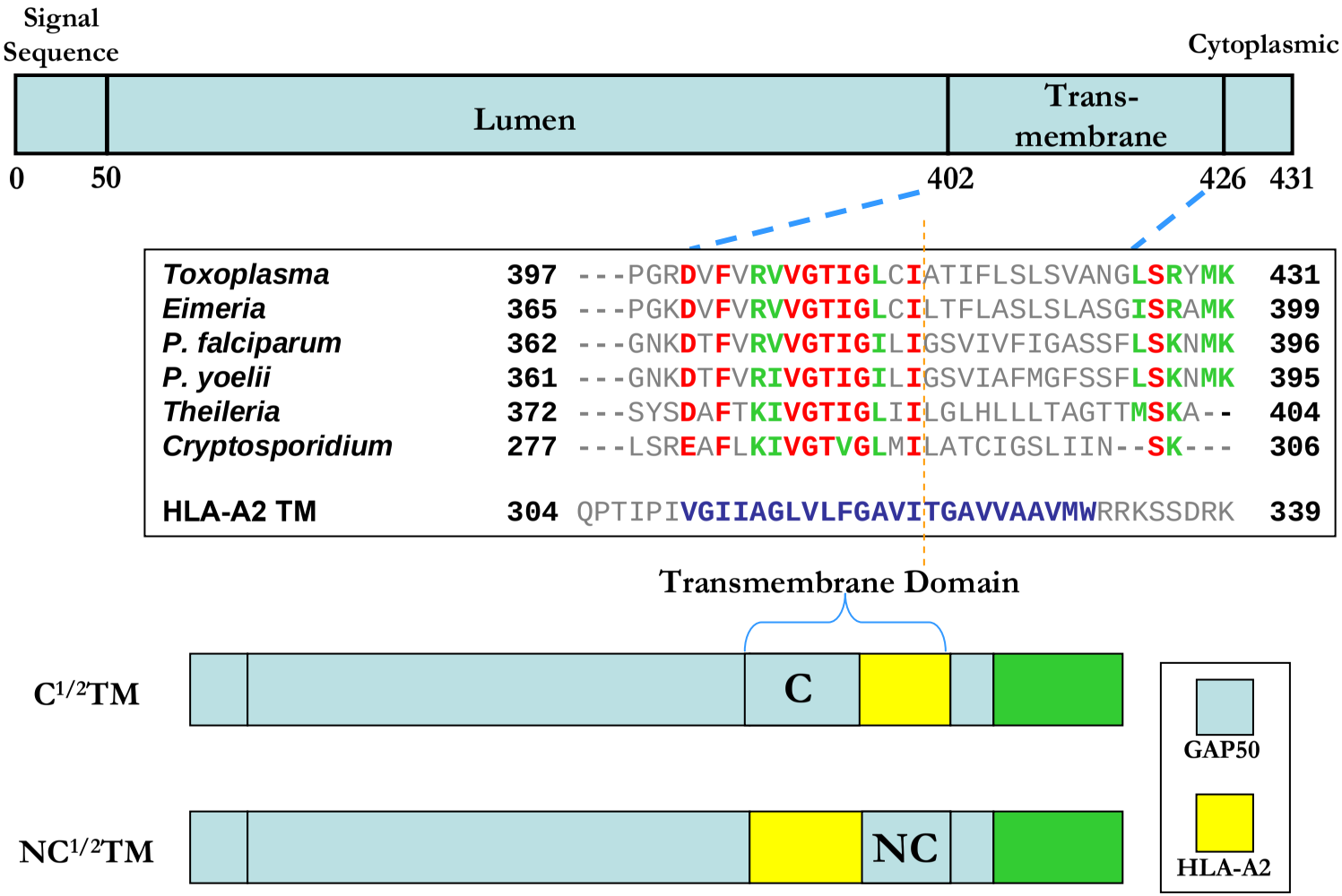


Figure 6. TgGAP50 transmembrane domain hybrids.

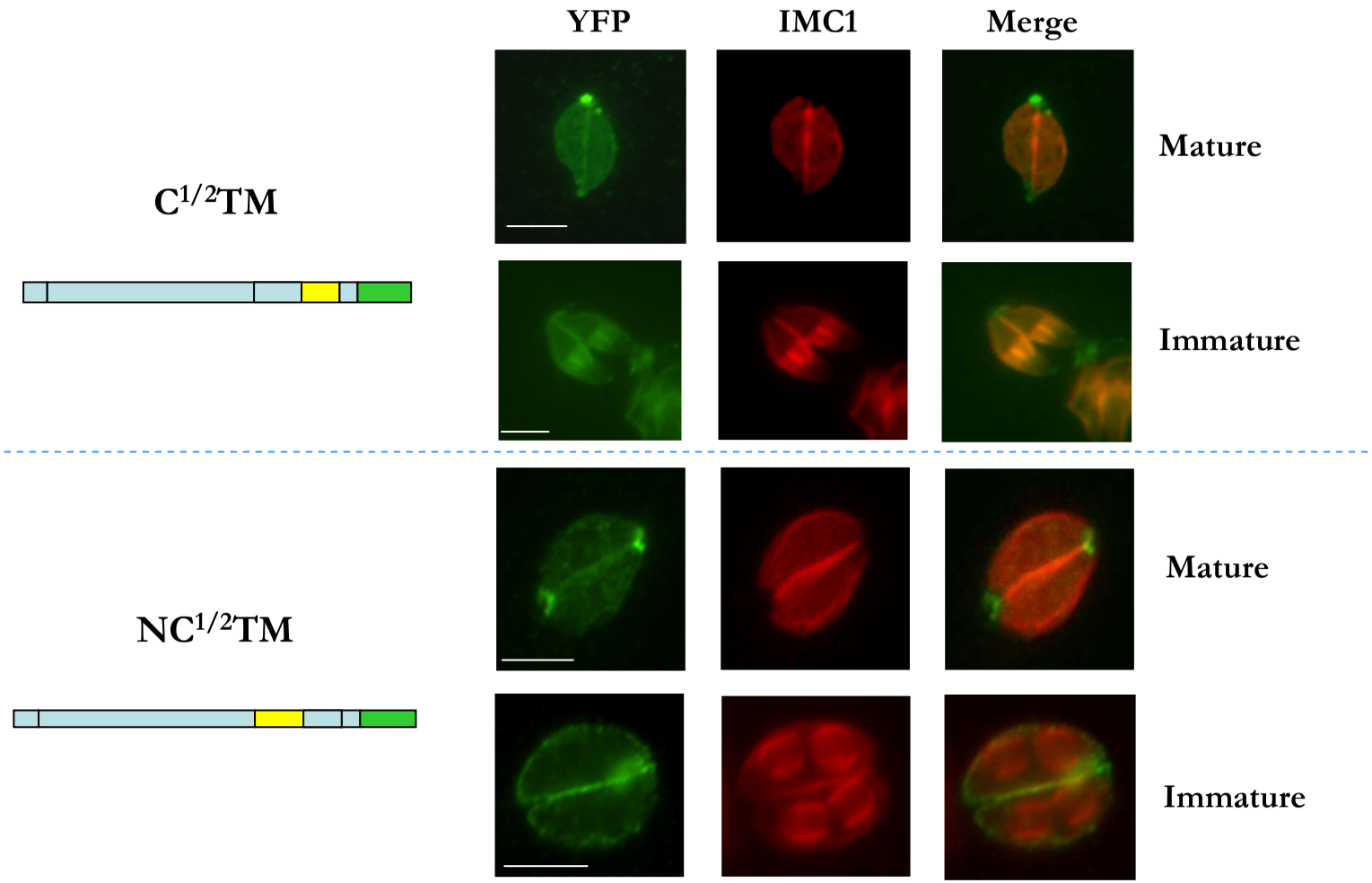


**Figure 7. Localization of TgGAP50 transmembrane domain hybrids.**

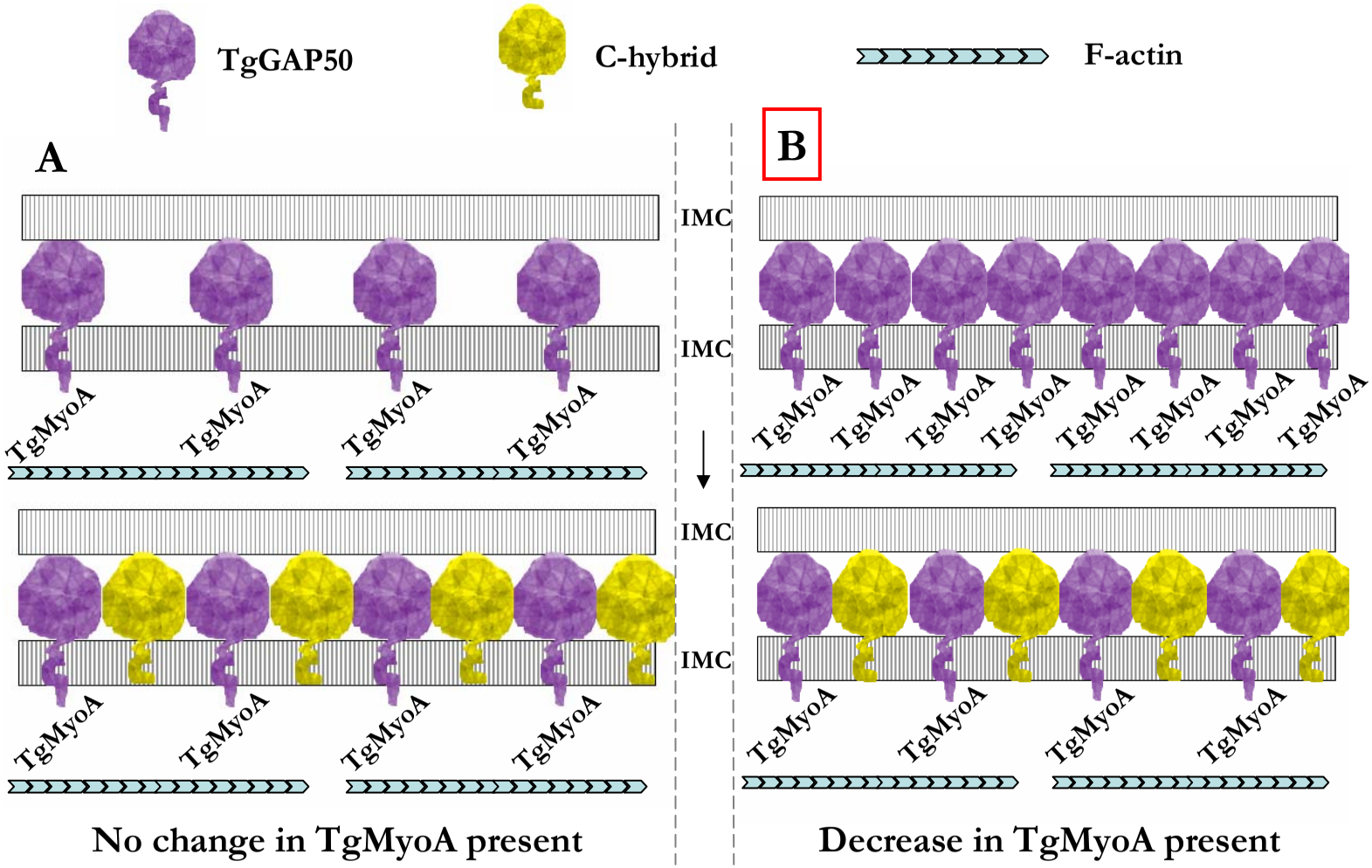


Figure 8. Model of TgGAP50 distribution in the IMC.

# CHAPTER IV

# CHARACTERIZATION OF THE TYPE XIV MYOSIN COMPLEX

## Introduction

*Toxoplasma gondii,* a parasite that can cause blindness and brain damage in immunocompromised individuals, and the malaria parasite *Plasmodium* are of the Phylum Apicomplexa, which are obligate intracellular parasites that utilize an active mode of host-cell entry. This motility is not dependent on a typical motility structure, such as a flagellum or lamellipodia, and the cell moves without changing shape. Instead they use a substrate-dependent type of motility, called gliding motility, which is essential for invasion and migration across biological barriers.

Gliding motility is dependent on a heterotetramer complex called the glideosome that includes a type XIV myosin, TgMyoA. This motor protein is found at the periphery of the parasite, the pellicle, where it associates with the inner membrane complex (IMC). The IMC consists of two closely apposed membranes just interior of the plasma membrane (PM), which together form the triple bilayer of the pellicle. Between the IMC and PM, TgMyoA associates with F-actin to provide motility for the parasite. The F-actin is bound to the host cell or substrate via protein interactions with adhesions that pass through the PM.

TgMyoA is anchored to the IMC, and therefore the cytoskeleton, by the integral membrane protein TgGAP50 (Gaskins et al., 2004). TgGAP50 immobilizes the glideosome to provide a mechanical base for TgMyoA force production (Johnson et

al., 2007). Aside from TgMyoA and TgGAP50, the glideosome contains two other proteins, TgMLC1, a calmodulin-like light chain, and TgGAP45, a novel protein that only shows homology to the same protein in other apicomplexans.

The glideosome is assembled in two stages, beginning with three proteins associating in the cytosol, TgMyoA, TgMLC1, and TgGAP45, to form the proto-glideosome (Gaskins et al., 2004)(Figure 1). TgGAP50 is co-translationally inserted into the IMC, where it eventually associates with the proto-glideosome at the periphery of mature parasites (Gaskins et al., 2004).

**TgGAP50**

TgGAP50 is an integral membrane glycoprotein that localizes to the IMC membranes of both daughter cells in replicating parasites and mature parasites. It is important to know how this glideosome anchoring protein is situated at the IMC, in order to form a model for glideosome participation in gliding motility. It has not been confirmed if TgGAP50 is only oriented in both faces of the IMC, or one direction, with the luminal domain between the two IMC membranes, the transmembrane domain passing through the outer membrane of the IMC, and the cytoplasmic domain located in the space between the IMC and PM. It is important to determine the sidedness of glideosome orientation to correctly form a model of gliding motility. In order to accomplish this, we can establish if TgGAP50 is present on one side of the IMC, or both.

**TgGAP45**

*Toxoplasma* motility depends upon TgMyoA function. Therefore, motility is dependent on proper glideosome assembly and function. Of the three TgMyoA

accessory proteins, the specific function has only been determined for one, TgGAP50, as the immobilized anchor for TgMyoA (Gaskins et al., 2004; Johnson et al., 2007). The role of TgGAP45 is unknown; however, it appears to be involved with targeting the proto-glideosome to the IMC. It has been demonstrated in *Plasmodium* that PfGAP45 is N-myristoylated and palmitoylated, the latter occurring once targeted to the IMC (Rees-Channer et al., 2006). The myristoylation event is sufficient to target PfGAP45 and TgGAP45 to the IMC, although the binding strength is estimated to be fairly weak (Rees-Channer et al., 2006; manuscript in preparation; Resh, 1999). The palmitoylation event may contribute to stabilizing the interaction between the glideosome and the IMC. TgGAP45 is heavily phosphorylated which may play a role in glideosome formation (Gilk et al., in preparation). Little is known about the structure of this protein, so we will examine the properties of TgGAP45 with a combination of experiments.

## Results

### TgGAP50 localizes to the outer face of the IMC

TgGAP50 localizes to the IMC in both replicating daughter cells and mature parasites (Gaskins et al., 2004). Most models for gliding motility suggest the protein may be localized to only one side of the IMC, where it interacts with actin on the outer face to move the parasite (Soldati and Meissner, 2004). Other models predict TgGAP50 may be found in both sides of the IMC, with its cytoplasmic domain available to anchor TgMyoA acting as a conveyor belt (Black and Boothroyd, 2000). For this model to be correct, actin would also be found on both sides of the IMC to associate with this TgGAP50-bound TgMyoA. To determine which face of the IMC TgGAP50 resides in, we used pre-embedded immuno-

electron microscopy to visualize TgGAP50-YFP. Parasites expressing TgGAP50-YFP were sonicated, to perturb the association of the IMC with the plasma membrane, and fixed for thin sectioning. Gold particles labeled the tagged protein, which was found only on the outer face of the IMC facing the plasma membrane (Figure 2A). As controls, the same procedure was done using antibodies to TgGAP45 and a cytoskeletal protein IMC1, which is found on the inner, cytoplasmic face if the IMC (Figure 2B and 2C).

**TgGAP45 does not oligomerize, but the N-terminal half may have an unusual elongated structure**

Our preliminary data show that the glideosome elutes as a complex of greater than 650 kD by gel filtration chromatography (Figure 3A). If each of the four glideosome proteins formed a monomer complex, the predicted size would be approximately 200 kD. In order to determine the oligomerization status of the glideosome, we utilized velocity sedimentation and found the complex has a sedimentation constant similar to that of catalase, a 230 kD protein (Figure 3B). To solve this discrepancy, we utilized a combination of both methods, beginning with velocity sedimentation (Figure 3C). Two peaks containing TgGAP45, as determined by Western blot, were subjected to gel filtration separately. These peaks correlated to the molecular weights of ~200 kD and ~45 kD judged by sedimentation patterns of controls. The ~200kD complex eluted as a ~660 kD complex, while the ~45 kD fraction eluted at ~230 kD (Figure 3C). TgMyoA, TgMLC1 and TgGAP50 were present in the larger 660 kD fraction at all stages indicating the complex remains tightly associated.

In order to determine if TgGAP45 was responsible for this unusual outcome, we expressed TgGAP45 in COS7 cells and analyzed the protein by gel filtration. We found that TgGAP45 by itself behaves as a ~200 kD protein during gel filtration (Figure 4A) while it co-sediments with a 29 kD standard protein during velocity sedimentation (Figure 4B). These data combined suggest that TgGAP45 has an unusual and perhaps elongated shape. This abnormal shape could be causing the entire complex to elute larger than expected during gel filtration.

To elucidate which element of TgGAP45 causes this discrepancy in size, we utilized two parasite cell lines: one that expresses the N-terminal half of TgGAP45, and another expressing the C-terminal half of TgGAP45, both tagged with YFP. Parasite lysates expressing these proteins were analyzed by gel filtration chromatography and it was determined that the N-terminal half of the protein, which is predicted to form a coiled-coil domain, is responsible for the increase in size (Figure 4C). This protein elutes as a protein approximately five times its predicted size, whereas the C-terminal protein elutes in the predicted fraction.

**Glideosome Purification**

We have purified the glideosome for visualization using a three-step strategy, beginning with a sequential detergent extraction. We have the ability to fractionate all proteins with this extraction process, first removing all plasma membrane and cytoplasmic contents, then solubilizing IMC proteins from the cytoskeletal elements (Johnson et al., 2007). We used this process to fractionate glideosome as a soluble complex after a second detergent extraction. The next step, actin cosedimentation, involves binding glideosome via TgMyoA to phalloidin-stabilized F-actin to remove non-actin binding proteins by centrifugation. Addition of ATP will remove the

glideosome from F-actin followed by a final centrifugation step to pellet actin. To further purify the sample from other proteins that may bind in an actin-dependent manner, we will utilize gel filtration. Glideosome elutes at its highly reproducible molecular weight, allowing us to pool fractions for analysis. All fractions were analyzed by Western blot to confirm the eluted glideosome location.

We were able to visualize the glideosome by negative staining in collaboration with Dr. Jack Griffith of UNC. Imaging by negative stain was performed as described previously (Walker, et al., 1995) in the lab of Dr. Jack Griffiths and samples were visualized using a transmission electron microscope. The glideosome, after elution from F-actin, appears to be 20-30 nm across in size (Figure 5A). Samples of the pelleted fraction prior to ATP incubation were also analyzed by negative stain imaging (Figure 5B). The individual complexes appear to bind F-actin with a periodicity of approximately 30 nm. Controls were carried out in which F-actin alone was imaged, to check for possible actin-binding proteins from the rabbit actin stock (Figure 5C). The supernatant from a mock actin knock-off was also visualized in which ATP allowed these actin-binding proteins to be released from F-actin (Figure 5C). This allowed us to visualize other actin-binding proteins to compare with glideosome eluted in the same manner. These particles were mostly globular and 2-5nm in diameter, much smaller than the glideosome complexes shown in Figure 5A. Further experiments are necessary to determine which domains of the imaged complex represent TgMyoA, TgGAP45, and TgMLC1.

## Discussion

*Toxoplasma* spreads amongst host cells and invades using a peculiar corkscrewing motility. Amongst the four proteins of the glideosome, the complex involved in gliding motility, the function is only known for two of those proteins, TgMyoA and TgGAP50. Here we demonstrate that TgGAP50 is only found in the outer face of the IMC as opposed to being oriented in both faces, as predicted by some models. We also demonstrate that TgGAP45 may have an elongated shape, possibly due to an unusual N-terminal region that may contain a variant coiled-coil. Finally, we are able to visualize glideosome, from a multi-step purification protocol, and image the complex by negative staining.

A previous model of gliding motility suggested TgMyoA was able to interact with filamentous actin along the interior of the plasma membrane and along the interior of the IMC, where the sub-pellicular cytoskeleton lies (Black and Boothroyd, 2000). This would involve TgGAP50 residing in both the inner and outer faces of the IMC, in order to place TgMyoA in the presence of actin filaments. The resulting motion would act as a conveyor belt, providing force from both sides of the IMC. Our results indicate that this is not the case, as TgGAP50 is only found to be present on the outer face of the IMC, facing the PM (Figure 2). This is consistent with the need for actin filaments to be associated with the substrate through adhesions (MIC2) and the glycolytic enzyme aldolase.

The glideosome elutes as a very large complex by gel filtration (Figure 3A), yet it does not appear to form oligomers as demonstrated by velocity sedimentation (Figure 3B). TgGAP45 alone does not seem to form dimers as judged by velocity sedimentation and gel filtration analysis (Figure 4A and 4B) however the N-terminal half of the protein is responsible for the size discrepancy seen (Figure 4C). TgGAP45 is predicted to have a coiled-coil region encompassing the entire N-

terminal half of the protein so this may represent an unusual structural region (Lupas et al., 1991). This may cause TgGAP45, and therefore the entire glideosome, to have an extended shape. Most myosins have a tail region that functions as part of the lever arm, binding to membranes or other proteins to provide stability for the myosin head (Foth et al., 2006). TgMyoA has a short tail compared to most myosins, so it is possible that TgGAP45 acts as a lever arm for TgMyoA, as it is known that TgGAP45 is heavily phosphorylated (Gilk et al., in preparation). These data combined suggest a role for GAP45 in glideosome targeting and assembly. In order to discern why TgGAP45 shows unique shape characteristics, visualization of the protein within the complex is necessary.

In some cases, the easiest way to determine if a protein or complex has an unusual shape it to visualize it. In this case, purification of the glideosome allowed us to image the complex with TgMyoA in both bound and unbound actin conformations. We are not able to discern much information about the complex structurally, except that it is not globular as a whole. It appears to have one or two lobes protruding from the center, which may be TgMyoA, TgGAP45, or both. It will be important to repeat these types of experiments using markers that label either protein, in order to determine the specifics of the complex. Averaging software can then be used to predict actual structural information. This method of purification is useful in that other assays that require pure protein, such as sliding filament assays, can be now be performed using purified glideosome.

## Materials and Methods

### Immuno-electron Microscopy

Parasites expressing TgGAP50-YFP (Gaskins et al., 2004) were isolated from freshly lysed cultures by passage through 18G and 25G needles and centrifugation at room temperature for 5 minutes at 800 x g. Parasites were resuspended in 4mL PBS and sonicated at 50% power for 10 seconds then cooled on ice for 10 seconds, repeated five times. Membranes were collected by centrifugation at 10,000rpm for 10 minutes and supernatant was removed. Insoluble material was blocked in 3% (w/v) BSA in PBS for 20 minutes, then antisera to GFP was added (1:50) and incubated at 4°C for 2 hours. Centrifugation was repeated as above and insoluble material was incubated overnight at 4°C in anti-rabbit 10nm gold particles (1:25) (Electron Microscopy Sciences [EMS], Ft. Washington, PA) in 3% (w/v) BSA in PBS. Samples were washed twice in PBS.

Insoluble parasite material was incubated in 1% glutaraldehyde (EMS) in PBS for 20 minutes on ice. Material was washed in PBS and collected by centrifugation at 16,000 x g for 10 minutes at 4°C. Samples were then resuspended in 1% tannic acid (EMS) for 20 minutes on ice, washed again, and incubated in 1% OsO4 (EMS) for 20 minutes at room temperature. Material was washed twice in PBS, dehydrated in a 50-100% ethanol series and after two washes, propylene oxide embedded in epon. The polymerized blocks were sectioned at 60 nm with a Leica Ultracut UCT ultramicrotome (Leica Microsystems Inc., Bannockburn, IL). Sections were stained with 2% uranyl acetate and Sato's lead stain, and viewed on an FEI Tecnai 12 electron microscope (FEI Company, Hillsboro, OR). Images were collected with a Gatan model 794 multi-scan digital camera (Gatan Inc., Pleasanton, CA).

**Cell culture and protein expression**

The RH (HXGPRT-) strain of *Toxoplasma gondii* and its derivatives expressing various fusion proteins were maintained in human foreskin fibroblasts (HFF) as described previously (Gaskins et al., 2004). TgGAP45-YFP constructs were made by Nicolette DeVore. Plasmid constructs were transfected into parasites by electroporation, and stable transfectants were obtained by selection with chloramphenicol (Mann et al., 2002). Parasites were isolated from recently lysed cultures by passage through 18G and 25G needles and centrifugation at room temperature (RT) for 5 minutes at 800 x g. TgGAP45 was cloned into pcDNA3.1 (Invitrogen, Carlsbad, CA) and plasmid constructs were transfected into COS7 cells using Lipofectamine (Invitrogen).

**Gel Filtration Chromatography**

After one wash in PBS, parasites were extracted for 10 minutes on ice in TBS buffer (150 mM NaCl, 25 mM Tris-HCl pH 7.4) containing 1% (v/v) TX100. Insoluble material was removed by centrifugation for 10 minutes at 14,000 x g and 4°C, and the supernatant spun through a 5 μm spin filter to remove any remaining debris (Millipore, Bedford MA). Samples were then loaded onto a Superdex200 column of an AKTA FPLC system (GE Biosciences, Piscataway, NJ) equilibrated in TBS buffer containing 1% (w/v) CHAPS, and 0.5 ml fractions collected. Fractions were precipitated with trichloroacetic acid (TCA) and acetone, resuspended in reducing SDS-PAGE sample buffer containing 4% (v/v) β-mercaptoethanol (Laemmli, 1970)), run on 12% SDS-PAGE mini-gels, and transferred to nitrocellulose for immunoblotting as described previously (Mann and Beckers, 2001). Marker proteins with known molecular weights (thyroglobulin 660 kD;

catalase, 232 kD; ovalbumin 45 kD [Amersham Biosciences]) were analyzed in parallel with the parasite lysates.

**Velocity Sedimentation**

Parasite lysates were prepared as described above in TBS buffer containing 1% (v/v) TX100. A 400 µl aliquot of supernatant equivalent to ~2.5 x $10^7$ parasites was loaded onto a 5 ml 10-40% linear sucrose gradient prepared in 13x51 mm tubes and centrifuged for 12.5 hours at 268,000 x g and 4°C in a MLS50 rotor (Beckman Coulter, Fullerton, CA). Twelve 450 µl fractions were collected from the bottom. Proteins were precipitated with trichloroacetic acid (TCA) and acetone and analyzed by SDS-PAGE and immunoblotting. Sucrose solutions were prepared in 10 mM Tris-HCl pH8. Marker proteins with known molecular weights (catalase, 232 kD; aldolase 160 kD; ovalbumin 45 kD [Amersham Biosciences]) were analyzed in parallel with the parasite lysates.

**Glideosome Purification**

**Sequential detergent extractions**

Purified parasites (3 x $10^7$) were extracted for 10 minutes on ice in TX100/PBS buffer (1% Triton X-100, 154 mM NaCl, 1.54 mM $KH_2PO_4$, 2.71 mM $Na_2HPO_4$ pH 7.4) in the presence of protease inhibitors (1:100) (Sigma-Aldrich). The TX100/PBS-soluble and insoluble material was collected by centrifugation at 16,000 x g for 10 minutes at 4°C. The TX100/PBS-insoluble material was subsequently extracted for 10 minutes on ice in TX100/TBS (1% Triton X-100, 150 mM NaCl, 25 mM Tris-HCl pH 7.4) in the presence of protease inhibitors (1:100) (Sigma-Aldrich). The TX100/TBS soluble and insoluble material was collected by

centrifugation as described above. This second soluble fraction was used for actin cosedimentation experiments detailed below.

**Actin cosedimentation**

DTT (25µM) was added to the second soluble fraction described above which was subsequently combined with General actin buffer (GAB) (5mMTris-HCl pH 8.0, 0.2mM $CaCl_2$, 1mM DTT) containing 400µg/mL phalloidin stabilized rabbit actin (Cytoskeleton, Denver, CO) and incubated at room temperature for 30 minutes. Samples were subjected to centrifugation at 50,000 rpm for 1 hour at 15 ºC in a Beckman Ultracentrifuge. Pelleted material was either used to analyze glideosome as an actin-bound sample, or resuspended in GAB for actin knock-off. After the addition of 3mM ATP samples were incubated at RT for 15 minutes, and centrifugation was repeated as above to pellet actin and collect protein previously bound to actin.

**Negative stain**

Following sequential detergent extraction and actin cosedimentation, purified protein was concentrated to approximately 50µg/ml in 20 mM Tris-HCl, pH 7.5, 50 mM NaCl, and 5 mM $MgCl_2$, using a BIORAD Micro Bio-Spin 30 Column (BIORAD, Hercules, CA). Protein was adsorbed to a thin carbon foil according to the method of Valentine and Green (1967), and negatively stained with 2% uranyl acetate. Transmission electron microscopy was performed using a Philips CM12 electron microscope (Mahkov et al., 2004). The micrographs were recorded at a x 60,000 magnification and scanned using a Nikon LS4500 film scanner.

## Figure Legends

**Figure 1. The *Toxoplasma* glideosome is assembled in two stages.** TgMyoA, TgMLC1 and TgGAP45 associate in the cytosol forming the proto-glideosome while TgGAP50 is co-translationally inserted into the IMC. Only TgGAP50 associates with the immature IMC, and it eventually associates with the three proteins of the proto-glideosome at the periphery of mature parasites (Gaskins et al., 2004).

**Figure 2. TgGAP50 is only localized in the outer face of the IMC.** Pre-embedded Immuno-electron Microscopy was used to determine TgGAP50 orientation in the IMC. A. Parasites expressing TgGAP50-YFP were incubated with anitsera to GFP. Parasites were incubated with antisera to TgGAP45 (B) or TgIMC1 (C) (Gaskins et al., 2004). All samples were labeled with 10nm gold particles. Green lines or arrows indicate microtubules. Scale bars, 200nm.

**Figure 3. Analysis of glideosome size and shape.**
A. The glideosome elutes approximately three times larger (~600-700 kD) than its predicted size (~200 kD) by gel filtration. B. The glideosome sediments at its predicted size (~200 kD) by velocity sedimentation. Standards are indicated above each figure. C. A combination of the two methods, where two velocity sedimentation fractions were subsequently analyzed by gel filtration, shows that glideosome does not oligomerize, and appears to act as a larger complex than predicted.

**Figure 4. Analysis of TgGAP45 shape and size.**
A. By gel filtration, TgGAP45 expressed in COS7 cells elutes larger (~200 kD) than its predicted size of 27 kD. B. By velocity sedimentation analysis, TgGAP45 expressed in COS7 cells sediments at its predicted size. C. Gel filtration analysis of whole TgGAP45, N-terminal and C-terminal halves of TgGAP45 expressed in parasites, all expressing a C-terminal YFP tag, show the whole protein and the N-terminal half elute as a larger protein than predicted and the C-terminal half elutes at its predicted size.

**Figure 5. Purified glideosome visualized by negative stain.**
Negative stained images of A. glideosome eluted off actin following co-sedimentation (scale bars, 20nm and 50nm), B. glideosome bound to actin, prior to ATP incubation (scale bars, 20nm), C. polymerized rabbit F-actin with all protein eluted (scale bar 20 nm), and D. the actin binding proteins not including glideosome (scale bar, 20 nm).

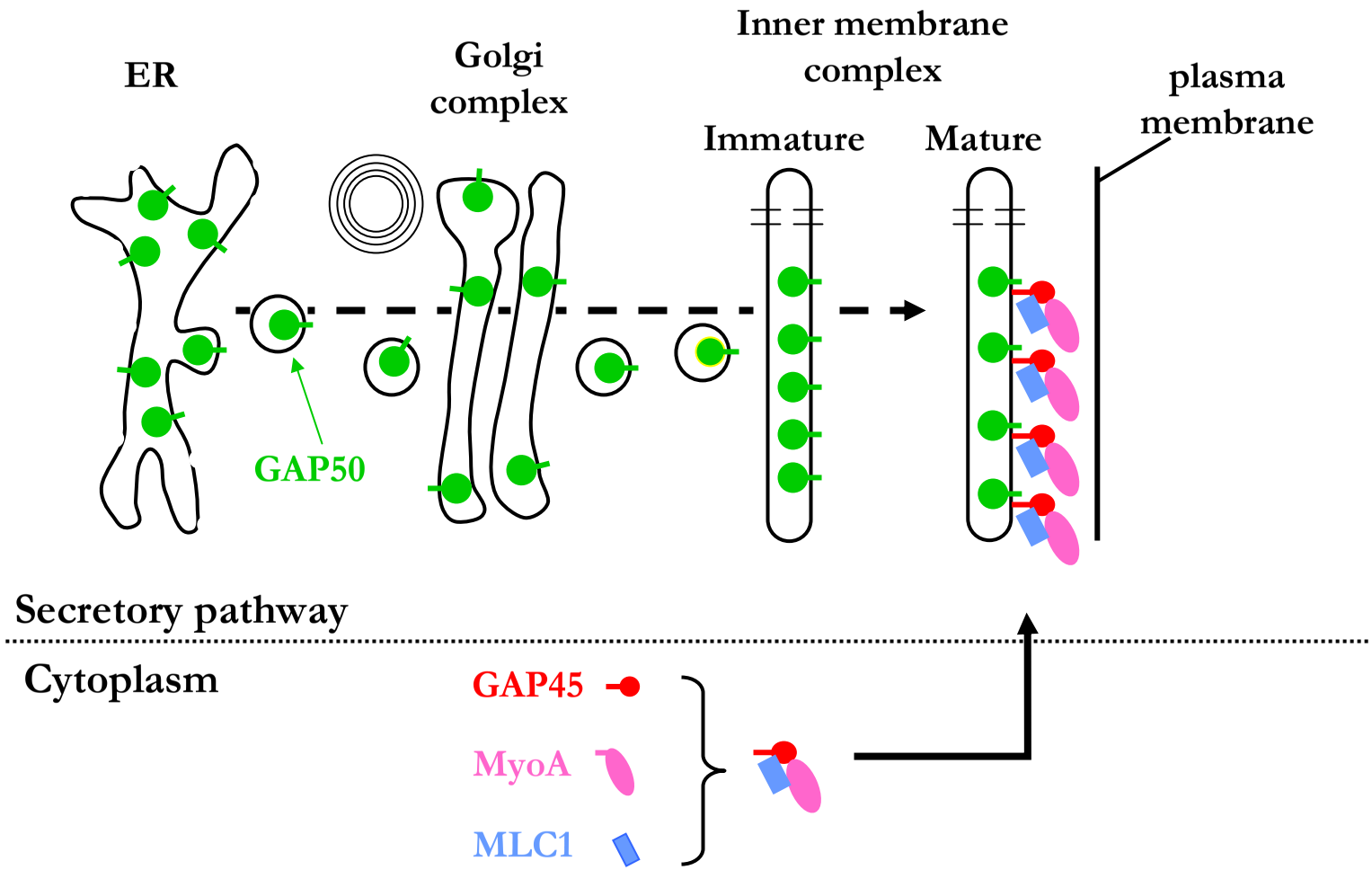


Figure 1. The *Toxoplasma* glideosome is assembled in two stages.

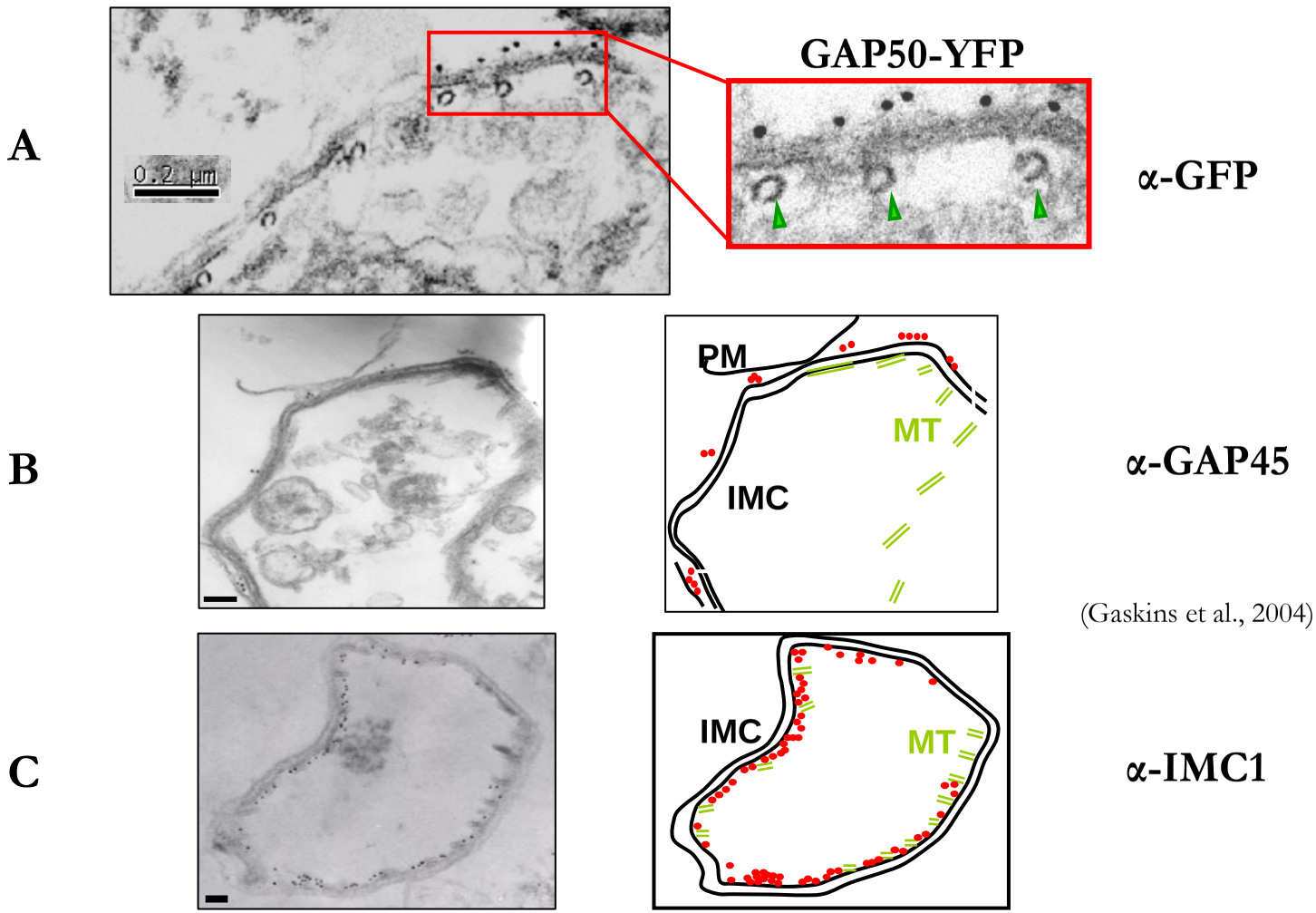


**Figure 2. TgGAP50 is only localized in the outer face of the IMC.**

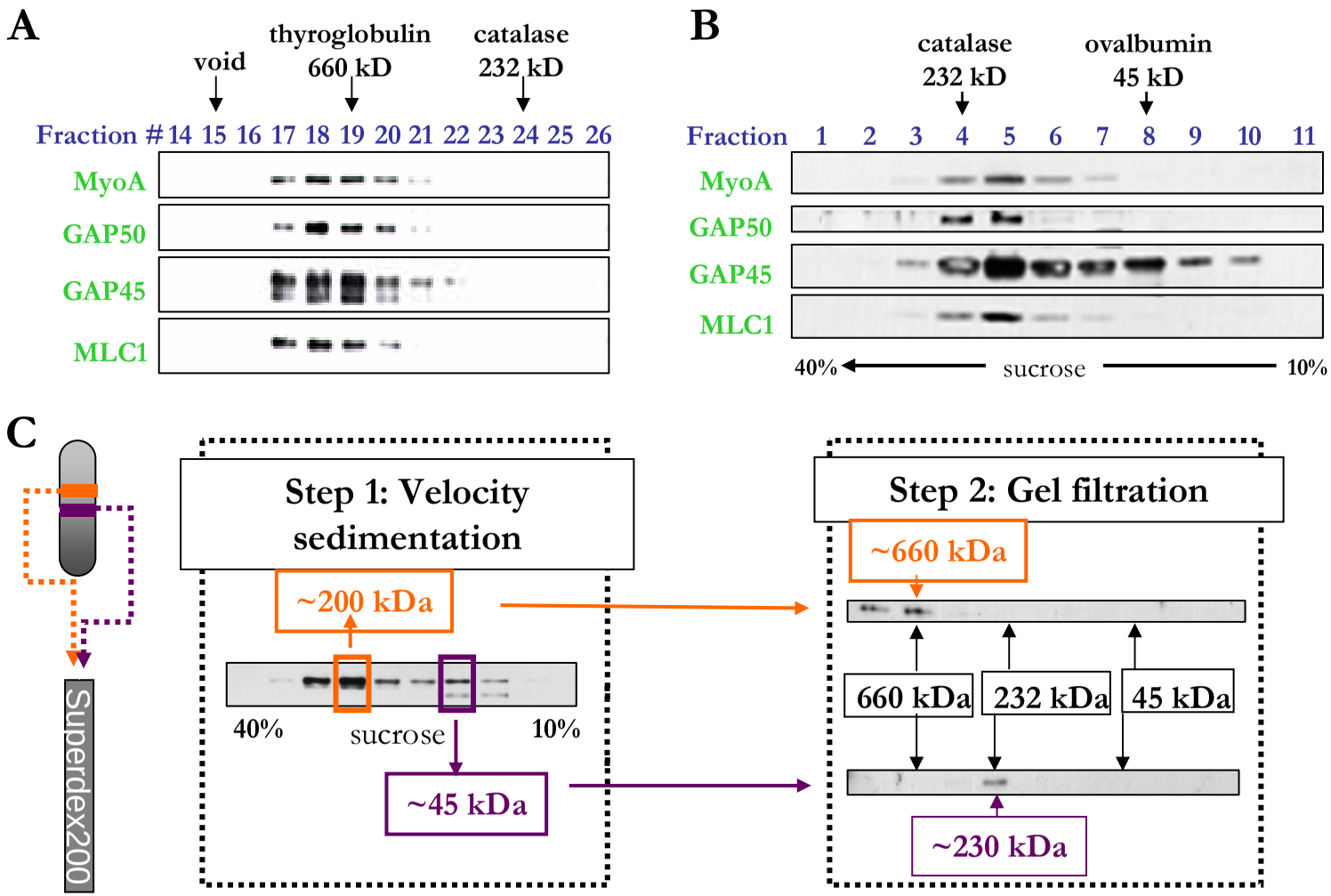


Figure 3. Analysis of glideosome size and shape.

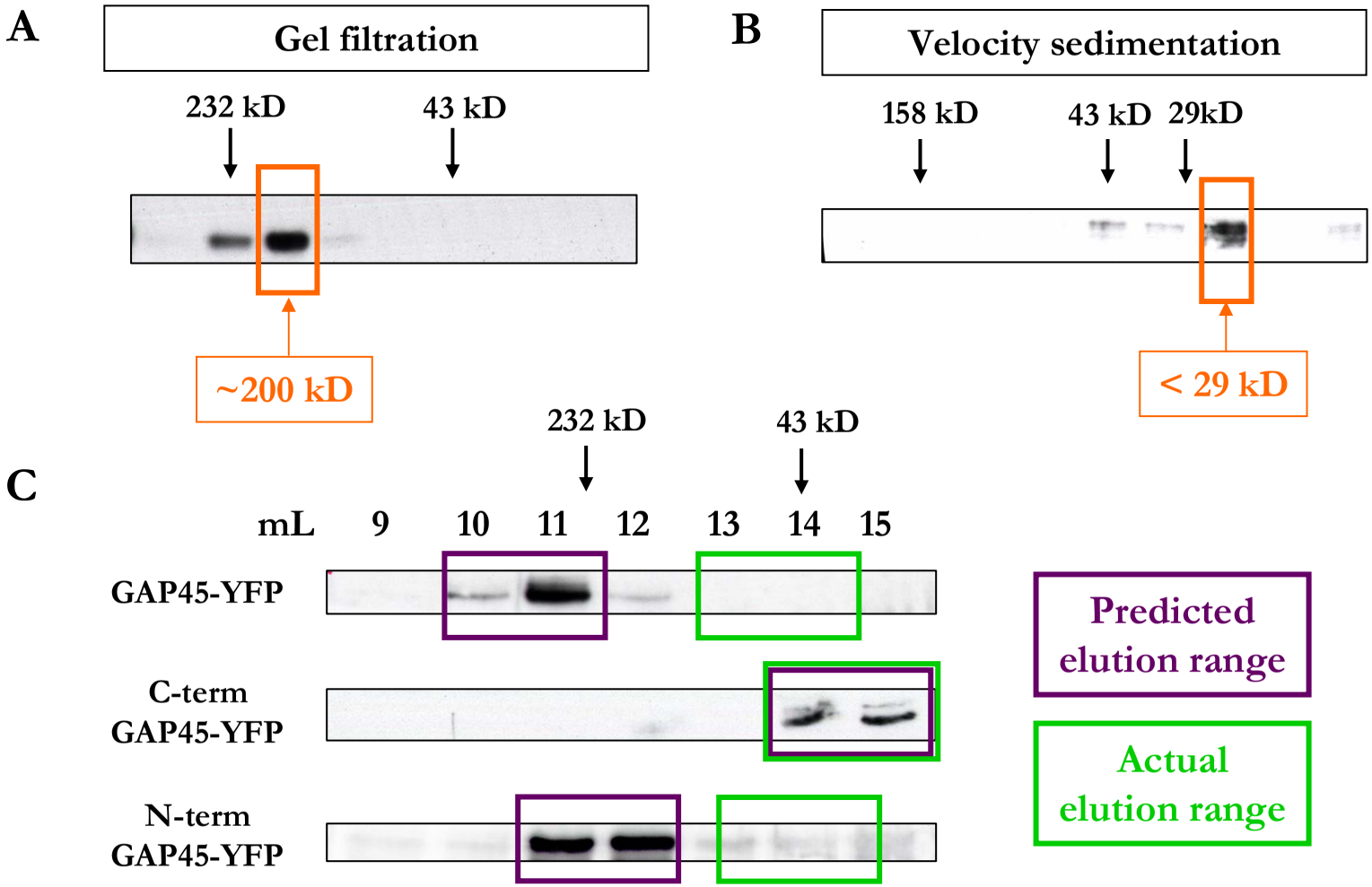


Figure 4. Analysis of TgGAP45 shape and size.

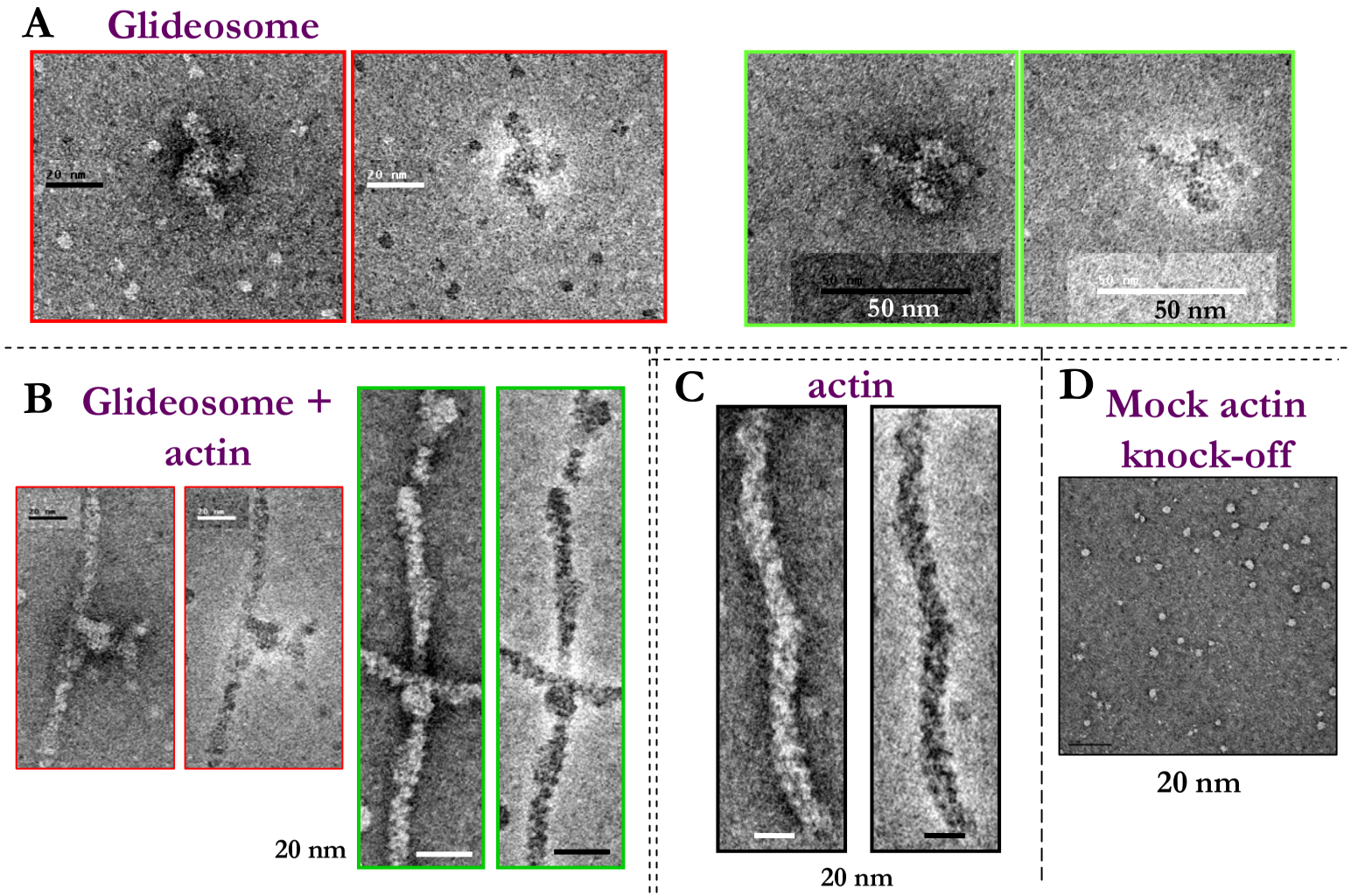


**Figure 5. Purified glideosome visualized by negative stain.**

# CHAPTER 5

# DISCUSSION AND FUTURE DIRECTIONS

## Summary

*Toxoplasma gondii* virulence relies on its mechanisms for rapid host cell invasion and its similarities to other parasites, such as *Plasmodium*, making it a parasite of concern. The overall goal of this research was to elucidate functional attributes of the gliding motility complex in apicomplexans, the glideosome. This complex encompasses half of the machinery that powers this unique actomyosin system in both invasion and motility of these parasites. This thesis focuses on two of the accessory proteins TgGAP50 and TgGAP45 that accompany the driving myosin motor, TgMyoA. What we have discovered is fundamental to understanding the mechanism of force generation by TgMyoA, as its anchor, TgGAP50, is immobilized in the IMC (Chapter 2). We have also determined that the lumenal domain and the first half of the transmembrane domain of TgGAP50 are critical for targeting of the protein, while the cytoplasmic domain is necessary for glideosome formation and therefore motility (Chapter 3). Lastly we have uncovered an unusual structural characteristic of TgGAP45, potentially alluding to its function in motility, and established a method for glideosome purification (Chapter 4). These results will reveal information about basic cellular processes such as cell motility and may eventually reveal new targets for therapeutic interventions for diseases caused by apicomplexans such as toxoplasmosis and malaria.

## Significance

We have learned that TgGAP50 only resides in the outer face of the IMC, a principle that was assumed, but not proven until now. This observation is important for the localization of actomyosin interactions and how other proteins or elements located in this space between the IMC and PM play a role in motility.

We know that TgGAP50 is immobilized in the IMC and that the IMC is largely composed of cholesterol, a rigidifying membrane lipid. The IMC cholesterol seems to be found in detergent resistant raft-like domains as judged by glideosome solubility at varied temperatures. We have shown that the removal of cholesterol leads to the dissociation of TgGAP50 with the IMC, suggesting TgGAP50 is anchored in a cholesterol-dependent manner.

We know that the first half of the transmembrane domain is required for proper targeting of TgGAP50, while the second half is not. This may be due to an interaction with the one side of the membrane this sequence spans, or being embedded within raft-like domains. There may be many small domains, or the entire layer may be a large cholesterol-rich membrane. The lumenal domain is also required for targeting, although the large size may play a role in proper membrane insertion.

TgGAP45 appears to have an unusual structural characteristic in the N-terminal half of the protein, causing it to behave as a large extended protein. This may play a role in assisting the short-tailed myosin TgMyoA, by acting as a pseudo-tail, or in actin binding, as the similarly behaving protein, tropomyosin.

We have developed a method for parasite fractionation using a combination of detergent extractions. This differential extraction is based on the use of a non-ionic detergent, TritonX-100, in buffers containing either phosphate or tris. This

method can be used to study compartmentalized molecules in the parasite, from the plasma membrane or cytosolic fraction, the IMC, or the cytoskeleton. The reasons for this buffer effect are not known, but this discovery can be exploited for many uses that require separation of cellular components.

Finally, we have developed a method for glideosome purification using a combination of detergent extractions, gel filtration, and actin cosedimentation. This protocol can be used for a variety of experiments in which functional TgMyoA is required, such as sliding filament assays, or it can be visualized further using other methods such as atomic force microscopy.

## Model

In 1981, a model was proposed for apicomplexan gliding motility based on a few observations (King et al., 1981). It was known that motility was an actin-dependent process, and that a transmembrane adhesive protein moved backwards on parasites at a speed roughly similar to the speed of invasion and forward motion (Russell and Sinden, 1981). This capping model proposed that transmembrane proteins linked the substrate to the interior of the parasite, and the gliding resulted from a capping of surface molecules driven by an actin-dependent motor (King et al., 1981; Russell and Sinden, 1981). In the past 26 years, more information has been added to this model, which has proven the initial model to be essentially correct despite the lack of detail at the time. The proteins of the glideosome have been identified, and the mechanism of actin-substrate interactions is mostly known (reviewed in Soldati and Meissner, 2004).

We are now able to add to the model of gliding motility based on our findings (Figure 1). We know that TgGAP50 is immobilized in the IMC, yet we have been

unable to detect protein-protein interactions that may be responsible. TgGAP50 may be involved in a type of protein-protein interaction with other TgGAP50 molecules, filling the IMC lumen with TgGAP50 therefore inhibiting its lateral movement through the membrane (Figure 2). We have discovered that the IMC is largely composed of cholesterol and the removal of this cholesterol leads to the dissociation of TgGAP50 with the IMC. The cholesterol may be enclosing the lattice of TgGAP50 lumenal domains, providing more stability.

The inability of the proto-glideosome to bind TgGAP50 missing the cytoplasmic tail appears to inhibit motility, but only if this TgGAP50 hybrid still localizes to the IMC. One would expect that if there are a set number of glideosome complexes spaced periodically on the outer face of the IMC, there would be enough endogenous TgGAP50 interacting with TgMyoA to move the parasite at a normal rate. The overexpressed hybrid would take up space in the IMC, but if this space was not previously occupied by TgGAP50, it will not have an effect on motility (Figure 2A). However, if the TgGAP50 molecules are tightly packed in the IMC, replacement of endogenous molecules with non-glideosome-binding TgGAP50 would have an effect on motility, as there would be fewer molecules of TgMyoA available to interact with polymerizing actin (Figure 2B).

**Future Directions: TgGAP50**

The lipid composition of the IMC still remains unknown, aside from the presence of cholesterol, but this information is critical to understanding targeting and immobilization of TgGAP50 and other potential IMC proteins. Is it not known if one face of the IMC differs in composition, so developing a method to separate these layers would be of use. It should be determined if there are many raft-like

domains, and if so, what is the size of these domains? It is also possible that one or both faces of the IMC are in fact large raft-like domains as a whole. To investigate this, we would need to utilize microscopy with high resolution in combination with markers, such as Laurdan, for areas of liquid ordered membranes versus liquid disordered membranes (Parasassi, 1998). With this compound, the fluorescence excitation and emission spectra differ between the two phospholipid phases (Parasassi, 1994).

Finally, the model supports a hypothesis that TgGAP50 molecules are tightly packed within the IMC, not allowing for lateral motility within the membrane (Figure 2B). One method for determining the spacing between TgGAP50 molecules would be to use Fluorescence resonance energy transfer (FRET) (Clegg, 2002).

Preliminary studies show that a serine at position 427 of the TgGAP50 cytoplasmic domain may be critical for motility, where overexpression of TgGAP50-YFP with serine-427 mutated to a glycine show a reduction in motility (data not shown). Phosphate incorporation experiments will determine if this serine is modified by phosphorylation and potentially regulating motility. Additionally, mutation of this serine to alanine and glutamic acid will correlate the modification with the motility defect.

It will also be of use to determine the identity of other IMC proteins. We have been successful at separating the IMC from the other cellular components such as plasma membrane, cytoplasmic organelles and cytoskeleton, which will be useful to analyze by mass spectroscopy.

**Future Directions: TgGAP45**

TgGAP45 appears to have an irregular extended shape stemming from its N-terminal half. We also know that TgGAP45 is heavily phosphorylated at two positions in between the N-terminal and C-terminal halves, and this modification has an affect on glideosome formation (Gilk et al., in preparation). It will be interesting to assess the shape and structure of TgGAP45 in its phosphorylated and dephosphorylated states, to determine the presence of a conformational change or its association with other glideosome proteins. Further visualization of this protein in a purified form using atomic force microscopy, NMR, or electron microscopy with rotary shadowing is also necessary to understand the unique structural characteristics.

Additionally, TgGAP45 may play a role in actin binding. The predicted coiled-coil region has been analyzed by the Structural Bioinformatics Core Facility at UNC and it does not appear to form a coiled-coil upon itself (data not shown). This conclusion is based on hydrophobic and hydrophilic residues positioned so that a coiled-coil would not be energetically favorable to the protein. There does seem to be a periodicity in the protein structure, which may provide binding elements for the grooves of actin filaments similar to the mechanisms of tropomyosin (Hitchcock-DeGregori and Varnell, 1990) (Figure 3).

Since TgMyoA is a single headed, non-processive myosin, it is possible that TgGAP45 binds to actin filaments after the TgMyoA power stroke, to hold the filament in place for the next myosin head. Attempts to bind TgGAP45 alone to polymerized rabbit actin have not been successful (data not shown); however actin found in the parasite may be slightly different in structure from this mammalian actin. It is also known that TgGAP45 is heavily phosphorylated (Gilk et al., in

preparation) so the binding may be regulated by this modification. The fact that TgGAP45 is not similar to any protein other than apicomplexan GAP45 indicates its potential for targeted therapeutics.

**Future Directions: Glideosome**

Preliminary studies show that TgMLC1 and TgMyoA, in addition to TgGAP45, may be palmitoylated (data not shown). These modifications may assist TgGAP50 in anchoring the complex at the IMC. Critical cysteines in these proteins can be mutated to serines to determine the effects on glideosome formation and therefore motility.

We know that the cytoplasmic domain of TgGAP50 is required for full glideosome association, but we do not know which accessory protein, or proteins, it associates with amongst TgGAP45, TgMLC1, and TgMyoA. In *Plasmodium*, it is known that 17 residues of PfMLC1 bind to PfMyoA through amino acids 803-816 of the tail domain and brings this motor to its site of action (Bosch et al., 2007). Only the tail of TgMyoA is necessary for this association with TgGAP45 and TgMyoA (data not shown). The first nine amino acids of TgGAP45 are necessary and sufficient to target TgGAP45 to the IMC, through a myristoylation signal although TgGAP45 binds to TgMLC1 and TgMyoA through its C-terminal half (Rees-Channer et al., 2006; data not shown). It is unclear if this signal is what directs an associated TgMLC1 and TgMyoA to the IMC as well or if any other signals are responsible for proto-glideosome targeting. Two basic residues of the TgMyoA tail are sufficient to target it to the IMC, however it was not evaluated for the presence of TgGAP45 or TgMLC1 (Hettmann et al., 2000). These residues may be necessary for binding TgGAP45, which is responsible for targeting.

The proteins of the glideosome are critical for parasite motility. Understanding their mode of action at the molecular level will shed light on basic cellular processes such as cell motility and cell-cell interactions and may reveal new targets for drug interventions.

"Imagine a world where parasites are masters of chemical warfare and camouflage, able to cloak themselves with their hosts' own molecules….welcome to earth."

…… Carl Zimmer, *Parasite Rex*

## Figure Legends:

**Figure 1. Model of gliding motility.**
The model of apicomplexan gliding motility can be adjusted to include the cholesterol enriched IMC membrane as a feature of TgGAP50 anchoring. TgGAP50 is also presumed to be packed together closely to assist in glideosome immobilization (adapted from Baum et al., 2006).

**Figure 2. Model of TgGAP50 arrangement in the IMC.**
Overexpression of a hybrid lacking the cytoplasmic domain (C-hybrid) localizes to the IMC, but if this space was not previously occupied by a TgGAP50 molecule, it will not have an effect on motility as the number of TgMyoA molecules does not change (A). If the TgGAP50 molecules are tightly packed in the IMC, replacement of endogenous molecules with non-glideosome-binding TgGAP50 would have an effect on motility, as there would be fewer molecules of TgMyoA available to interact with polymerizing actin (B). We do find a defect in motility in parasites overexpressing the C-hybrid, indicating B is more probable.

**Figure 3. Actin-binding properties of tropomyosin.**
TgGAP45 may bind to filamentous actin in the same manner as tropomyosin. The pockets in polymerized actin correspond to the amino acid shape of tropomyosin, allowing the two to fit together like a puzzle (A). If mutations are made to decrease the spacing of actin pockets by ½ (B) or 2/3 (C) of a site, binding no longer occurs; however shifting the pockets by one whole site restores actin binding (D), indicating the periodicity is required (Hitchcock-DeGregori and Varnell, 1990).

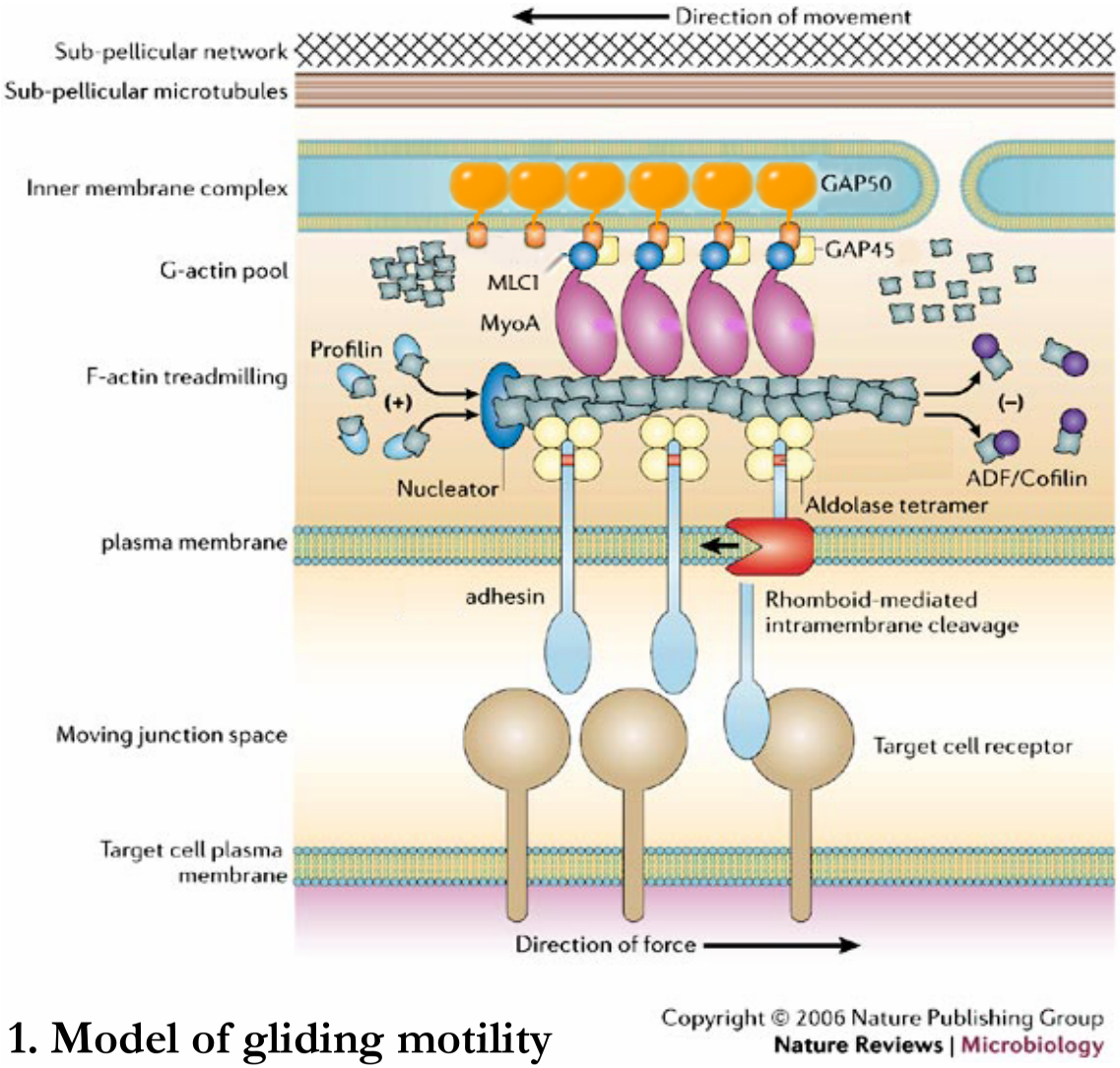


**Figure 1. Model of gliding motility**

Modified from Baum et al., 2006

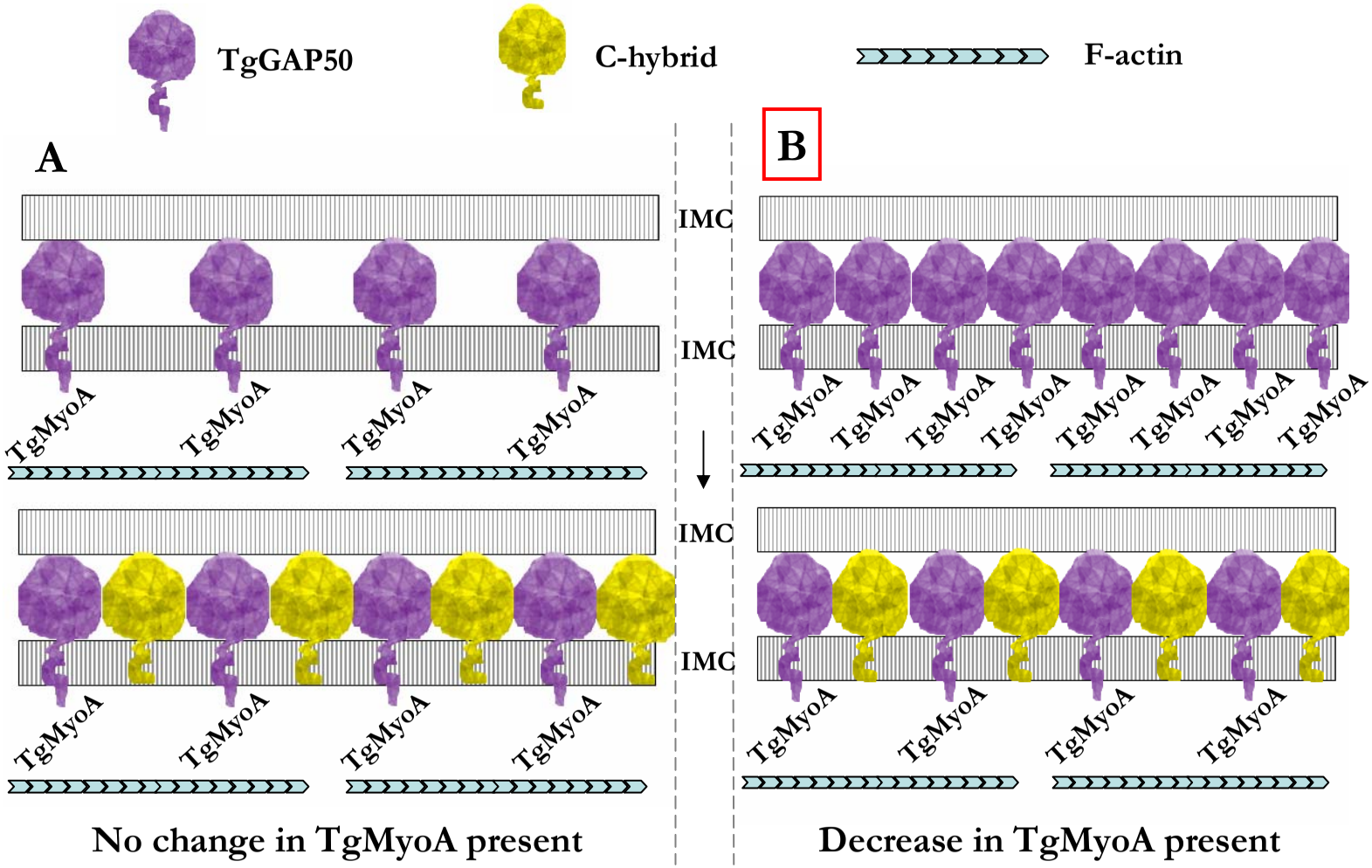


Figure 2. Model of TgGAP50 arrangement in the IMC

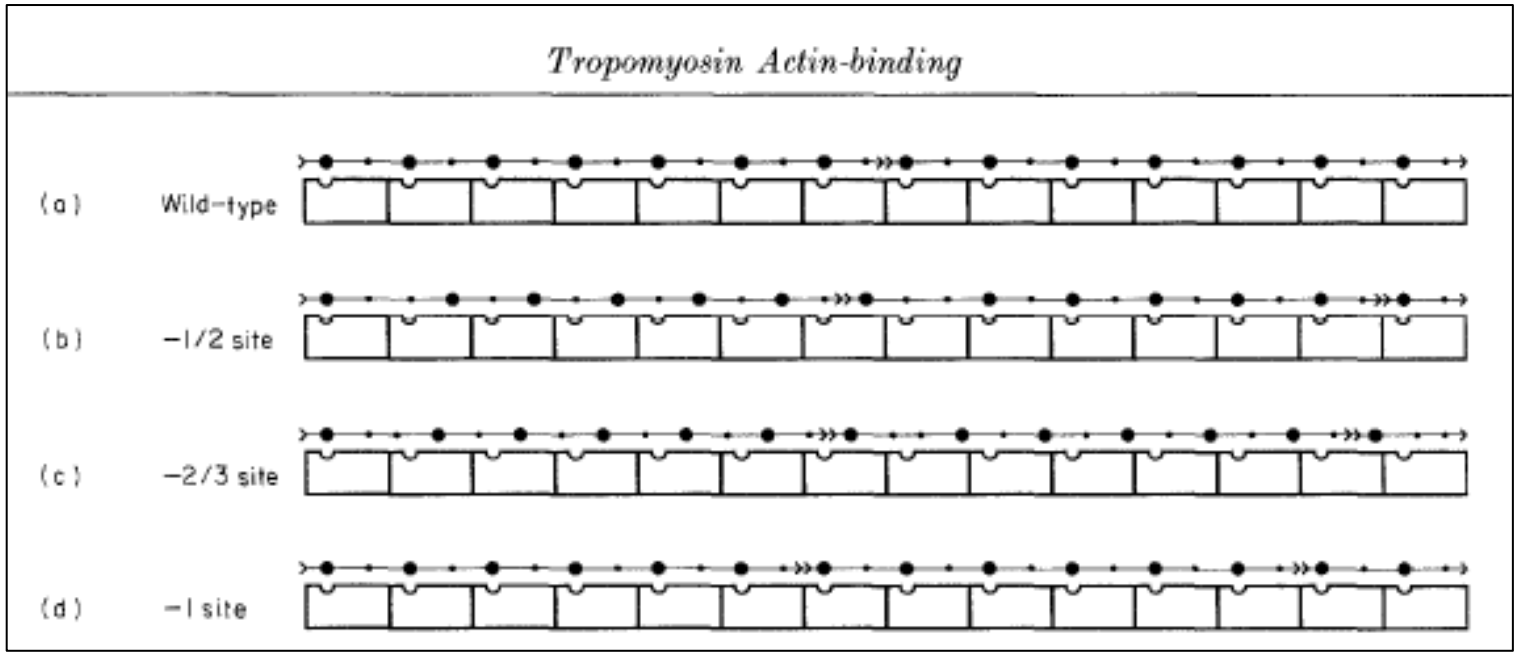


(Hitchcock-DeGregori and Varnell, 1990)

**Figure 3. Actin-binding properties of tropomyosin**

**COMPREHENSIVE BIBLIOGRAPHY**


Aikawa, M. and Beaudoin, R.L. (1968). Studies on nuclear division of a malarial parasite under pyrimethamine treatment. J Cell Biol *39*, 749-754.

Allen, M.L., Dobrowolski, J.M., Muller, H., Sibley, L.D., and Mansour, T.E. (1997). Cloning and characterization of actin depolymerizing factor from *Toxoplasma gondii*. Mol Biochem Parasitol *88*, 43-52.

Arvanitis, D.N., Min, W., Gong, Y., Heng, Y.M., and Boggs, J.M. (2005). Two types of detergent-insoluble, glycosphingolipid/cholesterol-rich membrane domains from isolated myelin. J Neurochem *94*, 1696-1710.

Barman, S., Adhikary, L., Chakrabarti, A.K., Bernas, C., Kawaoka, Y., and Nayak, D.P. (2004). Role of transmembrane domain and cytoplasmic tail amino acid sequences of influenza a virus neuraminidase in raft association and virus budding. J Virol *78*, 5258-5269.

Barry, M., and Bleackley, R.C. (2002) Cytotoxic T lymphocytes: all roads lead to death. Nat Rev Immunol 2: 401–409.

Baum, J., Richard, D., Healer, J., Rug, M., Krnajski, Z., Gilberger, T.W., Green, J.L., Holder, A.A., and Cowman, A.F. (2006). A conserved molecular motor drives cell invasion and gliding motility across malaria life cycle stages and other apicomplexan parasites. J Biol Chem *281*, 5197-5208.

Bement, W.M., and Mooseker, M.S. (1995). TEDS rule: a molecular rationale for differential regulation of myosins by phosphorylation of the heavy chain head. Cell Motil Cytoskeleton *31*, 87-92.

Bergman, L.W., Kaiser, K., Fujioka, H., Coppens, I., Daly, T.M., Fox, S., Matuschewski, K., Nussenzweig, V., and Kappe, S.H. (2003). Myosin A tail domain interacting protein (MTIP) localizes to the inner membrane complex of *Plasmodium* sporozoites. J Cell Sci *116*, 39-49.

Black, M.W., and Boothroyd, J.C. (2000). Lytic cycle of *Toxoplasma gondii*. Microbiol Mol Biol Rev *64*, 607-623.

Bligh, E.G., and Dyer, W.J. (1959). A rapid method of total lipid extraction and purification. Can J Biochem Physiol *37*, 911-917.

Bosch, J., Turley, S., Daly, T.M., Bogh, S.M., Villasmil, M.L., Roach, C., Zhou, N., Morrisey, J.M., Vaidya, A.B., Bergman, L.W., and Hol, W.G. (2006). Structure of the MTIP-MyoA complex, a key component of the malaria parasite invasion motor. Proc Natl Acad Sci U S A *103*, 4852-4857.

Bosch, J., Turley, S., Roach, C.M., Daly, T.M., Bergman, L.W., and Hol, W.G. (2007). The Closed MTIP-Myosin A-Tail Complex from the Malaria Parasite Invasion Machinery. J Mol Biol.

Bradley, P.J., Ward, C., Cheng, S.J., Alexander, D.L., Coller, S., Coombs, G.H., Dunn, J.D., Ferguson, D.J., Sanderson, S.J., Wastling, J.M., and Boothroyd, J.C. (2005). Proteomic analysis of rhoptry organelles reveals many novel constituents for host-parasite interactions in *Toxoplasma gondii*. J Biol Chem *280*, 34245-34258.

Bretscher, M.S., and Munro, S. (1993). Cholesterol and the Golgi apparatus. Science *261*, 1280-1281.

Brown, D.A., and Rose, J.K. (1992). Sorting of GPI-anchored proteins to glycolipid-enriched membrane subdomains during transport to the apical cell surface. Cell *68*, 533-544.

Brown, E.L., and Lyles, D.S. (2003). A novel method for analysis of membrane microdomains: vesicular stomatitis virus glycoprotein microdomains change in size during infection, and those outside of budding sites resemble sites of virus budding. Virology *310*, 343-358.

Buscaglia, C.A., Coppens, I., Hol, W.G., and Nussenzweig, V. (2003). Sites of interaction between aldolase and thrombospondin-related anonymous protein in *plasmodium*. Mol Biol Cell *14*, 4947-4957.

Carmen, J.C., and Sinai, A.P. (2007). Suicide prevention: disruption of apoptotic pathways by protozoan parasites. Mol Microbiol *64*, 904-916.

Carruthers, V.B., Sherman, G.D., and Sibley, L.D. (2000). The *Toxoplasma* adhesive protein MIC2 is proteolytically processed at multiple sites by two parasite-derived proteases. J Biol Chem *275*, 14346-14353.

Carruthers, V.B., and Sibley, L.D. (1997). Sequential protein secretion from three distinct organelles of *Toxoplasma gondii* accompanies invasion of human fibroblasts. Eur J Cell Biol *73*, 114-123.

Cavalier-Smith, T. (1993). Kingdom protozoa and its 18 phyla. Microbiol Rev *57*, 953-994.

Clegg, R.M. (2002). FRET tells us about proximities, distances, orientations and dynamic properties. J Biotechnol *82*, 177-179.

Coppens, I., and Joiner, K.A. (2003). Host but not parasite cholesterol controls *Toxoplasma* cell entry by modulating organelle discharge. Mol Biol Cell *14*, 3804-3820.

Coppens, I., Sinai, A.P., and Joiner, K.A. (2000). *Toxoplasma gondii* exploits host low-density lipoprotein receptor-mediated endocytosis for cholesterol acquisition. J Cell Biol *149*, 167-180.

Dobrowolski, J.M., Carruthers, V.B., and Sibley, L.D. (1997a). Participation of myosin in gliding motility and host cell invasion by *Toxoplasma gondii*. Mol Microbiol *26*, 163-173.

Dobrowolski, J.M., Niesman, I.R., and Sibley, L.D. (1997b). Actin in the parasite *Toxoplasma gondii* is encoded by a single copy gene, ACT1 and exists primarily in a globular form. Cell Motil Cytoskeleton *37*, 253-262.

Dobrowolski, J.M., and Sibley, L.D. (1996). *Toxoplasma* invasion of mammalian cells is powered by the actin cytoskeleton of the parasite. Cell *84*, 933-939.

Dowse, T.J., and Soldati, D. (2005). Rhomboid-like proteins in Apicomplexa: phylogeny and nomenclature. Trends Parasitol *21*, 254-258.

Du, Wayne. Pork Safety: Managing *Toxoplasma* In Swine. Ontario: Queens Printer for Ontario. Factsheet 2004.

Dubey, J.P. (1994). Toxoplasmosis. J Am Vet Med Assoc *205*, 1593-1598.

Dubey, J.P. (1998). Advances in the life cycle of *Toxoplasma gondii*. Int J Parasitol *28*, 1019-1024.

Dubremetz, J.F., and Elsner, Y.Y. (1979). Ultrastructural study of schizogony of Eimeria bovis in cell cultures. J Protozool *26*, 367-376.

Dubremetz, J.F., and Torpier, G. (1978). Freeze fracture study of the pellicle of an eimerian sporozoite (Protozoa, Coccidia). J Ultrastruct Res *62*, 94-109.

Flegr, J. (2007). Effects of *toxoplasma* on human behavior. Schizophr Bull *33*, 757-760.

Fleming, E.H., Kolokoltsov, A.A., Davey, R.A., Nichols, J.E., and Roberts, N.J., Jr. (2006). Respiratory syncytial virus F envelope protein associates with lipid rafts without a requirement for other virus proteins. J Virol *80*, 12160-12170.

Foth, B.J., Goedecke, M.C., and Soldati, D. (2006). New insights into myosin evolution and classification. Proc Natl Acad Sci U S A *103*, 3681-3686.

Foussard, F., Leriche, M.A., and Dubremetz, J.F. (1991). Characterization of the lipid content of *Toxoplasma gondii* rhoptries. Parasitology *102 Pt 3*, 367-370.

Frixione, E., Mondragon, R., and Meza, I. (1996). Kinematic analysis of *Toxoplasma gondii* motility. Cell Motil Cytoskeleton *34*, 152-163.

Fruth, I.A., and Arrizabalaga, G. (2007). *Toxoplasma gondii*: Induction of egress by the potassium ionophore nigericin. Int J Parasitol.

Fulton, J.D., and Spooner, D.F. (1960). Metabolic studies on *Toxoplasma gondii*. Exp Parasitol *9*, 293-301.

Gaskins, E., Gilk, S., DeVore, N., Mann, T., Ward, G., and Beckers, C. (2004). Identification of the membrane receptor of a class XIV myosin in *Toxoplasma gondii*. J Cell Biol *165*, 383-393.

Gilbert, R.E., Stanford, M.R., Jackson, H., Holliman, R.E., and Sanders, M.D. (1995). Incidence of acute symptomatic *toxoplasma* retinochoroiditis in south London according to country of birth. BMJ *310*, 1037-1040.

Gilk, S.D., Johnson, T.M., Gaskins, E., Ward, G.E., and Beckers, C.J.M. (in preparation) GAP45 phosphorylation controls assembly of the *Toxoplasma* myosin XIV complex.

Gilk, S.D., Raviv, Y., Hu, K., Murray, J.M., Beckers, C.J., and Ward, G.E. (2006). Identification of PhIL1, a novel cytoskeletal protein of the *Toxoplasma gondii* pellicle, through photosensitized labeling with 5-[125I]iodonaphthalene-1-azide. Eukaryot Cell *5*, 1622-1634.

Goder, V., and Spiess, M. (2001). Topogenesis of membrane proteins: determinants and dynamics. FEBS Lett *504*, 87-93.

Gordon, G.W., Berry, G., Liang, X.H., Levine, B., and Herman, B. (1998). Quantitative fluorescence resonance energy transfer measurements using fluorescence microscopy. Biophys J *74*, 2702-2713.

Gordon, J.L., and Sibley, L.D. (2005). Comparative genome analysis reveals a conserved family of actin-like proteins in apicomplexan parasites. BMC Genomics *6*, 179.

Gupta, N., and DeFranco, A.L. (2003). Visualizing lipid raft dynamics and early signaling events during antigen receptor-mediated B-lymphocyte activation. Mol Biol Cell *14*, 432-444.

Hakansson, S., Morisaki, H., Heuser, J., and Sibley, L.D. (1999). Time-lapse video microscopy of gliding motility in *Toxoplasma gondii* reveals a novel, biphasic mechanism of cell locomotion. Mol Biol Cell *10*, 3539-3547.

Heintzelman, M.B., and Schwartzman, J.D. (1997). A novel class of unconventional myosins from *Toxoplasma gondii*. J Mol Biol *271*, 139-146.

Heintzelman, M.B., and Schwartzman, J.D. (1999). Characterization of myosin-A and myosin-C: two class XIV unconventional myosins from *Toxoplasma gondii*. Cell Motil Cytoskeleton *44*, 58-67.

Hepler, P.K., Huff, C.G., and Sprinz, H. (1966). The fine structure of the exoerythrocytic stages of *Plasmodium fallax*. J Cell Biol *30*, 333-358.

Herm-Gotz, A., Weiss, S., Stratmann, R., Fujita-Becker, S., Ruff, C., Meyhofer, E., Soldati, T., Manstein, D.J., Geeves, M.A., and Soldati, D. (2002). *Toxoplasma gondii* myosin A and its light chain: a fast, single-headed, plus-end-directed motor. Embo J *21*, 2149-2158.

Hettmann, C., Herm, A., Geiter, A., Frank, B., Schwarz, E., Soldati, T., and Soldati, D. (2000). A dibasic motif in the tail of a class XIV apicomplexan myosin is an essential determinant of plasma membrane localization. Mol Biol Cell *11*, 1385-1400.

Hitchcock-DeGregori, S.E., and Varnell, T.A. (1990). Tropomyosin has discrete actin-binding sites with sevenfold and fourteenfold periodicities. J Mol Biol *214*, 885-896.

Hu, K., Mann, T., Striepen, B., Beckers, C.J., Roos, D.S., and Murray, J.M. (2002). Daughter cell assembly in the protozoan parasite *Toxoplasma gondii*. Mol Biol Cell *13*, 593-606.

Huynh, M.H., Rabenau, K.E., Harper, J.M., Beatty, W.L., Sibley, L.D., and Carruthers, V.B. (2003). Rapid invasion of host cells by *Toxoplasma* requires secretion of the MIC2-M2AP adhesive protein complex. Embo J *22*, 2082-2090.

Jewett, T.J., and Sibley, L.D. (2003). Aldolase forms a bridge between cell surface adhesins and the actin cytoskeleton in apicomplexan parasites. Mol Cell *11*, 885-894.

Johnson, T.M., Rajfur, Z., Jacobson, K., and Beckers, C.J. (2007). Immobilization of the Type XIV Myosin Complex in *Toxoplasma gondii*. Mol Biol Cell *18*, 3039-3046.

Jordan, B.R., Caillol, D., Damotte, M., Delovitch, T., Ferrier, P., Kahn-Perles, B., Kourilsky, F., Layet, C., Le Bouteiller, P., Lemonnier, F.A., and et al. (1985). HLA class I genes: from structure to expression, serology and function. Immunol Rev *84*, 73-92.

Kappe, S., Bruderer, T., Gantt, S., Fujioka, H., Nussenzweig, V., and Menard, R. (1999). Conservation of a gliding motility and cell invasion machinery in Apicomplexan parasites. J Cell Biol *147*, 937-944.

Karsten, V., Qi, H., Beckers, C.J., Reddy, A., Dubremetz, J.F., Webster, P., and Joiner, K.A. (1998). The protozoan parasite *Toxoplasma gondii* targets proteins to dense granules and the vacuolar space using both conserved and unusual mechanisms. J Cell Biol *141*, 1323-1333.

Keeley, A., and Soldati, D. (2004). The glideosome: a molecular machine powering motility and host-cell invasion by Apicomplexa. Trends Cell Biol *14*, 528-532.

Kieschnick, H., Wakefield, T., Narducci, C.A., and Beckers, C. (2001). *Toxoplasma gondii* attachment to host cells is regulated by a calmodulin-like domain protein kinase. J Biol Chem *276*, 12369-12377.

King, C.A. (1981). Cell surface interaction of the protozoan *Gregarina* with concanavalin A beads - implications for models of gregarine gliding. Cell Biol Int Rep *5*, 297-305.

Kinose, F., Wang, S.X., Kidambi, U.S., Moncman, C.L., and Winkelmann, D.A. (1996). Glycine 699 is pivotal for the motor activity of skeletal muscle myosin. J Cell Biol *134*, 895-909.

Klein, S.L. (2005). Parasite manipulation of host behavior: mechanisms, ecology, and future directions. Behav Processes *68*, 219-221.

Laemmli, U.K. (1970). Cleavage of structural proteins during the assembly of the head of bacteriophage T4. Nature *227*, 680-685.

Lafferty, K.D. (2006). Can the common brain parasite, *Toxoplasma gondii*, influence human culture? Proc Biol Sci *273*, 2749-2755.

Lauer, S., VanWye, J., Harrison, T., McManus, H., Samuel, B.U., Hiller, N.L., Mohandas, N., and Haldar, K. (2000). Vacuolar uptake of host components, and a role for cholesterol and sphingomyelin in malarial infection. Embo J *19*, 3556-3564.

Lecordier, L., Mercier, C., Sibley, L.D., and Cesbron-Delauw, M.F. (1999). Transmembrane insertion of the *Toxoplasma gondii* GRA5 protein occurs after soluble secretion into the host cell. Mol Biol Cell *10*, 1277-1287.

Liscum, L., and Munn, N.J. (1999). Intracellular cholesterol transport. Biochim Biophys Acta *1438*, 19-37.

Lou, H., Smith, A.M., Coates, L.C., Cawley, N.X., Loh, Y.P., and Birch, N.P. (2007). The transmembrane domain of the prohormone convertase PC3: a key motif for targeting to the regulated secretory pathway. Mol Cell Endocrinol *267*, 17-25.

Lovett, J.L., Marchesini, N., Moreno, S.N., and Sibley, L.D. (2002). *Toxoplasma gondii* microneme secretion involves intracellular Ca(2+) release from inositol 1,4,5-triphosphate (IP(3))/ryanodine-sensitive stores. J Biol Chem *277*, 25870-25876.

Lovett, J.L., and Sibley, L.D. (2003). Intracellular calcium stores in *Toxoplasma gondii* govern invasion of host cells. J Cell Sci *116*, 3009-3016.

Lucero, H.A., and Robbins, P.W. (2004). Lipid rafts-protein association and the regulation of protein activity. Arch Biochem Biophys *426*, 208-224.

Lupas, A., Van Dyke, M., and Stock, J. (1991). Predicting coiled coils from protein sequences. Science *252*, 1162-1164.

Makhov AM, Subramanian D, Holley-Guthrie E, Kenney SC, Griffith JD. (2004). The Epstein-Barr virus polymerase accessory factor BMRF1 adopts a ring-shaped structure as visualized by electron microscopy. J Biol Chem. 279(39):40358-61.

Mann, T., and Beckers, C. (2001). Characterization of the subpellicular network, a filamentous membrane skeletal component in the parasite *Toxoplasma gondii*. Mol Biochem Parasitol *115*, 257-268.

Mann, T., Gaskins, E., and Beckers, C. (2002). Proteolytic processing of TgIMC1 during maturation of the membrane skeleton of *Toxoplasma gondii*. J Biol Chem *277*, 41240-41246.

Meissner, M., Schluter, D., and Soldati, D. (2002). Role of *Toxoplasma gondii* myosin A in powering parasite gliding and host cell invasion. Science *298*, 837-840.

Mercier, C., Cesbron-Delauw, M.F., and Sibley, L.D. (1998). The amphipathic alpha helices of the *toxoplasma* protein GRA2 mediate post-secretory membrane association. J Cell Sci *111 ( Pt 15)*, 2171-2180.

Morrissette, N.S., Murray, J.M., and Roos, D.S. (1997). Subpellicular microtubules associate with an intramembranous particle lattice in the protozoan parasite *Toxoplasma gondii*. J Cell Sci *110 ( Pt 1)*, 35-42.

Morrissette, N.S., and Sibley, L.D. (2002a). Cytoskeleton of apicomplexan parasites. Microbiol Mol Biol Rev *66*, 21-38; table of contents.

Morrissette, N.S., and Sibley, L.D. (2002b). Disruption of microtubules uncouples budding and nuclear division in *Toxoplasma gondii*. J Cell Sci *115*, 1017-1025.

Mortensen, P.B., Norgaard-Pedersen, B., Waltoft, B.L., Sorensen, T.L., Hougaard, D., Torrey, E.F., and Yolken, R.H. (2007). *Toxoplasma gondii* as a risk factor for early-onset schizophrenia: analysis of filter paper blood samples obtained at birth. Biol Psychiatry *61*, 688-693.

Moudy, R., Manning, T.J., and Beckers, C.J. (2001). The loss of cytoplasmic potassium upon host cell breakdown triggers egress of *Toxoplasma gondii*. J Biol Chem *276*, 41492-41501.

Murphy, D.J. (2001). The biogenesis and functions of lipid bodies in animals, plants and microorganisms. Prog Lipid Res *40*, 325-438.

Newton, C.R., and Warrell, D.A. (1998). Neurological manifestations of falciparum malaria. Ann Neurol *43*, 695-702.

Nichols, B.A., and Chiappino, M.L. (1987). Cytoskeleton of *Toxoplasma gondii*. J Protozool *34*, 217-226.

Nichols, B.A., Chiappino, M.L., and Pavesio, C.E. (1994). Endocytosis at the micropore of *Toxoplasma gondii*. Parasitol Res *80*, 91-98.

Ogino, N., and Yoneda, C. (1966). The fine structure and mode of division of *Toxoplasma gondii*. Arch Ophthalmol *75*, 218-227.

Opitz, C., and Soldati, D. (2002). 'The glideosome': a dynamic complex powering gliding motion and host cell invasion by *Toxoplasma gondii*. Mol Microbiol *45*, 597-604.

Ortega, Y. R. Food Microbiology And Food Safety Series, Foodborne Parasites. Springer US, 2006.109-133.

Ossorio, P.N., Dubremetz, J.F., and Joiner, K.A. (1994). A soluble secretory protein of the intracellular parasite *Toxoplasma gondii* associates with the parasitophorous vacuole membrane through hydrophobic interactions. J Biol Chem *269*, 15350-15357.

Parasassi, T., Di Stefano, M., Loiero, M., Ravagnan, G., and Gratton, E. (1994). Influence of cholesterol on phospholipid bilayers phase domains as detected by Parasassi T., Krasnowska E.K., Bagatolli L.and Gratton E. (1998). Laurdan and Prodan as Polarity-Sensitive Fluorescent Membrane Probes. J Fluor. *8*, 365-373. Laurdan fluorescence. Biophys J *66*, 120-132.

Parfrey, H., Mahadeva, R., Ravenhill, N.A., Zhou, A., Dafforn, T.R., Foreman, R.C., and Lomas, D.A. (2003). Targeting a surface cavity of alpha 1-antitrypsin to prevent conformational disease. J Biol Chem *278*, 33060-33066.

Perrotto, J., Keister, D.B., and Gelderman, A.H. (1971). Incorporation of precursors into *Toxoplasma* DNA. J Protozool *18*, 470-473.

Pfefferkorn, E.R. (1984). Interferon gamma blocks the growth of *Toxoplasma gondii* in human fibroblasts by inducing the host cells to degrade tryptophan. Proc Natl Acad Sci U S A *81*, 908-912.

Pike, L.J. (2004). Lipid rafts: heterogeneity on the high seas. Biochem J *378*, 281-292.

Porchet, E., and Torpier, G. (1977). [Freeze fracture study of *Toxoplasma* and *Sarcocystis* infective stages (author's transl)]. Z Parasitenkd *54*, 101-124.

Porchet-Hennere, E., and Nicolas, G. (1983). Are rhoptries of *Coccidia* really extrusomes? J Ultrastruct Res *84*, 194-203.

Poupel, O., Boleti, H., Axisa, S., Couture-Tosi, E., and Tardieux, I. (2000). Toxofilin, a novel actin-binding protein from *Toxoplasma gondii*, sequesters actin monomers and caps actin filaments. Mol Biol Cell *11*, 355-368.

Prior, I.A., Muncke, C., Parton, R.G., and Hancock, J.F. (2003). Direct visualization of Ras proteins in spatially distinct cell surface microdomains. J Cell Biol *160*, 165-170.

Proellocks, N.I., Kovacevic, S., Ferguson, D.J., Kats, L.M., Morahan, B.J., Black, C.G., Waller, K.L., and Coppel, R.L. (2007). *Plasmodium falciparum* Pf34, a novel GPI-anchored rhoptry protein found in detergent-resistant microdomains. Int J Parasitol.

Rayner, J.C., and Pelham, H.R. (1997). Transmembrane domain-dependent sorting of proteins to the ER and plasma membrane in yeast. Embo J *16*, 1832-1841.

Rees-Channer, R.R., Martin, S.R., Green, J.L., Bowyer, P.W., Grainger, M., Molloy, J.E., and Holder, A.A. (2006). Dual acylation of the 45 kDa gliding-associated protein (GAP45) in *Plasmodium falciparum* merozoites. Mol Biochem Parasitol *149*, 113-116.

Resh, M.D. (1999). Fatty acylation of proteins: new insights into membrane targeting of myristoylated and palmitoylated proteins. Biochim Biophys Acta *1451*, 1-16.

Robibaro, B., Stedman, T.T., Coppens, I., Ngo, H.M., Pypaert, M., Bivona, T., Nam, H.W., and Joiner, K.A. (2002). *Toxoplasma gondii* Rab5 enhances cholesterol acquisition from host cells. Cell Microbiol *4*, 139-152.

Russell, D.G., and Burns, R.G. (1984). The polar ring of coccidian sporozoites: a unique microtubule-organizing centre. J Cell Sci *65*, 193-207.

Russell, D.G., and Sinden, R.E. (1981). The role of the cytoskeleton in the motility of coccidian sporozoites. J Cell Sci *50*, 345-359.

Saeij, J.P., Coller, S., Boyle, J.P., Jerome, M.E., White, M.W., and Boothroyd, J.C. (2007). *Toxoplasma* co-opts host gene expression by injection of a polymorphic kinase homologue. Nature *445*, 324-327.

Schmitz, S., Grainger, M., Howell, S., Calder, L.J., Gaeb, M., Pinder, J.C., Holder, A.A., and Veigel, C. (2005). Malaria parasite actin filaments are very short. J Mol Biol *349*, 113-125.

Schuler, H., and Matuschewski, K. (2006). Regulation of apicomplexan microfilament dynamics by a minimal set of actin-binding proteins. Traffic *7*, 1433-1439.

Schwab, J.C., Beckers, C.J., and Joiner, K.A. (1994). The parasitophorous vacuole membrane surrounding intracellular *Toxoplasma gondii* functions as a molecular sieve. Proc Natl Acad Sci U S A *91*, 509-513.

Schwartzman, J.D., and Pfefferkorn, E.R. (1982). *Toxoplasma gondii*: purine synthesis and salvage in mutant host cells and parasites. Exp Parasitol *53*, 77-86.

Shaw, M.K., and Tilney, L.G. (1999). Induction of an acrosomal process in *Toxoplasma gondii*: visualization of actin filaments in a protozoan parasite. Proc Natl Acad Sci U S A *96*, 9095-9099.

Sibley, L.D. (2003). *Toxoplasma gondii*: perfecting an intracellular life style. Traffic *4*, 581-586.

Sibley, L.D. (2004). Intracellular parasite invasion strategies. Science *304*, 248-253.

Simons, K., and Ikonen, E. (1997). Functional rafts in cell membranes. Nature *387*, 569-572.

Sinai, A.P., and Joiner, K.A. (2001). The *Toxoplasma gondii* protein ROP2 mediates host organelle association with the parasitophorous vacuole membrane. J Cell Biol *154*, 95-108.

Sinai, A.P., Webster, P., and Joiner, K.A. (1997). Association of host cell endoplasmic reticulum and mitochondria with the *Toxoplasma gondii* parasitophorous vacuole membrane: a high affinity interaction. J Cell Sci *110 ( Pt 17)*, 2117-2128.

Smith, J.E. (1995). A ubiquitous intracellular parasite: the cellular biology of *Toxoplasma gondii*. Int J Parasitol *25*, 1301-1309.

Soldati, D., and Meissner, M. (2004). *Toxoplasma* as a novel system for motility. Curr Opin Cell Biol *16*, 32-40.

Stokkermans, T.J., Schwartzman, J.D., Keenan, K., Morrissette, N.S., Tilney, L.G., and Roos, D.S. (1996). Inhibition of *Toxoplasma gondii* replication by dinitroaniline herbicides. Exp Parasitol *84*, 355-370.

Striepen, B., Jordan, C.N., Reiff, S., and van Dooren, G.G. (2007). Building the Perfect Parasite: Cell Division in Apicomplexa. PLoS Pathog *3*, e78.

Sultan, A.A., Thathy, V., Frevert, U., Robson, K.J., Crisanti, A., Nussenzweig, V., Nussenzweig, R.S., and Menard, R. (1997). TRAP is necessary for gliding motility and infectivity of *plasmodium* sporozoites. Cell *90*, 511-522.

Tardieux, I., Liu, X., Poupel, O., Parzy, D., Dehoux, P., and Langsley, G. (1998). A *Plasmodium falciparum* novel gene encoding a coronin-like protein which associates with actin filaments. FEBS Lett *441*, 251-256.

Tenant-Flowers, M., Boyle, M.J., Carey, D., Marriott, D.J., Harkness, J.L., Penny, R., and Cooper, D.A. (1991). Sulphadiazine desensitization in patients with AIDS and cerebral toxoplasmosis. Aids *5*, 311-315.

Thomas, F., Adamo, S., and Moore, J. (2005). Parasitic manipulation: where are we and where should we go? Behav Processes *68*, 185-199.

Torrey, E.F., and Yolken, R.H. (2003). *Toxoplasma gondii* and schizophrenia. Emerg Infect Dis *9*, 1375-1380.

Torrey, E.F., and Yolken, R.H. (2007). Schizophrenia and toxoplasmosis. Schizophr Bull *33*, 727-728.

Trotter, P.J., and Voelker, D.R. (1994). Lipid transport processes in eukaryotic cells. Biochim Biophys Acta *1213*, 241-262.

Valentine, R. C., and Green, N. M. (1967) J. Mol. Biol. 27**,** 615–617.

van der Zypen, E., and Piekarski, G. (1967). [Endodyogeny in *Toxoplasma gondii*. A morphological analysis]. Z Parasitenkd *29*, 15-35.

van der Zypen, E., and Piekarski G. (1968). Ultrastructure on endodyogeny in *Toxoplasma gondii*. Bol. Chil. Parasitol. 23:90-94. (In Spanish.)

Vial, H.J., Eldin, P., Tielens, A.G., and van Hellemond, J.J. (2003). Phospholipids in parasitic protozoa. Mol Biochem Parasitol *126*, 143-154.

Vyas, A., Kim, S.K., Giacomini, N., Boothroyd, J.C., and Sapolsky, R.M. (2007). Behavioral changes induced by *Toxoplasma* infection of rodents are highly specific to aversion of cat odors. Proc Natl Acad Sci U S A *104*, 6442-6447.

Website: www.dpd.cdc.gov

Walker, M., Trinick, J., and White, H. (1995). Millisecond time resolution electron cryo-microscopy of the M-ATP transient kinetic state of the acto-myosin ATPase. Biophys J *68*, 87S-91S.

Webster, J.P. (2007). The effect of *Toxoplasma gondii* on animal behavior: playing cat and mouse. Schizophr Bull *33*, 752-756.

Webster, J.P., Lamberton, P.H., Donnelly, C.A., and Torrey, E.F. (2006). Parasites as causative agents of human affective disorders? The impact of anti-psychotic, mood-stabilizer and anti-parasite medication on *Toxoplasma gondii*'s ability to alter host behaviour. Proc Biol Sci *273*, 1023-1030.

Wetzel, D.M., Hakansson, S., Hu, K., Roos, D., and Sibley, L.D. (2003). Actin filament polymerization regulates gliding motility by apicomplexan parasites. Mol Biol Cell *14*, 396-406.

Wong, S.Y., and Remington, J.S. (1993). Biology of *Toxoplasma gondii*. Aids *7*, 299-316.

Zhou, H., Gu, Q., Zhao, Q., Zhang, J., Cong, H., Li, Y., and He, S. (2007). *Toxoplasma gondii*: expression and characterization of a recombinant protein containing SAG1 and GRA2 in *Pichia pastoris*. Parasitol Res *100*, 829-835.